NASA TECHNICAL NOTE

NASA TN D-2037

NASA TN D-2037

AERODYNAMIC CHARACTERISTICS OF A SPOILER-SLOT-DEFLECTOR CONTROL ON A 45° SWEPTBACK-WING–FUSELAGE MODEL AT HIGH SUBSONIC SPEEDS

by Alexander D. Hammond
Langley Research Center
Langley Station, Hampton, Va.

NATIONAL AERONAUTICS AND SPACE ADMINISTRATION • WASHINGTON, D. C. • NOVEMBER 1963

TECHNICAL NOTE D-2037

AERODYNAMIC CHARACTERISTICS OF A SPOILER-SLOT-DEFLECTOR CONTROL ON A 45° SWEPTBACK-WING – FUSELAGE MODEL AT HIGH SUBSONIC SPEEDS

By Alexander D. Hammond

Langley Research Center
Langley Station, Hampton, Va.

NATIONAL AERONAUTICS AND SPACE ADMINISTRATION

NATIONAL AERONAUTICS AND SPACE ADMINISTRATION

TECHNICAL NOTE D-2037

AERODYNAMIC CHARACTERISTICS OF A SPOILER-SLOT-DEFLECTOR CONTROL ON A 45° SWEPTBACK-WING—FUSELAGE MODEL AT HIGH SUBSONIC SPEEDS[1]

By Alexander D. Hammond

SUMMARY

An investigation was made in the Langley high-speed 7- by 10-foot tunnel for a Mach number range from 0.60 to 0.95 to determine the lateral-control and hinge-moment characteristics of a spoiler-slot-deflector configuration on a half model of a 45° sweptback-wing—fuselage combination. The wing had an aspect ratio of 3.5, a taper ratio of 0.3, and NACA 65A005 airfoil sections parallel to the free-stream direction and was equipped with a 65-percent-semispan, 15-percent-wing-chord inboard spoiler-slot-deflector control. The spoiler and deflector were hinged about the 60- and 75-percent wing-chord lines, respectively. The tests were made at angles of attack from -4° to 20° or the angle of attack limited by tunnel power. The tests were made for spoiler projections from zero to 8-percent wing chord, with the deflector at various projections from zero to the projection of the spoiler or to a maximum, which was mechanically limited to 7 percent of the wing chord.

The results of the investigation indicate that a spoiler-slot-deflector configuration having an increasing ratio of deflector projection to spoiler projection with increasing control projection would have good rolling effectiveness and generally low total hinge moments throughout the angle-of-attack and Mach number range of the investigation. Comparison of the results of this investigation with results of another investigation of the same model at supersonic Mach numbers indicates that use of this control linkage would also result in good rolling effectiveness and generally low hinge moments up to the highest Mach number (2.01) of the investigation.

---

[1]Supersedes NASA Technical Memorandum X-205 by Alexander D. Hammond, 1960.

INTRODUCTION

There has been considerable interest shown in spoiler-type lateral controls for high-speed thin-wing configurations. These controls are desirable because of their good effectiveness transonically (ref. 1) and low aeroelastic effects as compared to more conventional trailing-edge ailerons. Recent investigations of spoiler-type controls have shown that the spoiler-slot-deflector has certain advantages over the plain flap-type spoiler, such as lower hinge moments and more effectiveness, particularly at high angles of attack. (For example, see refs. 2 to 8.) As a result of the advantages of spoiler-slot-deflector lateral controls indicated at subsonic and transonic speeds and the interest shown in them, an investigation was made in the Langley 4- by 4-foot supersonic pressure tunnel at Mach numbers of 1.61 and 2.01. The model used in that investigation had an inboard 65-percent-semispan, 15-percent wing-chord spoiler-slot-deflector on a half model of a 45° sweptback-wing—fuselage combination. The results of that investigation are reported in reference 9.

In order to define more completely the effect of Mach number on this configuration, it appeared desirable to obtain lateral-control characteristics at subsonic speeds. It is the purpose of this report, therefore, to present the results of a lateral-control and hinge-moment investigation using the same model as that of reference 9 in the Langley high-speed 7- by 10-foot tunnel. The tests were made for a range of angles of attack from -4° to 20° for spoiler projections from zero to 8-percent wing chord at Mach numbers from 0.60 to 0.95. The deflectors were tested through a projection range from zero to a projection equal to the spoiler at each spoiler projection tested, except that the maximum deflector projection was mechanically limited to a projection of 7-percent wing chord. The angle-of-attack range was limited for the tests at Mach numbers of 0.85 and above because of tunnel power limitations.

COEFFICIENTS AND SYMBOLS

The lift, drag, and pitching-moment coefficients are, of course, presented about the wind axes and the rolling- and yawing-moment coefficients are presented about the model body axes. The origin of the wind axes and the model body axes is on the model root at a longitudinal position corresponding to the quarter chord of the mean aerodynamic chord.

C_L lift coefficient, $\frac{\text{Twice semispan lift}}{qS}$

C_D drag coefficient, $\frac{\text{Twice semispan drag}}{qS}$

C_m pitching-moment coefficient referred to $0.25\bar{c}$, $\frac{\text{Twice semispan pitching moment}}{qS\bar{c}}$

C_l rolling-moment coefficient produced by control, $\frac{\text{Rolling moment}}{qSb}$

C_n yawing-moment coefficient produced by control, $\frac{\text{Yawing moment}}{qSb}$

C_h hinge-moment coefficient about control hinge axis, $\frac{\text{Hinge moment}}{2qQ}$

$C_{h,t}$ total hinge moment, $C_{h,s}\frac{Q_s}{Q_t} + \frac{d\delta_d}{d\delta_s}C_{h,d}\frac{Q_d}{Q_t}$

q free-stream dynamic pressure, lb/sq ft

Q area moment of control about its hinge line, cu ft

S twice area of semispan wing, 2.294 sq ft

c local wing chord, ft

$\bar{c}$ mean aerodynamic chord, $\frac{2}{S}\int_0^{b/2} c^2 dy$, ft

b twice span of half model, 2.833 ft

α angle of attack, deg

M Mach number

δ control projection measured perpendicular to the wing surface (negative for spoiler trailing edge above wing surface and deflector leading edge below wing surface), fraction of wing chord

Subscripts:

s	spoiler
d	deflector
t	total

APPARATUS AND MODEL

The half model of the 45° sweptback-wing—fuselage combination was mounted in the Langley high-speed 7- by 10-foot tunnel in such a manner that the tunnel ceiling served as a reflection plane. A small clearance was maintained between the model and the tunnel ceiling so that no part of the model came in contact with the tunnel structure. A small end plate was attached to the model root to minimize the effects on the flow over the model of air inflow into the tunnel test section through the clearance hole between the model and the tunnel ceiling. The half model was mounted on a five-component strain-gage balance which measured the forces and moments on the model. In addition, the spoiler and deflector were equipped with strain gages to measure moments about the hinge lines of each control. The forces and moments were measured simultaneously with calibrated recording potentiometers.

The geometric characteristics and dimensions of the half model of the sweptback-wing—fuselage combination are shown in figure 1. The wing, fuselage, and controls were made of steel. The wing had 45° sweepback of the quarter-chord line, an aspect ratio of 3.5, a taper ratio of 0.3, and NACA 65A005 airfoil sections parallel to the free stream and had no twist or dihedral. The wing was equipped with an inboard 65-percent-semispan, 15-percent-wing-chord spoiler-slot-deflector (fig. 1). The spoiler and deflector were hinged along the 60-percent and 75-percent wing-chord lines, respectively.

TESTS

All tests were made in the Langley high-speed 7- by 10-foot tunnel. Tests were made through a Mach number range from 0.60 to 0.95 for a range of spoiler projections from zero to 8 percent of the wing chord with a range of deflector projections from zero to a projection equal to that of the spoiler projection at each spoiler projection or to a maximum deflector projection of 7-percent wing chord. Additional tests were made for a spoiler projection of zero for deflector projections from zero to 7 percent of the wing chord. The tests were made through

an angle-of-attack range from -4° to 20° at Mach numbers of 0.60 and 0.80 and to the angles of attack limited by the tunnel power for Mach numbers of 0.85, 0.91, and 0.95. Reynolds numbers based on the wing mean aerodynamic chord varied from about 3.0×10^6 at $M = 0.60$ to about 3.9×10^6 at $M = 0.95$.

CORRECTIONS

Blockage corrections have been applied to the data according to the method of reference 10 to account for the constriction effects of the model on the tunnel free-stream flow. Jet-boundary corrections as determined by the method of reference 11 have been applied to the drag and angle of attack. No reflection-plane corrections have been applied to the rolling-moment data of this investigation because the variation of this correction with Mach number at subsonic and transonic speeds has not been established. The reflection-plane correction at low subsonic speeds, which will decrease the rolling moment, can be determined by the method of reference 12 by using the theoretical span-load distributions resulting from antisymmetric control deflection (ref. 13) and symmetrical control deflection (ref. 14). At supersonic speeds no reflection-plane corrections are required.

RESULTS AND DISCUSSION

The model lift, drag, and pitching-moment characteristics for various spoiler-slot-deflector-control projections for deflector-to-spoiler projection ratios (δ_d/δ_s) of 0, 0.25, 0.50, 0.75, and 1.00 are presented in figures 2 to 6, respectively. The variation of the rolling-moment and yawing-moment characteristics of these model configurations is presented in figures 7 and 8. In figures 9 to 13 the variation of the spoiler and deflector hinge-moment coefficients with deflector projection is presented for various spoiler projections. All of the data in figures 2 to 13 are shown for Mach numbers from 0.60 to 0.95 for the angle-of-attack range from -4° to 20° or for the angle of attack limited by tunnel power.

It should be pointed out that the data presented in figures 2 to 8 were determined from strain-gage-balance readings where both the semispan wing and the half fuselage were mounted on the balance. In contrast, the supersonic data for this model presented in reference 9 were determined from strain-gage-balance readings where the semispan wing was mounted on the balance in the presence of the half fuselage. Because of the differences in model mountings, the longitudinal data of

figures 2 to 6 represent the lift, drag, and pitching-moment characteristics of the semispan wing and the half fuselage; whereas the data of reference 9 represent only the lift, drag, and pitching-moment characteristics of the semispan wing in the presence of the fuselage. However, since the rolling-moment and yawing-moment coefficients of the present report and the rolling-moment coefficients of reference 9 are presented as the increments resulting from control deflection, the rolling-moment data are comparable. Also, since for both investigations the model mounting had no effect on the determination of the control hinge moments, which were measured with strain-gage beams that were separate from the main balance, the control hinge-moment data of this report and of reference 9 are comparable.

Longitudinal Characteristics

The variation of the lift coefficient with angle of attack for the various control configurations (figs. 2 to 6) indicates that a decrease in lift coefficient occurs with an increase in control projection. However, as the ratio of deflector projection to spoiler projection (δ_d/δ_s) is increased, a larger loss in lift coefficient occurs with increase in control projection particularly at the angles of attack near wing stall. For example, at Mach numbers of 0.60 and 0.80 the plain spoiler $(\delta_d/\delta_s = 0)$ shows a small decrease in lift with increase in control projection at 20° angle of attack (figs. 2(a) and 2(b)); whereas, the spoiler-slot-deflector having $\delta_d/\delta_s = 1.00$ shows a much larger decrease in lift with increase in control projection (figs. 6(a) and 6(b)).

The data of figures 2 to 6 indicate that there is an increase in the drag coefficient with either an increase in control projection for a given δ_d/δ_s or with an increase in δ_d/δ_s for a given control projection.

The static longitudinal stability of all of the spoiler-slot-deflector configurations investigated was about the same at a given Mach number (figs. 2 to 6) throughout the control-projection range investigated. However, projection of the spoiler-slot-deflector resulted in a positive increment of pitching-moment coefficient at a given lift coefficient. Increasing the ratio of the deflector projection to spoiler projection at a given spoiler projection generally resulted in a larger positive increment of pitching moment at given lift coefficient.

Rolling-Moment and Yawing-Moment Characteristics

Both the rolling-moment and yawing-moment coefficients generally show an increase with increase in control projection for a given δ_d/δ_s

or with increase in (δ_d/δ_s) at all Mach numbers and angles of attack investigated (figs. 7 and 8). Exceptions occurred, however, in the lower angle-of-attack range where increases in control-projection ratio (δ_d/δ_s) above about 0.5 caused decreases in rolling-moment effectiveness. The increase in rolling- and yawing-moment coefficients resulting from increase in δ_d/δ_s is especially notable at angles of attack near the wing stall. When the results of the trends of the variation of rolling effectiveness with angle of attack, control deflection, and control-projection ratio are considered, the data indicate that a spoiler-slot-deflector configuration having an increasing control-deflection ratio (δ_d/δ_s) with increasing control deflection would have good rolling effectiveness throughout the angle-of-attack and Mach number range investigated. In general, the results shown here for the rolling effectiveness agree with those found for the model investigated in reference 6. Although the magnitude of the rolling effectiveness obtained for the model of this investigation at subsonic speeds is somewhat higher than the magnitude of the rolling effectiveness at supersonic speeds presented in reference 9 for the same model, as would be expected, the trends of the variation of the rolling effectiveness with angle of attack, control projection, and control projection ratio δ_d/δ_s are in general agreement.

Hinge-Moment Characteristics

In general the data of figures 9 to 13 indicate that increasing the spoiler projection at a given deflector projection results in a positive increment in spoiler hinge-moment coefficients for angles of attack below 20°. Increasing the spoiler projection also generally resulted in a positive increment in deflector hinge-moment coefficient except for the higher spoiler projections investigated.

For deflector projections above approximately 3/8 of the spoiler projection, an increase in deflector projection generally resulted in a negative increment in spoiler hinge-moment coefficient. At low angles of attack increasing the deflector projection above approximately 0.005c results in a negative increment in deflector hinge moment.

Increasing the angle of attack up to about 8° had little effect on the spoiler hinge-moment coefficients, and further increase in angle of attack generally results in a decrease in the magnitude of the spoiler hinge-moment coefficient for a given spoiler projection. Increasing the angle of attack had a relatively small effect on the deflector hinge moment at high deflector projections. However, the deflector hinge-moment coefficient for medium and small deflector projections become substantially more positive with increasing angle of attack (figs. 9 to 13).

Increasing the Mach number generally had small effects on the magnitude of the spoiler and deflector hinge-moment coefficients for the Mach number range investigated.

The general trends of the variation of the spoiler and deflector hinge moments with deflector projection presented in figures 9 to 13 are similar to those shown in reference 6 for a spoiler-slot-deflector configuration on a 35° sweptback wing at high subsonic speeds and with the trends obtained for the model of this investigation at supersonic speeds (ref. 9).

Total Hinge-Moment Characteristics

It has been pointed out in both references 6 and 9 that since the hinge-moment coefficients for the spoiler and deflector are of opposite sign, if the spoiler and deflector are properly linked the total hinge moments will be considerably reduced as compared to either the deflector or spoiler hinge moment. The total hinge-moment coefficients $C_{h,t}$ obtained on the model of this investigation at supersonic speeds (ref. 9) show that a linear linkage having a constant $\delta_d/\delta_s = 0.5$ for all control projections results in minimum hinge moments for the control at supersonic speeds. However, at the subsonic Mach numbers of this investigation a linear linkage having a constant $\delta_d/\delta_s = 0.5$ would not result in desirable hinge moments particularly at low control deflections. The data for low control deflections (figs. 9 to 13) at subsonic speeds indicate that the minimum hinge moments would occur for control-projection ratios of less than 0.5 and that the linkage recommended in reference 6 (increasing δ_d/δ_s with increasing control projection) would give generally desirable values of $C_{h,t}$ throughout the subsonic Mach number range investigated. A further analysis of the total hinge moments of reference 9 indicate that while using a linkage having an increasing ratio of δ_d/δ_s with increasing control projection would not result in minimum values of $C_{h,t}$ this linkage would result in generally low values of $C_{h,t}$ at supersonic speeds. It can therefore be concluded that for the model of this investigation if a control linkage having an increasing ratio of δ_d/δ_s with increasing control deflection were used, generally low total hinge moments would result through the Mach number range up to the highest Mach number of the investigation (M = 2.01).

CONCLUSIONS

A wind-tunnel investigation at Mach numbers from 0.60 to 0.95 was made to determine the lateral-control and hinge-moment characteristics of an inboard 65-percent-semispan, 15-percent-chord inboard spoiler-slot-deflector control on a half model of a 45° sweptback-wing—fuselage configuration. The wing had an aspect ratio of 3.5, a taper ratio of 0.3, and NACA 65A005 airfoil sections parallel to the free-stream direction. The spoiler and deflector were hinged about the 60- and 75-percent wing-chord lines, respectively. The tests were made at angles of attack from -4° to 20° or the angle of attack limited by tunnel power. Tests were made for spoiler projections from zero to 8-percent wing chord with the deflector at various projections from zero to the projection of the spoiler or to a projection mechanically limited to 7 percent of the wing chord. The results of the investigation led to the following conclusions:

1. The rolling-moment data indicate that a spoiler-slot-deflector configuration having an increasing ratio of deflector projection to spoiler projection with increasing control projection would have good rolling effectiveness and generally low total hinge moments throughout the angle-of-attack and Mach number range investigated.

2. Comparison of the results of this investigation with the results of another investigation of the same model at supersonic Mach numbers indicates that use of this control linkage would also result in good rolling effectiveness and generally low total hinge moments up to the highest Mach number (2.01) of the investigation.

Langley Research Center,
National Aeronautics and Space Administration,
Langley Field, Va., September 9, 1959.

REFERENCES

1. Lowry, John G.: Data on Spoiler-Type Ailerons. NACA RM L53I24a, 1953.

2. Vogler, Raymond D.: Wind-Tunnel Investigation at High Subsonic Speeds of a Spoiler-Slot-Deflector Combination on an NACA 65A006 Wing With Quarter-Chord Line Swept Back 32.6°. NACA RM L53D17, 1953.

3. Scallion, William I.: Full-Scale Wind-Tunnel Tests of a 35° Swept-Wing Fighter Airplane With a Spoiler-Slot-Deflector Lateral Control System. NACA RM I56D18, 1956.

4. West, F. E., Jr., Whitcomb, Charles F., and Schmeer, James W.: Investigation of Spoiler-Slot-Deflector Ailerons and Other Spoiler Ailerons on a 45° Sweptback-Wing—Fuselage Combination at Mach Numbers From 0.60 to 1.03. NACA RM L56F15, 1956.

5. Hammond, Alexander D.: Low-Speed Investigation of the Lateral-Control Characteristics of a Flap-Type Spoiler and a Spoiler-Slot-Deflector on a 30° Sweptback Wing-Fuselage Model Having an Aspect Ratio of 3, a Taper Ratio of 0.5, and NACA 65A004 Airfoil Section. NACA RM L56F18, 1956.

6. Hammond, Alexander D., and Brown, Albert E.: The Results of an Investigation at High Subsonic Speeds To Determine the Lateral-Control and Hinge-Moment Characteristics of a Spoiler-Slot-Deflector Configuration on a 35° Sweptback Wing. NACA RM L57C20, 1957.

7. Hammond, Alexander D., and Huffman, Jarrett K.: Wind-Tunnel Investigation of the Effect of Aspect Ratio and Chordwise Location on Effectiveness of Spoiler-Slot-Deflector Controls on Thin Untapered Wings at Transonic Speeds. NACA RM L57G08a, 1957.

8. Hammond, Alexander D., and McKinney, Linwood W.: Wind-Tunnel Investigation of the Effect of Sweep and Taper Ratio on Effectiveness of Spoiler-Slot-Deflector Controls on Aspect-Ratio-4 Wings at Transonic Speeds. NACA RM L58E29, 1958.

9. Lord, Douglas R., and Moring, Robert: Aerodynamic Characteristics of a Spoiler-Slot-Deflector Control on a 45° Sweptback Wing at Mach Numbers of 1.61 and 2.01. NACA RM L57E16a, 1957.

10. Herriot, John G.: Blockage Corrections for Three-Dimensional-Flow Closed-Throat Wind Tunnels, With Consideration of the Effect of Compressibility. NACA Rep. 995, 1950. (Supersedes NACA RM A7B28.)

11. Polhamus, Edward C.: Jet-Boundary-Induced-Upwash Velocities for Swept Reflection-Plane Models Mounted Vertically in 7- by 10-Foot, Closed, Rectangular Wind Tunnels. NACA TN 1752, 1948.

12. Swanson, Robert S., and Toll, Thomas A.: Jet-Boundary Corrections for Reflection-Plane Models in Rectangular Wind Tunnels. NACA Rep. 770, 1943. (Supersedes NACA WR L-458.)

13. DeYoung, John: Theoretical Antisymmetric Span Loading for Wings of Arbitrary Plan Form at Subsonic Speeds. NACA Rep. 1056, 1951. (Supersedes NACA TN 2140.)

14. DeYoung, John: Theoretical Symmetric Span Loading Due to Flap Deflection for Wings of Arbitrary Plan Form at Subsonic Speeds. NACA Rep. 1071, 1952. (Supersedes NACA TN 2278.)

Wing data:

Area (twice area of semispan), sq ft	2.294
Aspect ratio	3.500
Taper ratio	0.300
Mean aerodynamic chord, ft	0.888
Airfoil section (parallel to plane of symmetry)	NACA 65A005

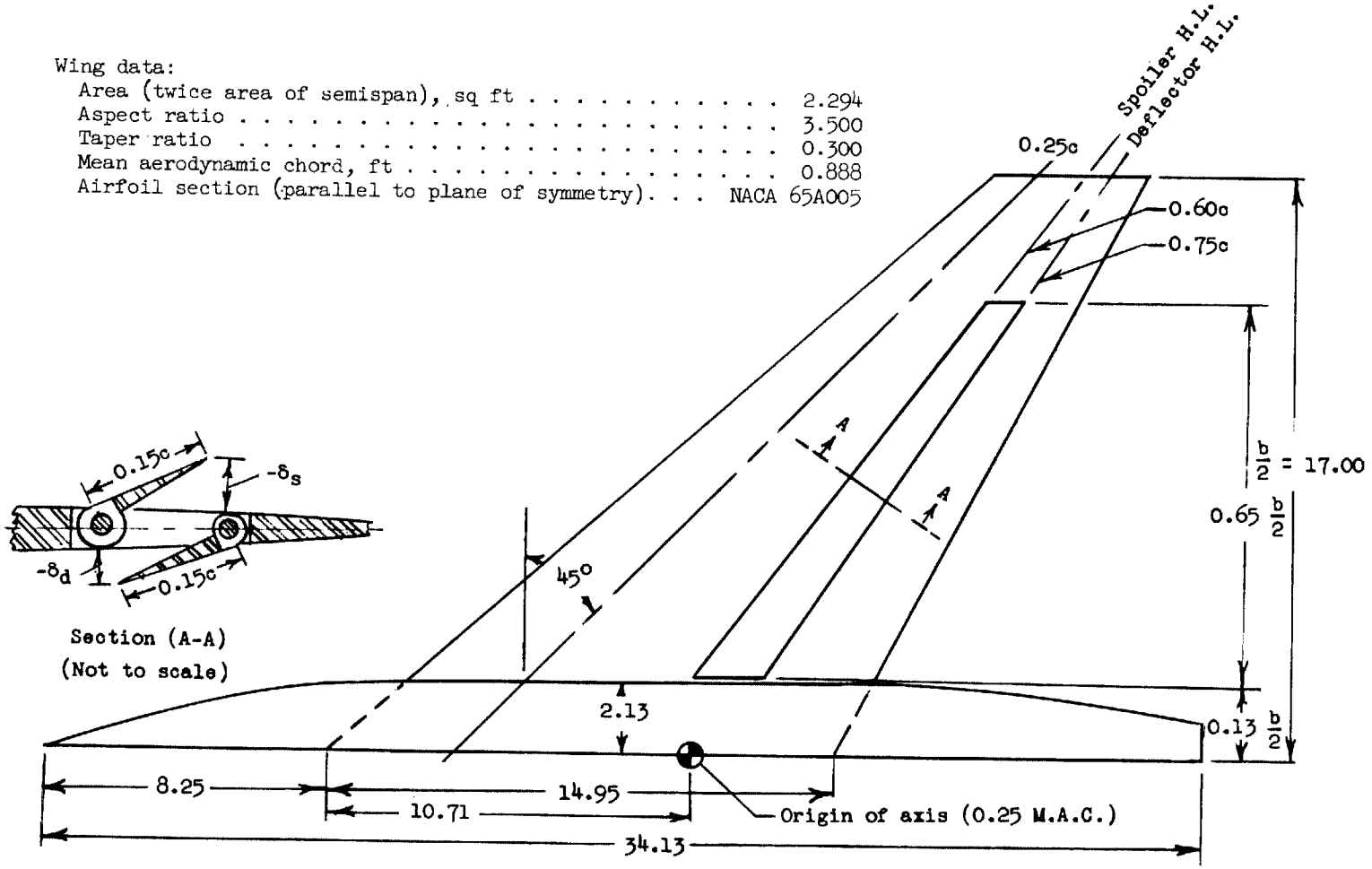

Figure 1.- Geometric characteristics of 45° sweptback-wing—fuselage model equipped with a spoiler-slot-deflector. All dimensions are in inches unless otherwise noted.

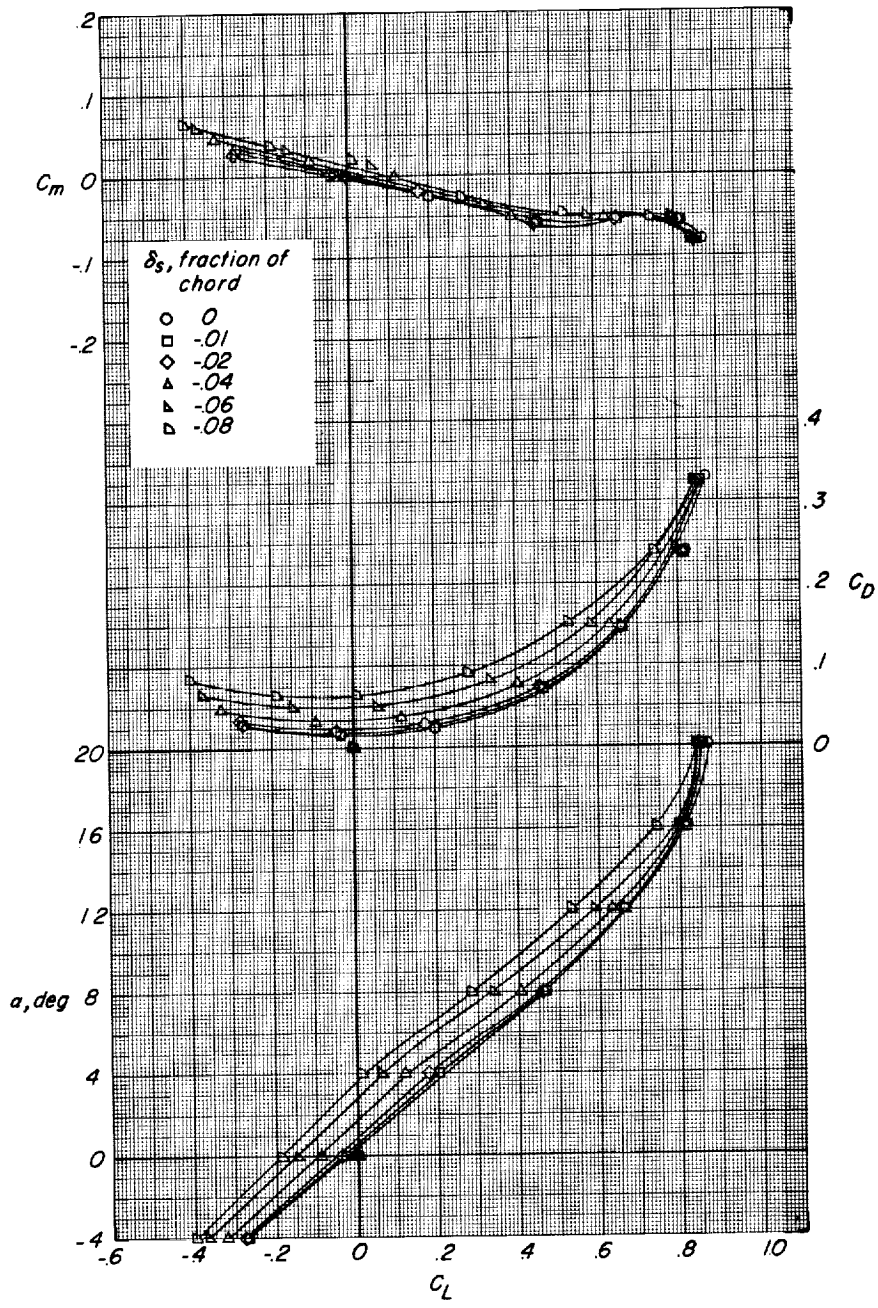

(a) M = 0.60.

Figure 2.- Variation of the longitudinal aerodynamic characteristics of the 45° sweptback wing equipped with a plain spoiler configuration ($\delta_d/\delta_s = 0$).

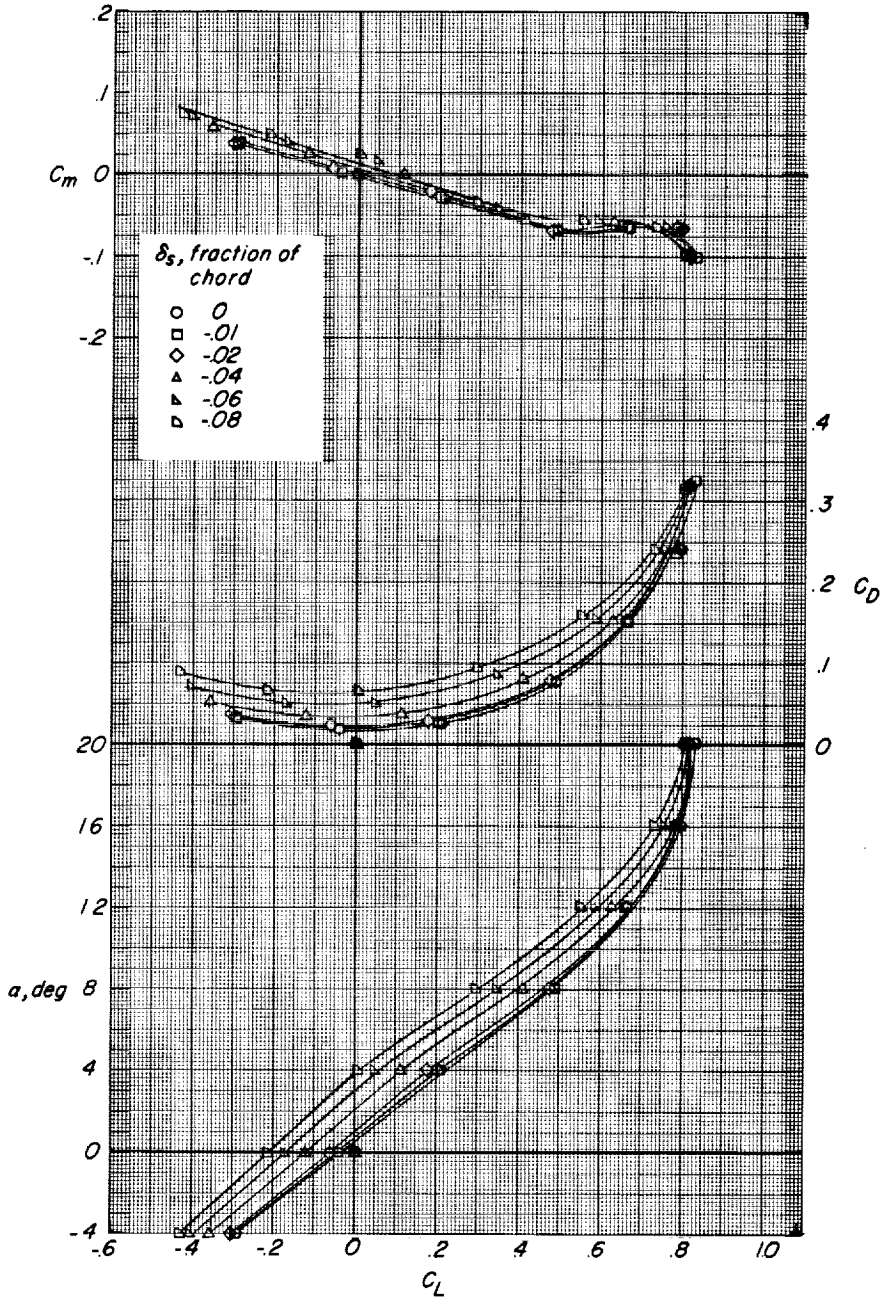

(b) M = 0.80.

Figure 2.- Continued.

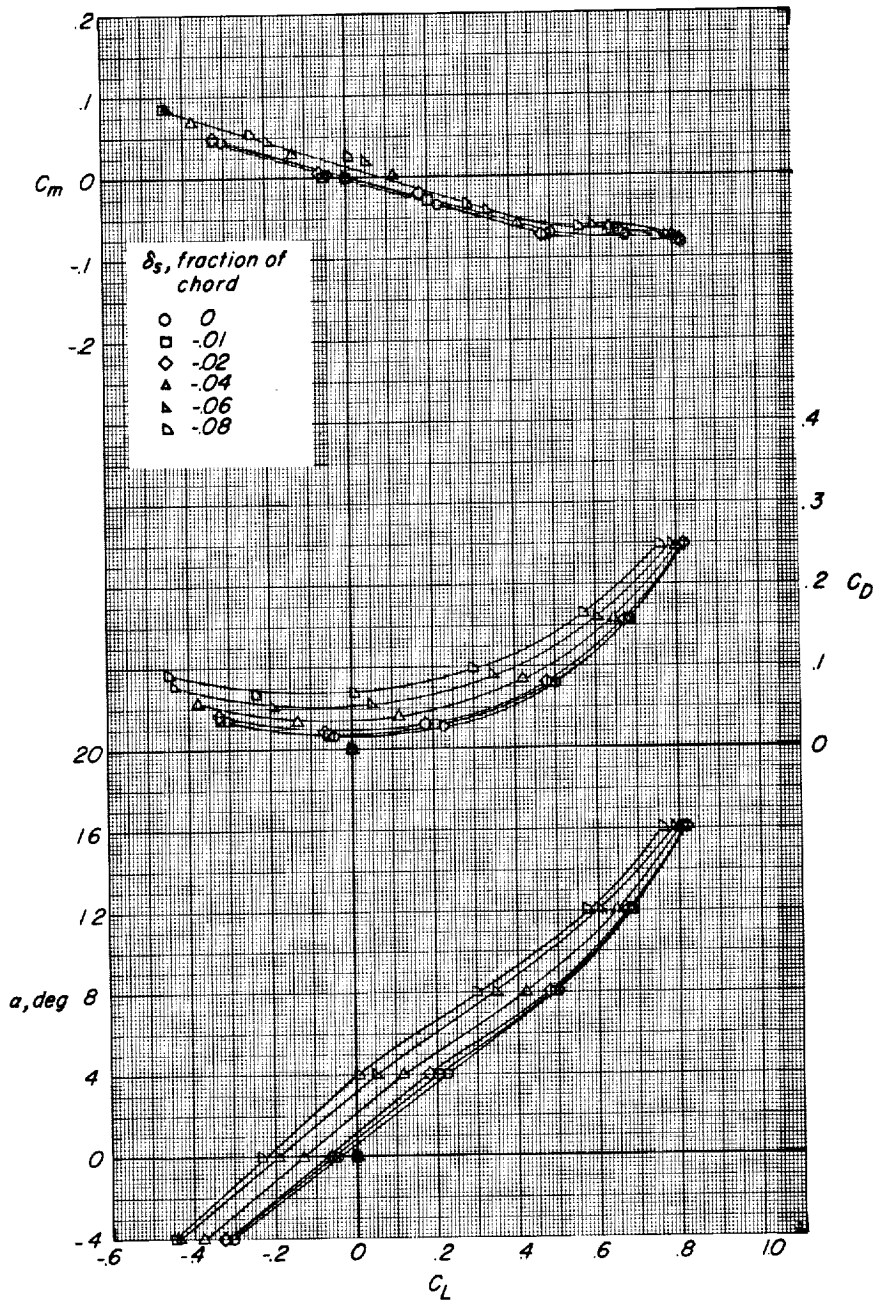

(c) M = 0.85.

Figure 2.- Continued.

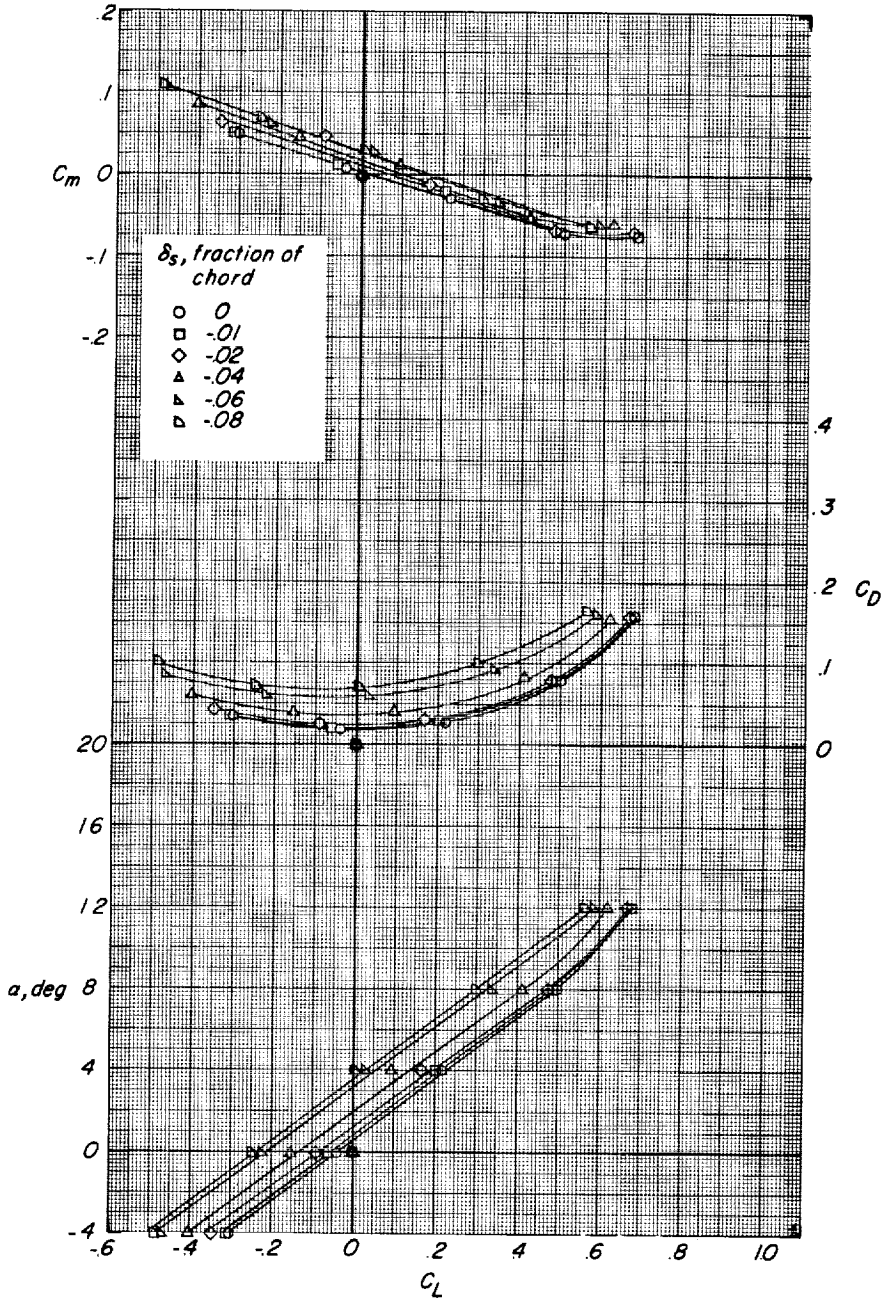

(d) M = 0.91.

Figure 2.- Continued.

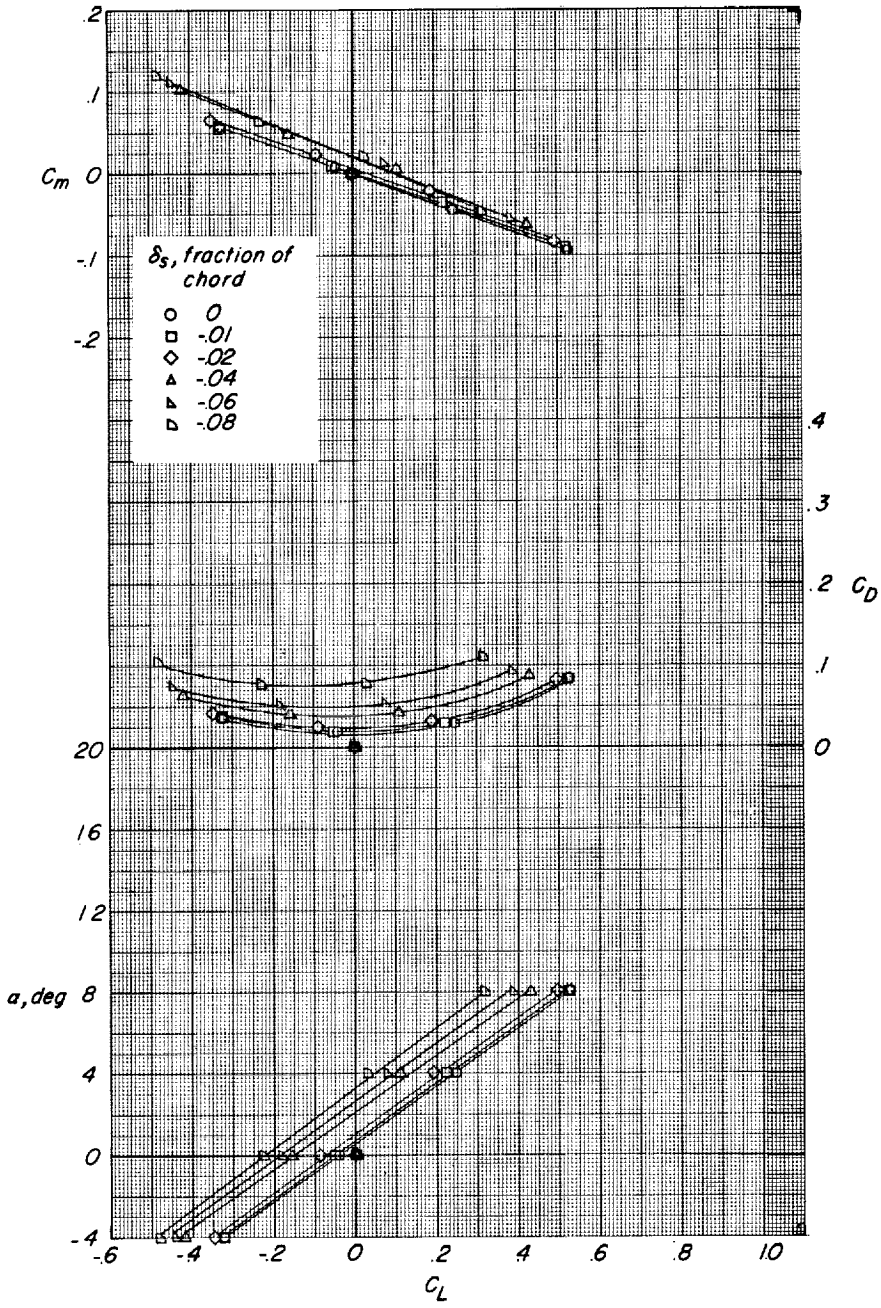

(e) M = 0.95.

Figure 2.- Concluded.

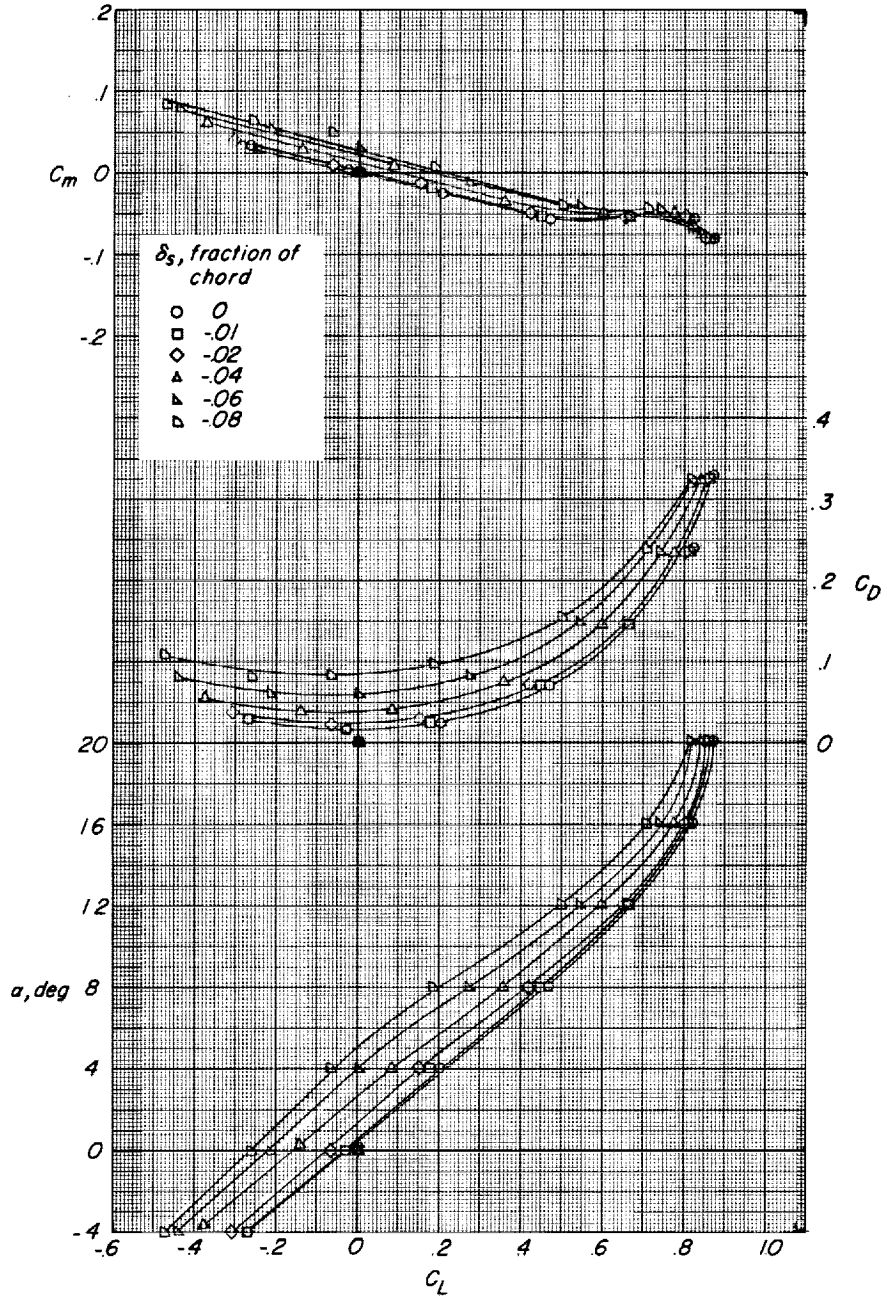

(a) M = 0.60.

Figure 3.- Variation of the longitudinal aerodynamic characteristics of the 45° sweptback wing equipped with a spoiler-slot-deflector configuration having a deflector-to-spoiler projection ratio (δ_d/δ_s) of 0.25.

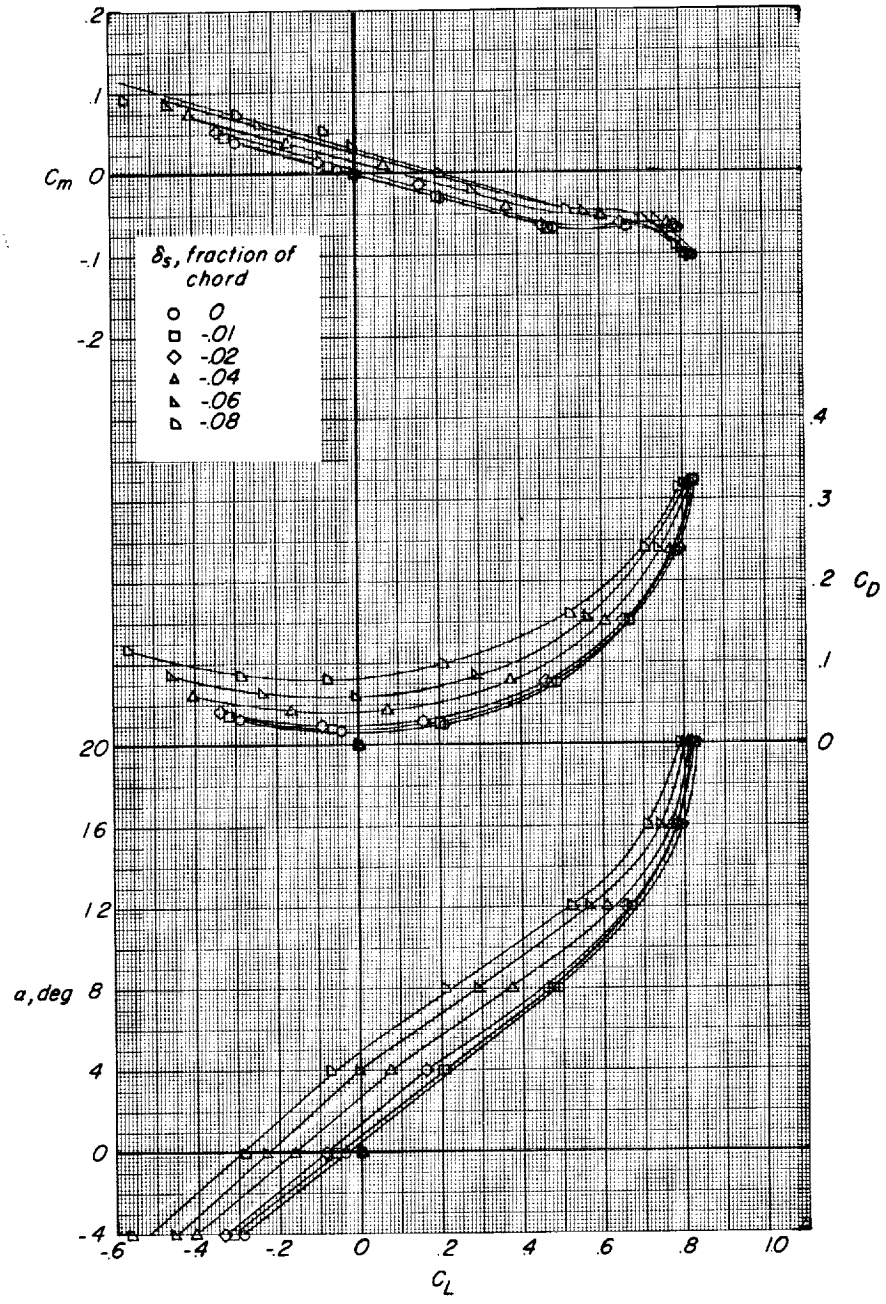

(b) M = 0.80.

Figure 3.- Continued.

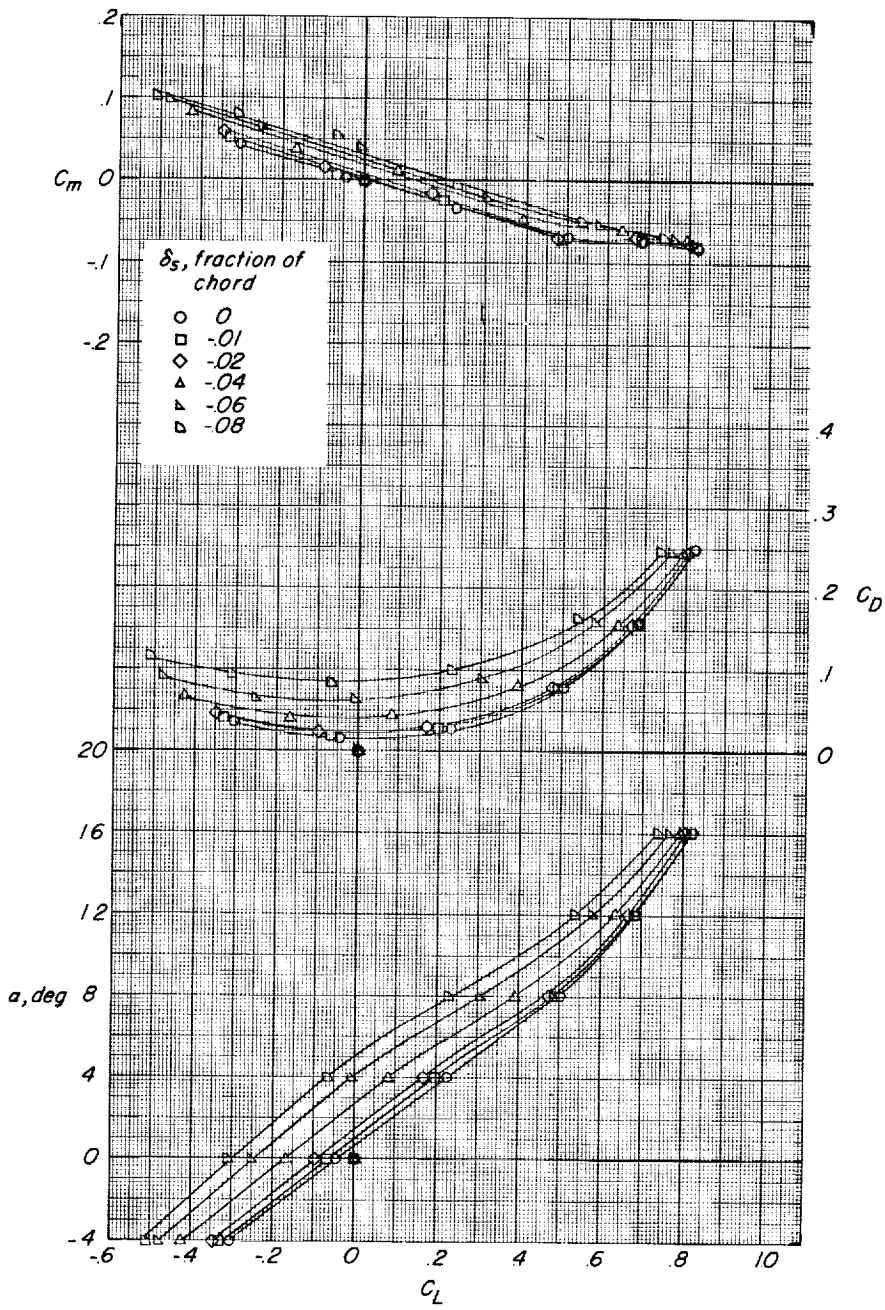

(c) M = 0.85.

Figure 3.- Continued.

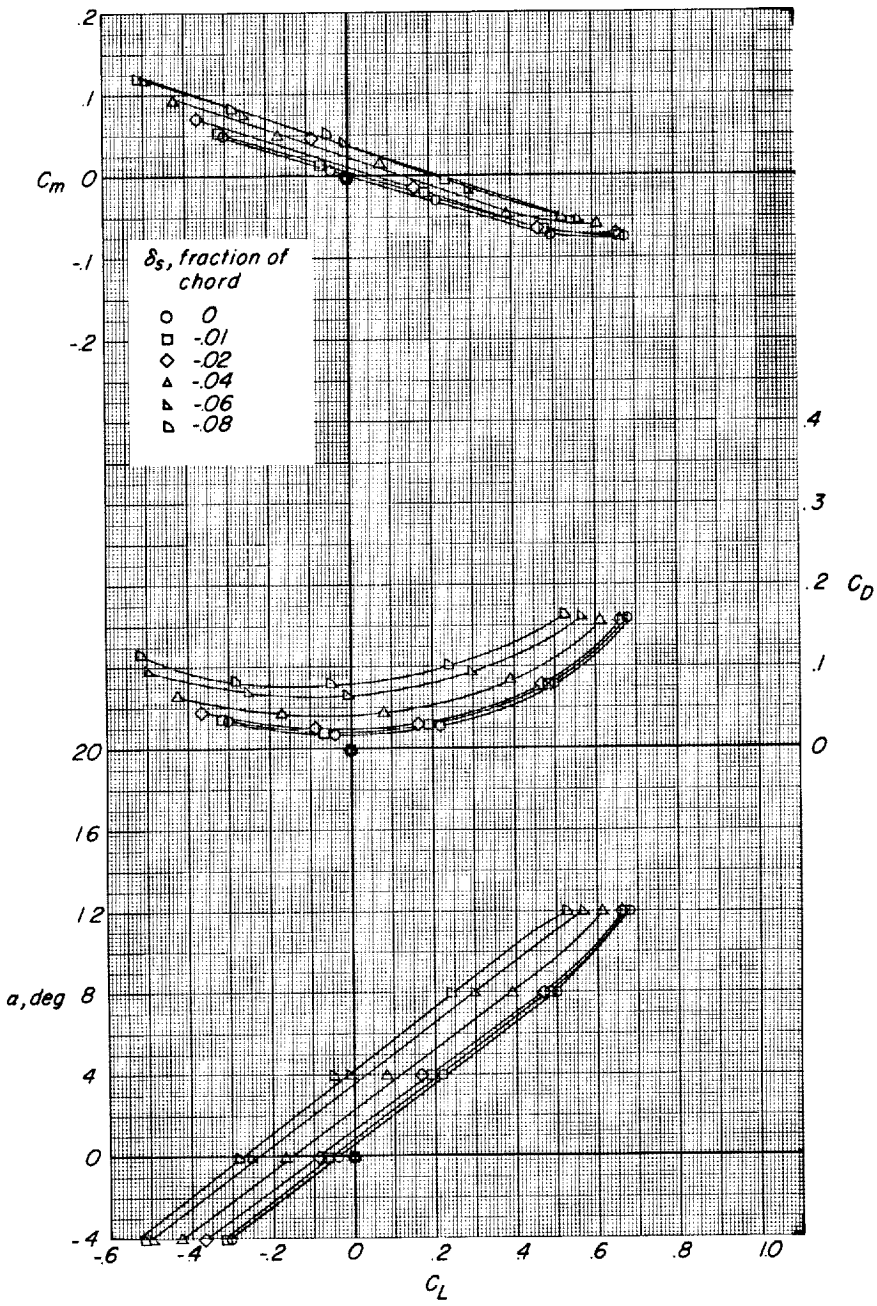

(d) M = 0.91.

Figure 3.- Continued.

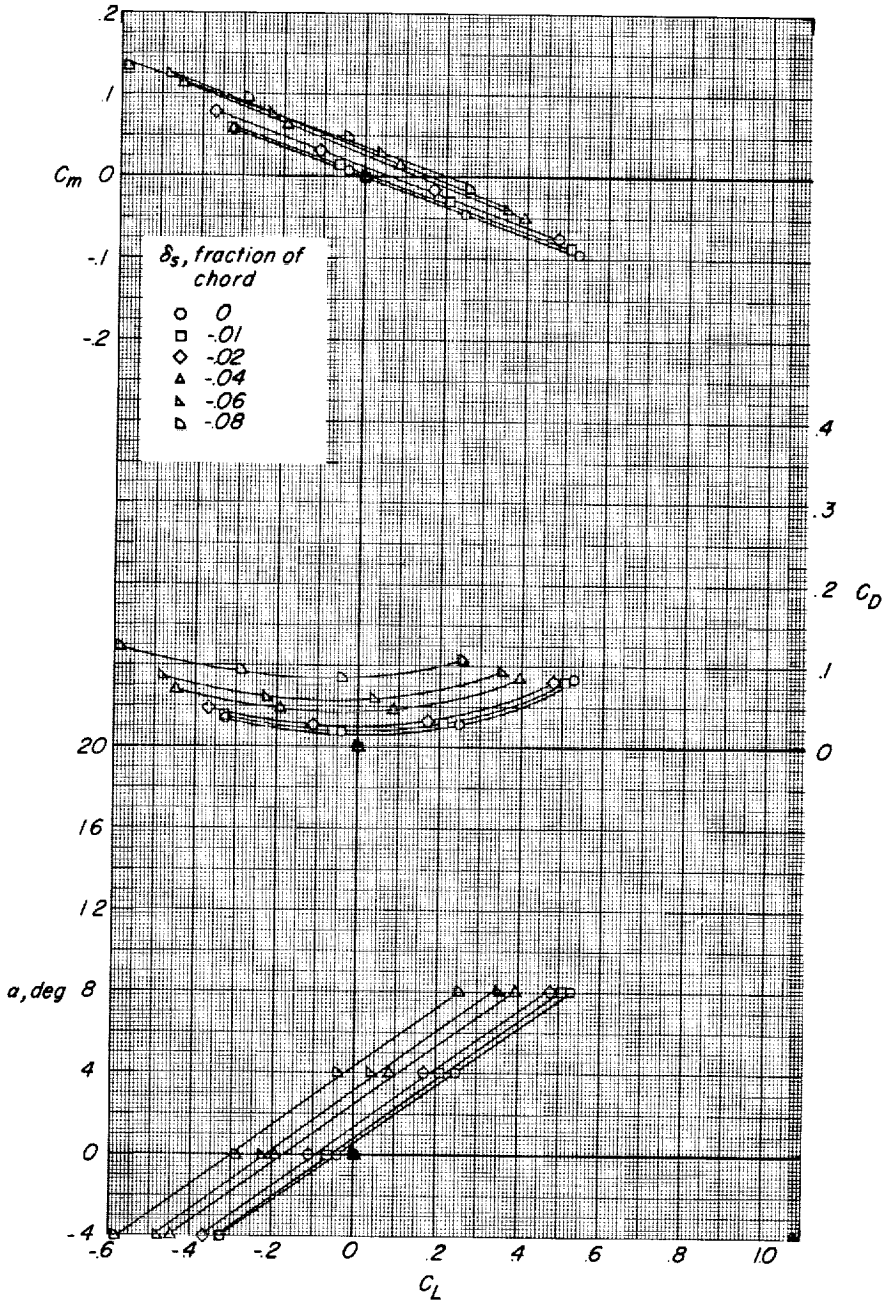

(e) M = 0.95.

Figure 3.- Concluded.

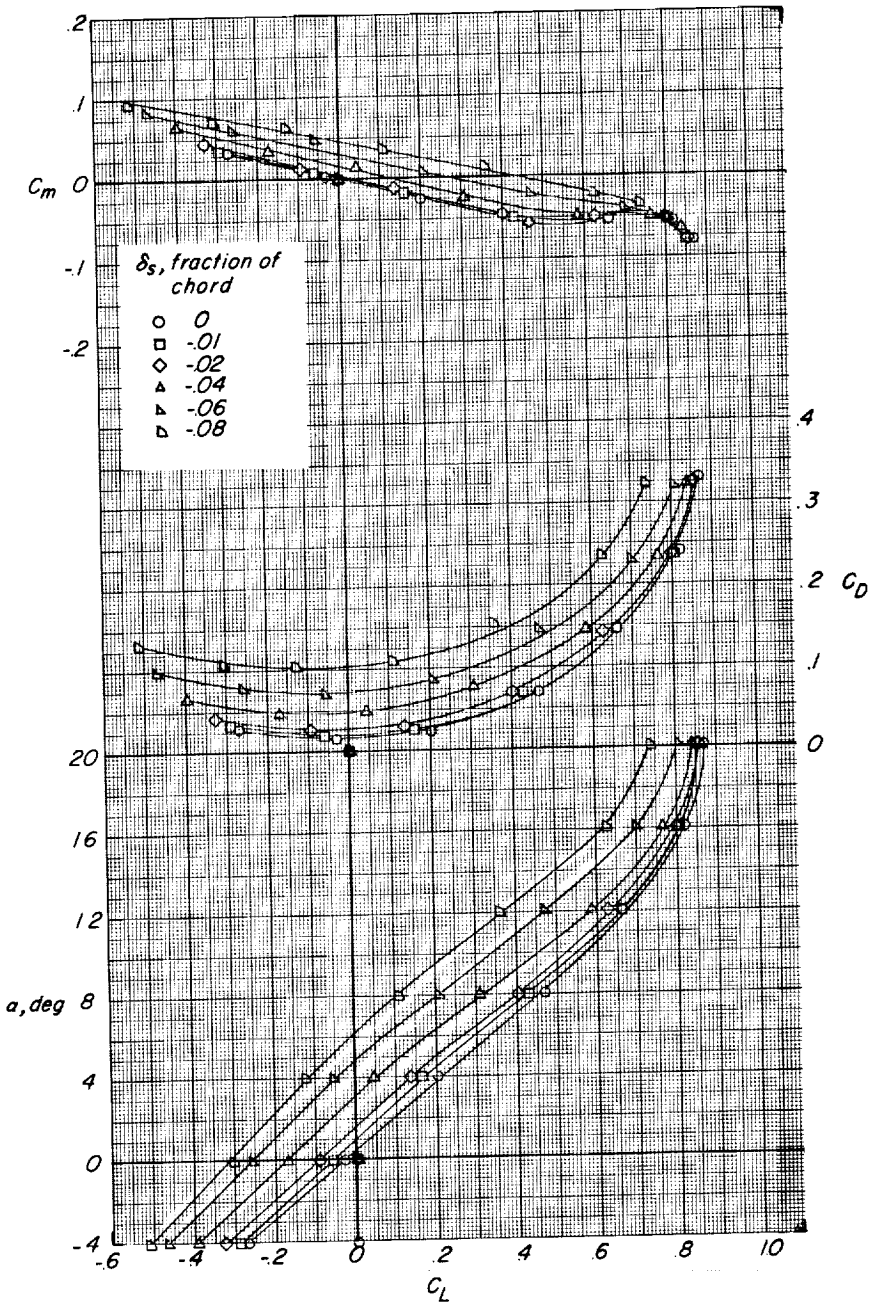

(a) M = 0.60.

Figure 4.- Variation of the longitudinal aerodynamic characteristics of the 45° sweptback wing equipped with a spoiler-slot-deflector configuration having a deflector-to-spoiler projection ratio (δ_d/δ_s) of 0.50.

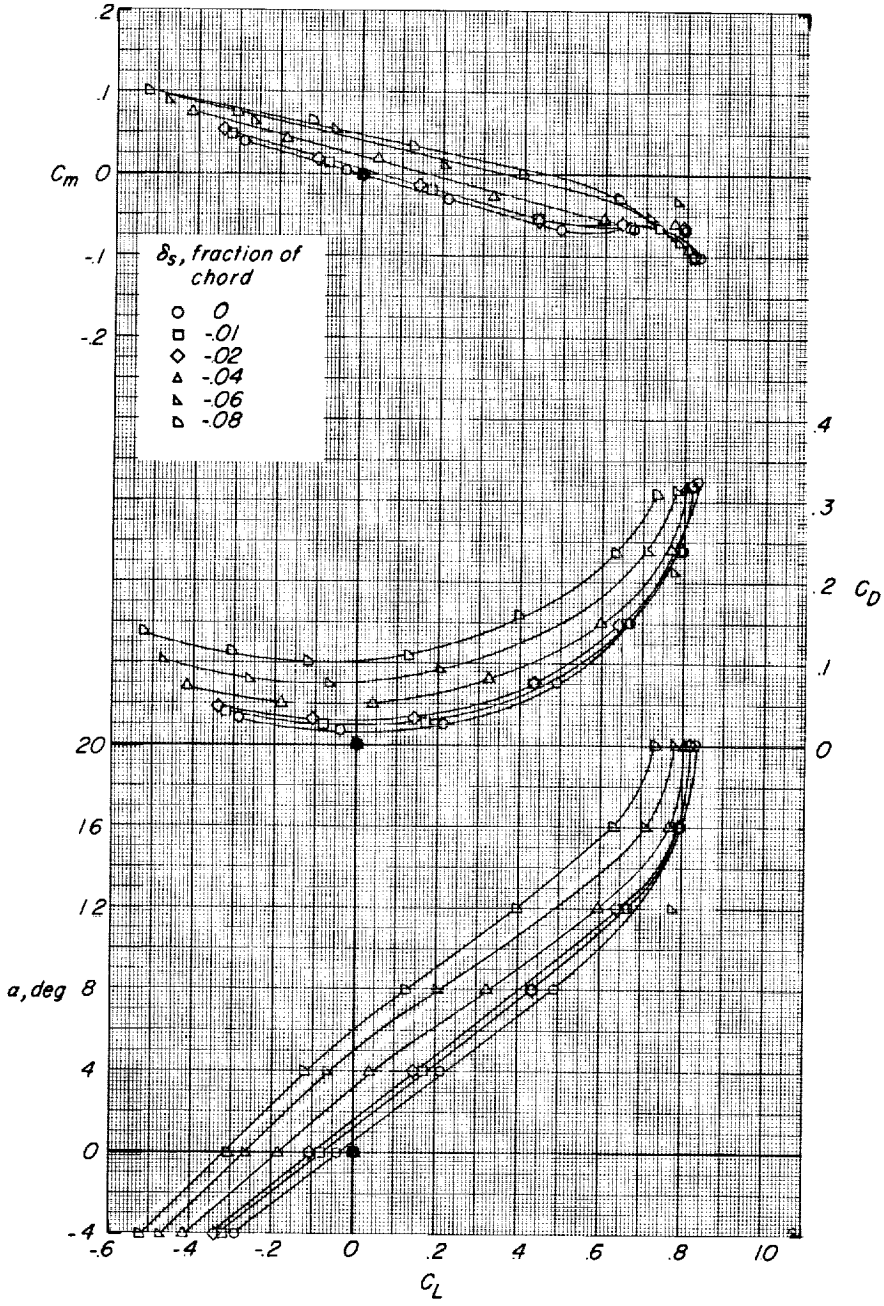

(b) M = 0.80.

Figure 4.- Continued.

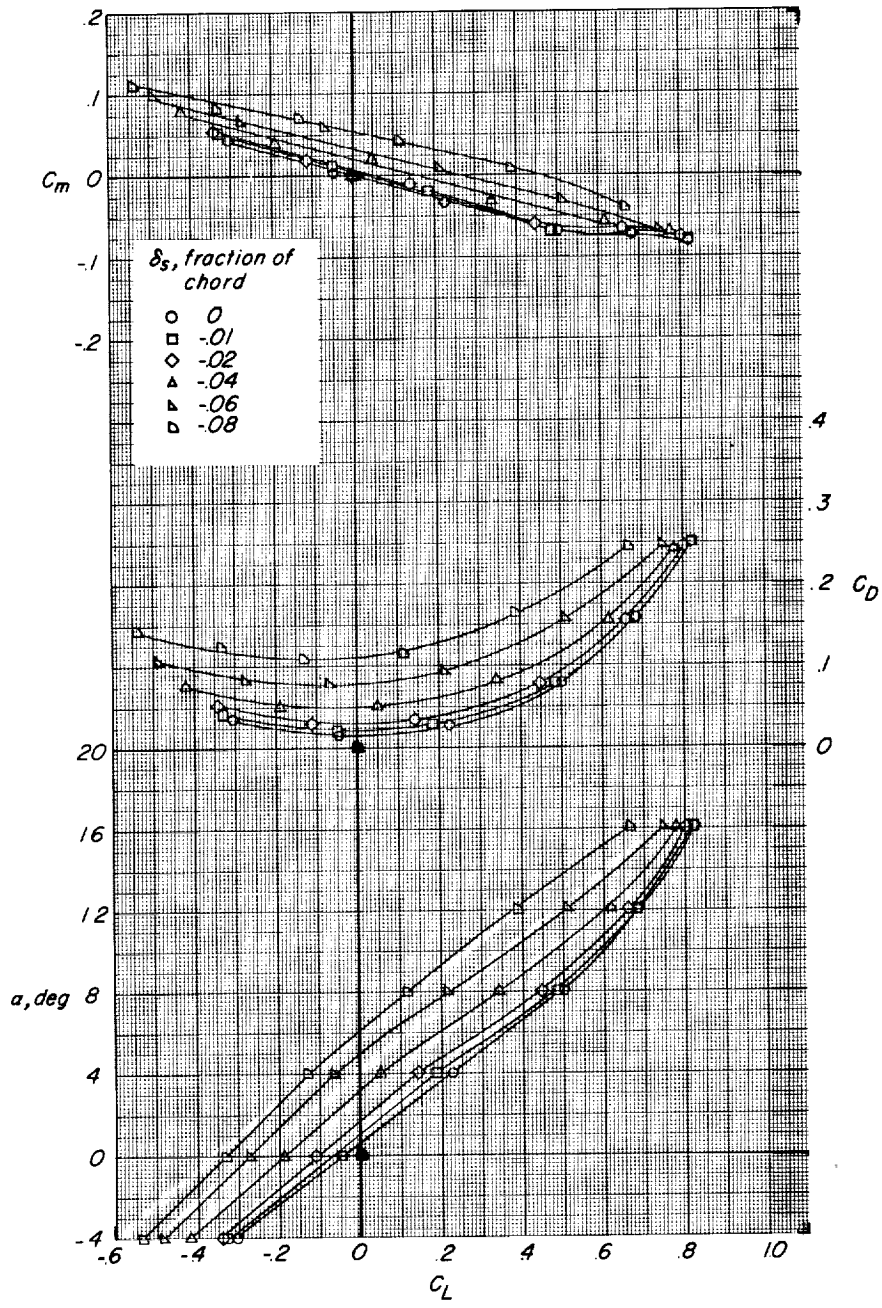

(c) M = 0.85.

Figure 4.- Continued.

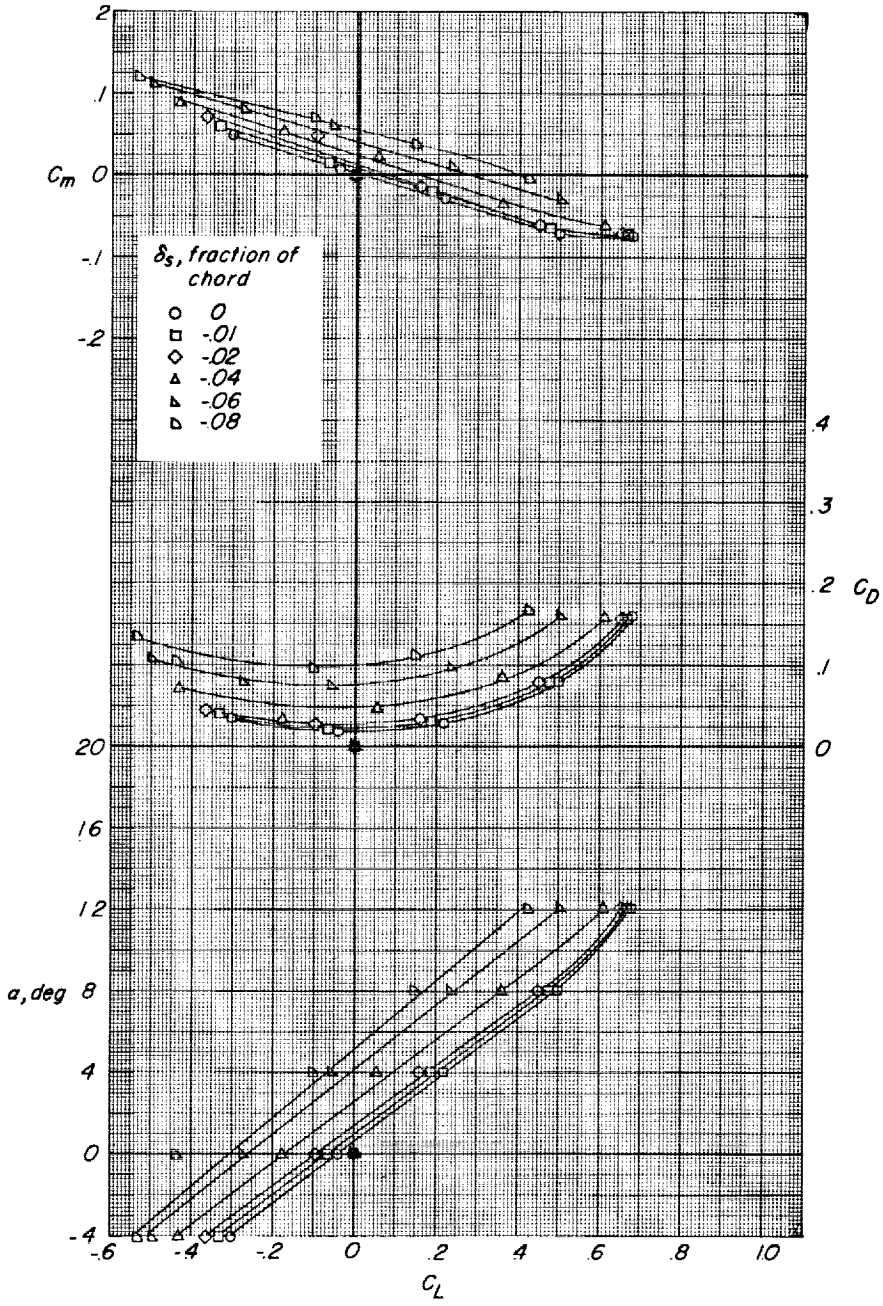

(d) M = 0.91.

Figure 4.- Continued.

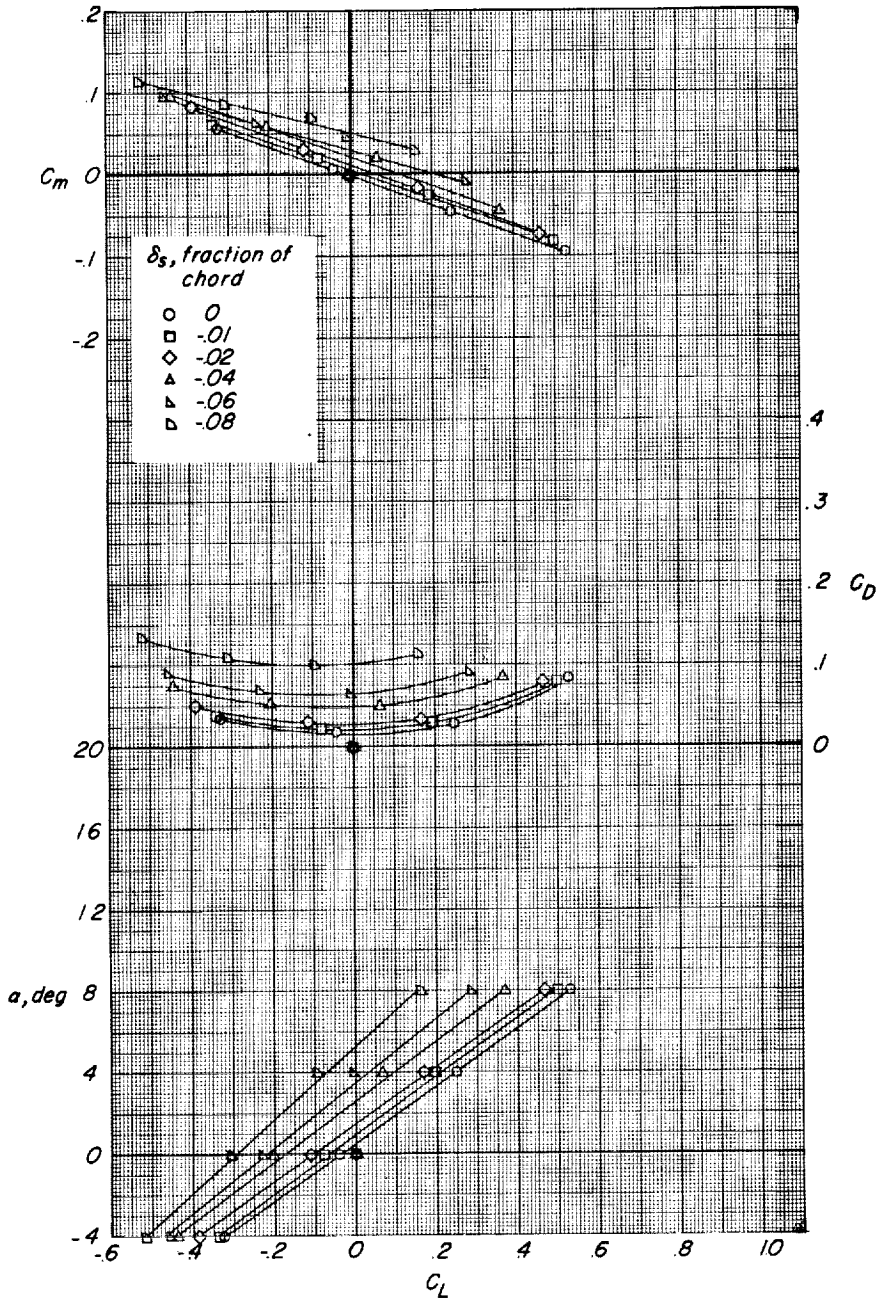

(e) M = 0.95.

Figure 4.- Concluded.

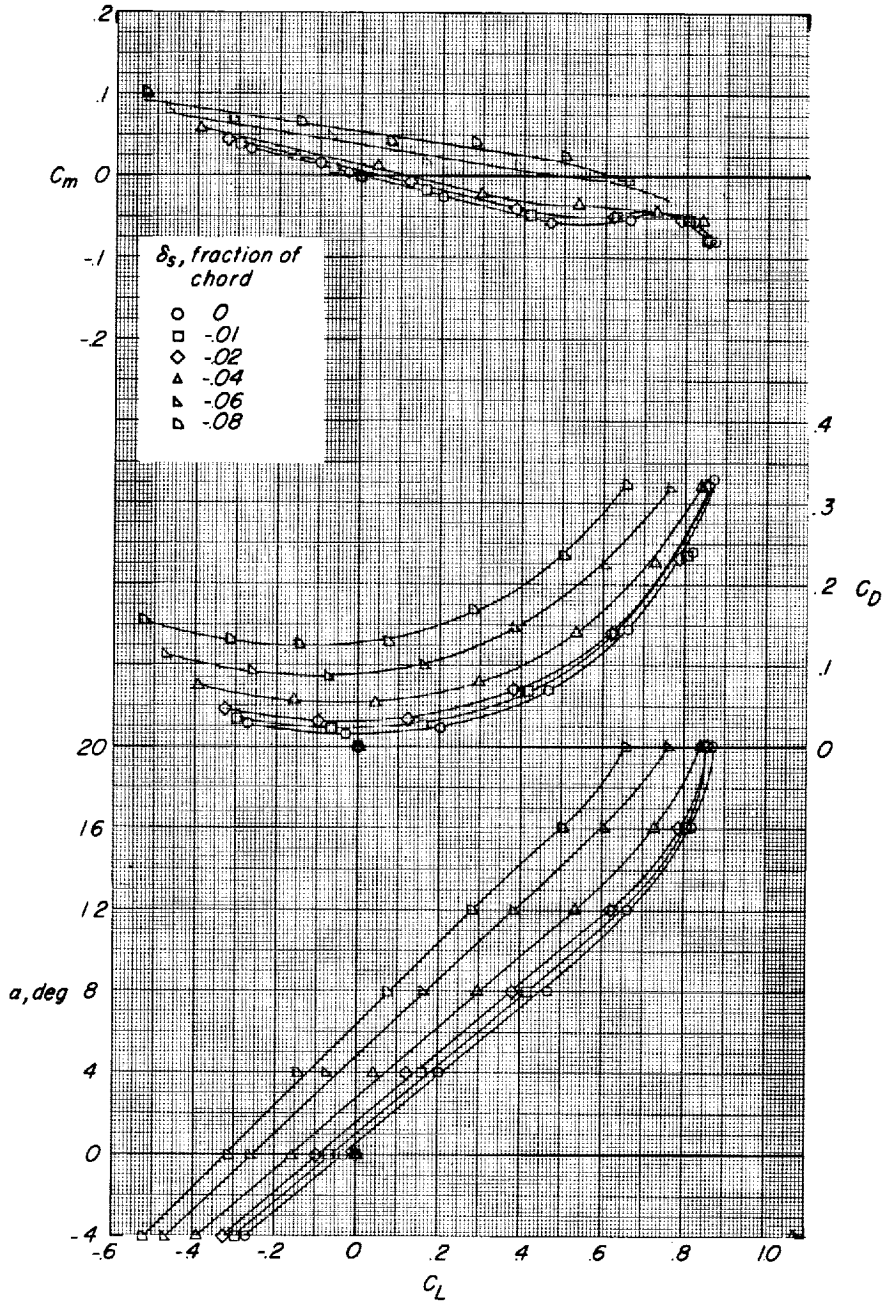

(a) M = 0.60.

Figure 5.- Variation of the longitudinal aerodynamic characteristics of the 45° sweptback wing equipped with a spoiler-slot-deflector configuration having a deflector-to-spoiler projection ratio (δ_d/δ_s) of 0.75.

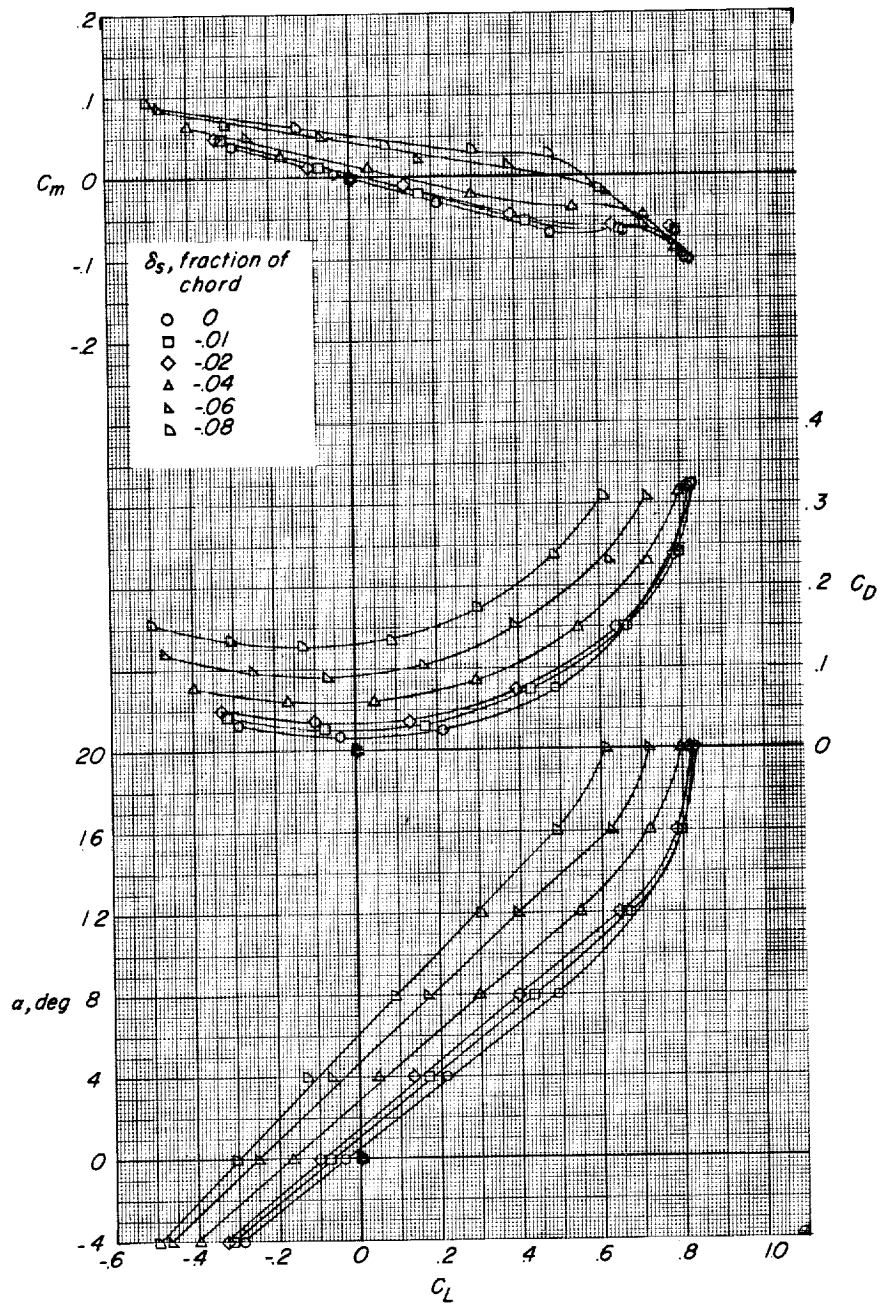

(b) M = 0.80.

Figure 5.- Continued.

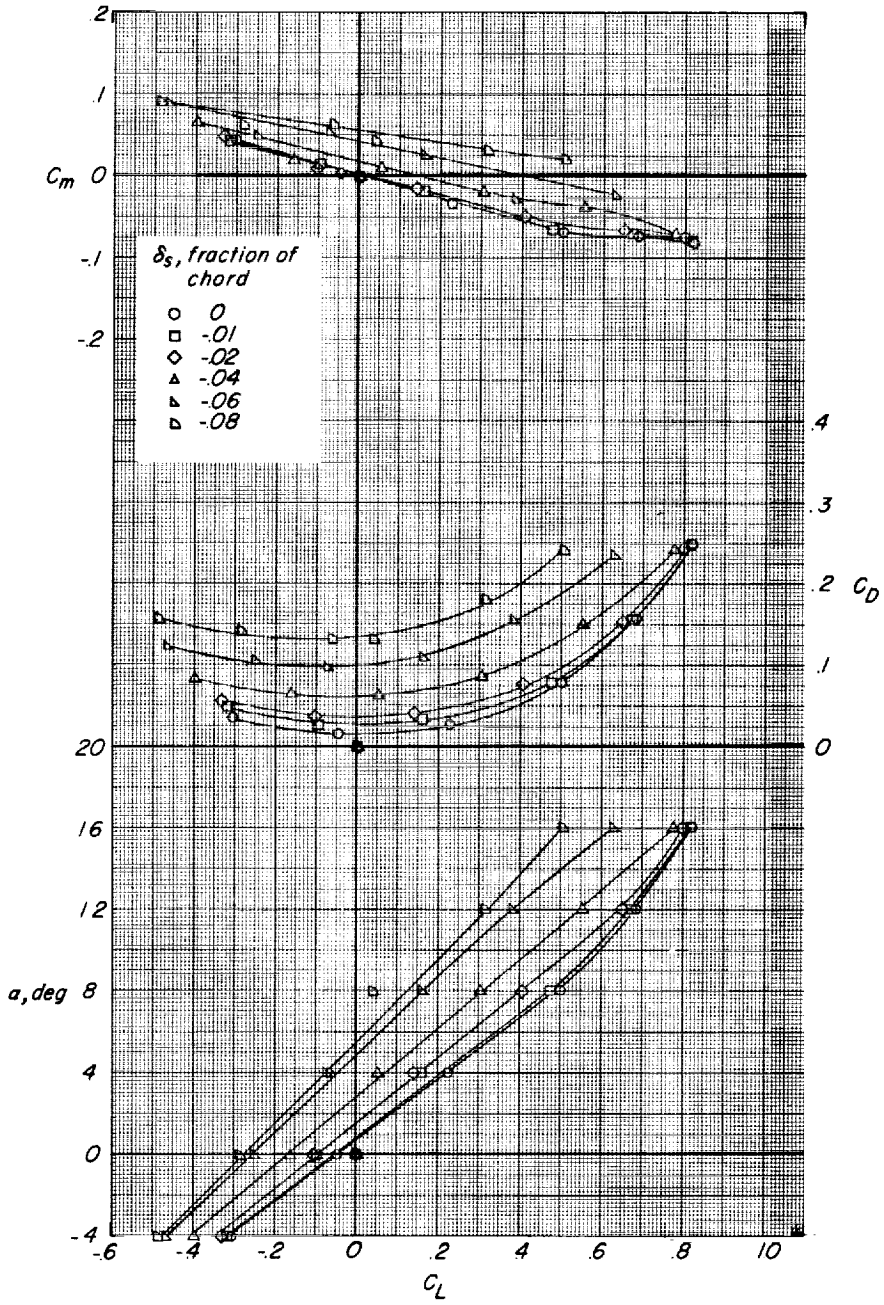

(c) M = 0.85.

Figure 5.- Continued.

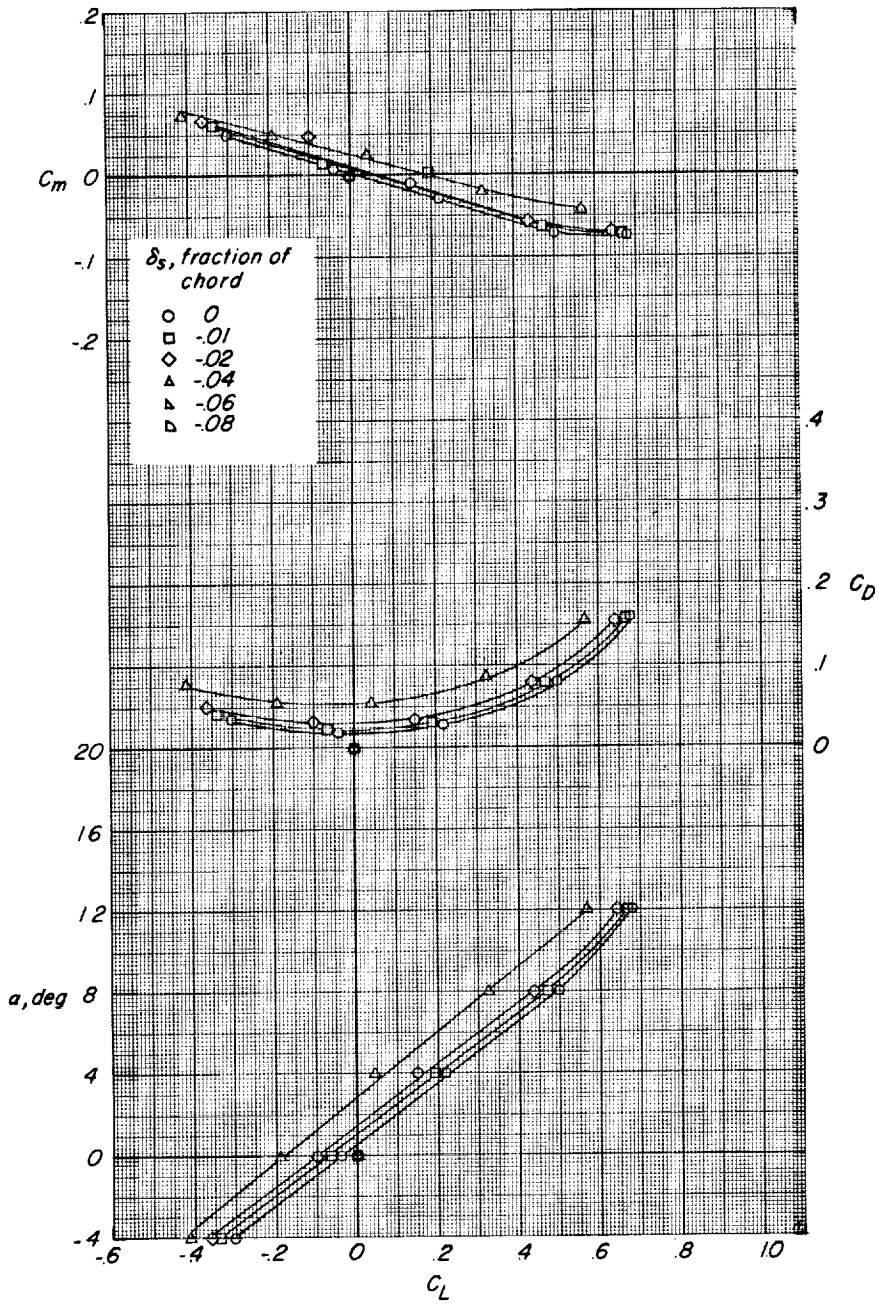

(d) M = 0.91.

Figure 5.- Continued.

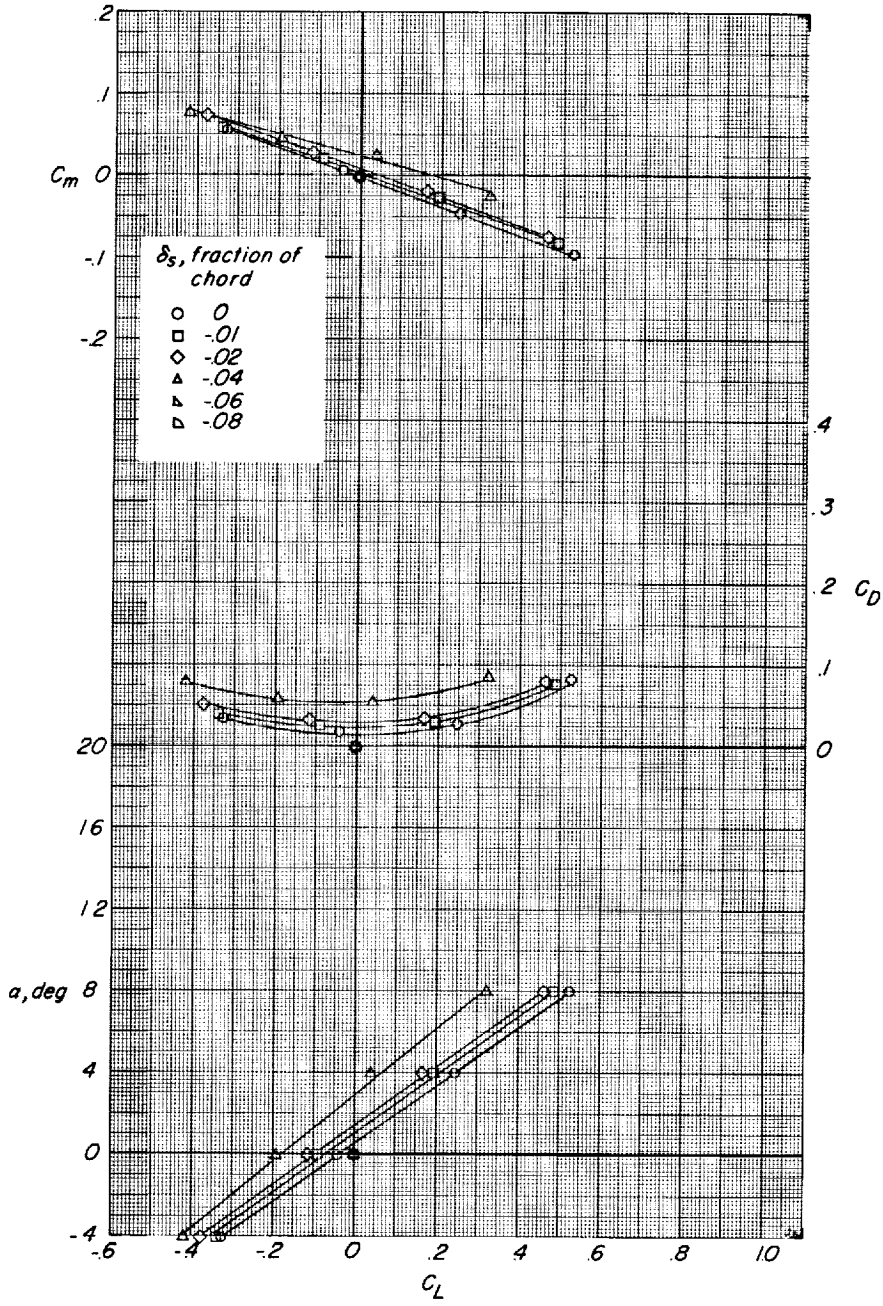

(e) M = 0.95.

Figure 5.- Concluded.

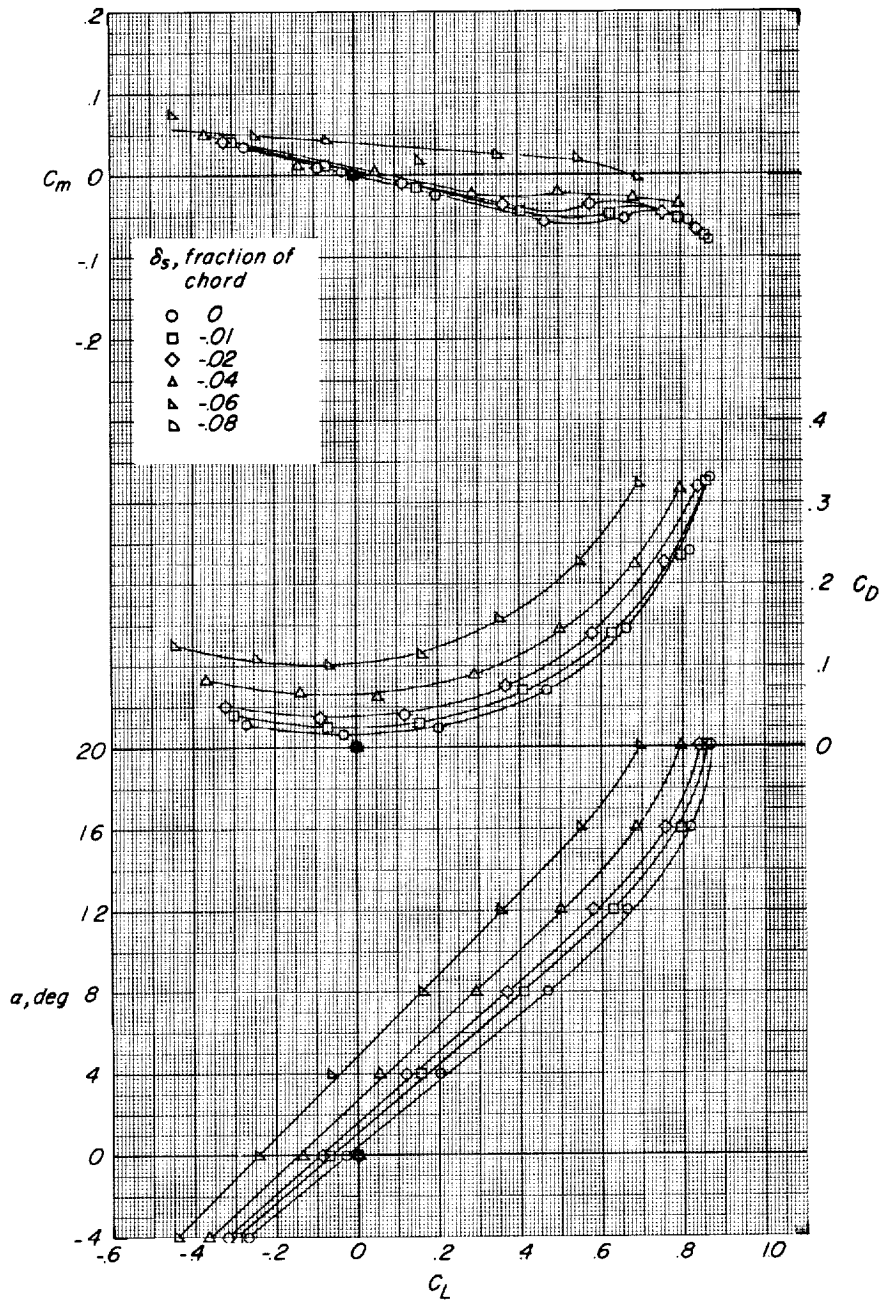

(a) M = 0.60.

Figure 6.- Variation of the longitudinal aerodynamic characteristics of the 45° sweptback wing equipped with a spoiler-slot-deflector configuration having a deflector-to-spoiler projection ratio (δ_d/δ_s) of 1.00.

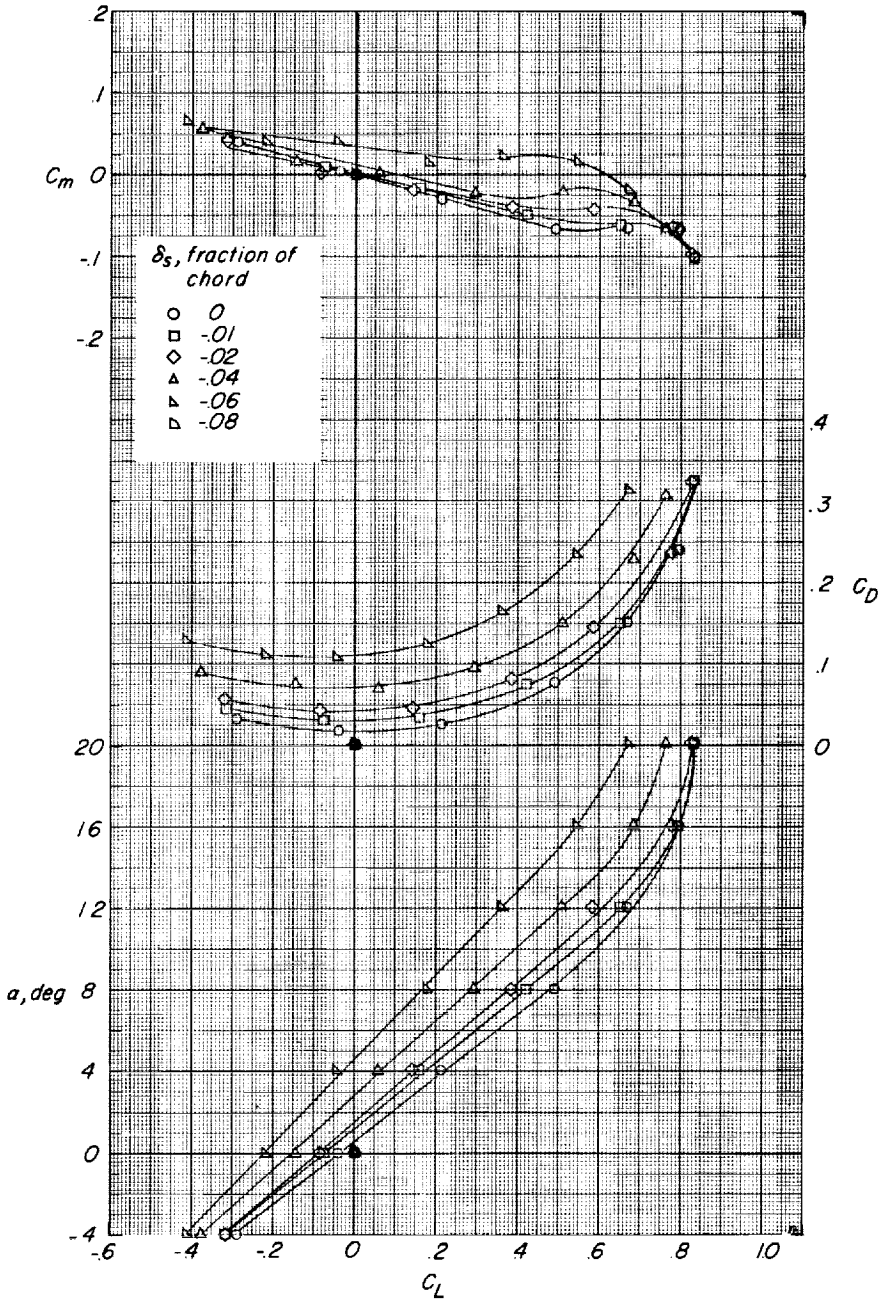

(b) M = 0.80.

Figure 6.- Continued.

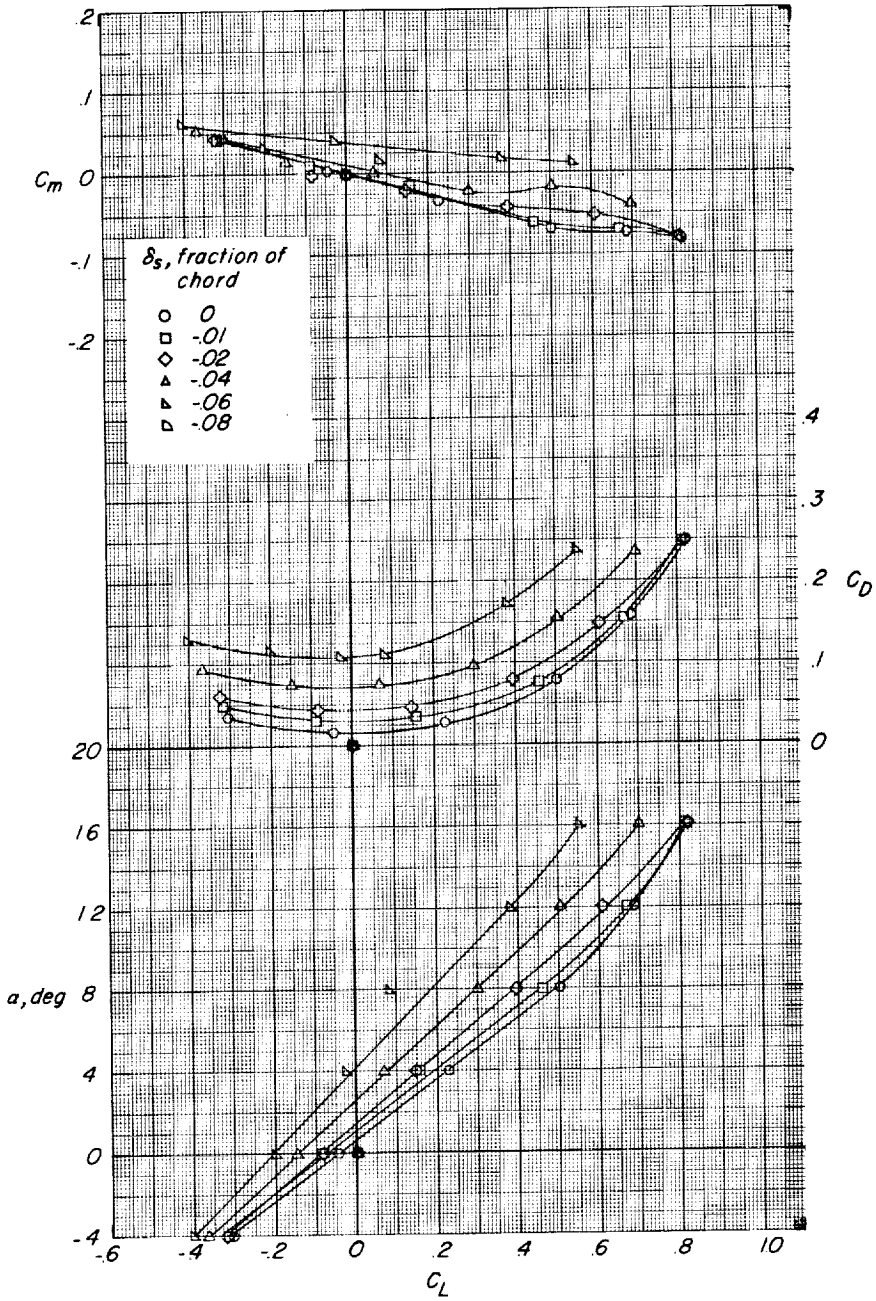

(c) M = 0.85.

Figure 6.- Continued.

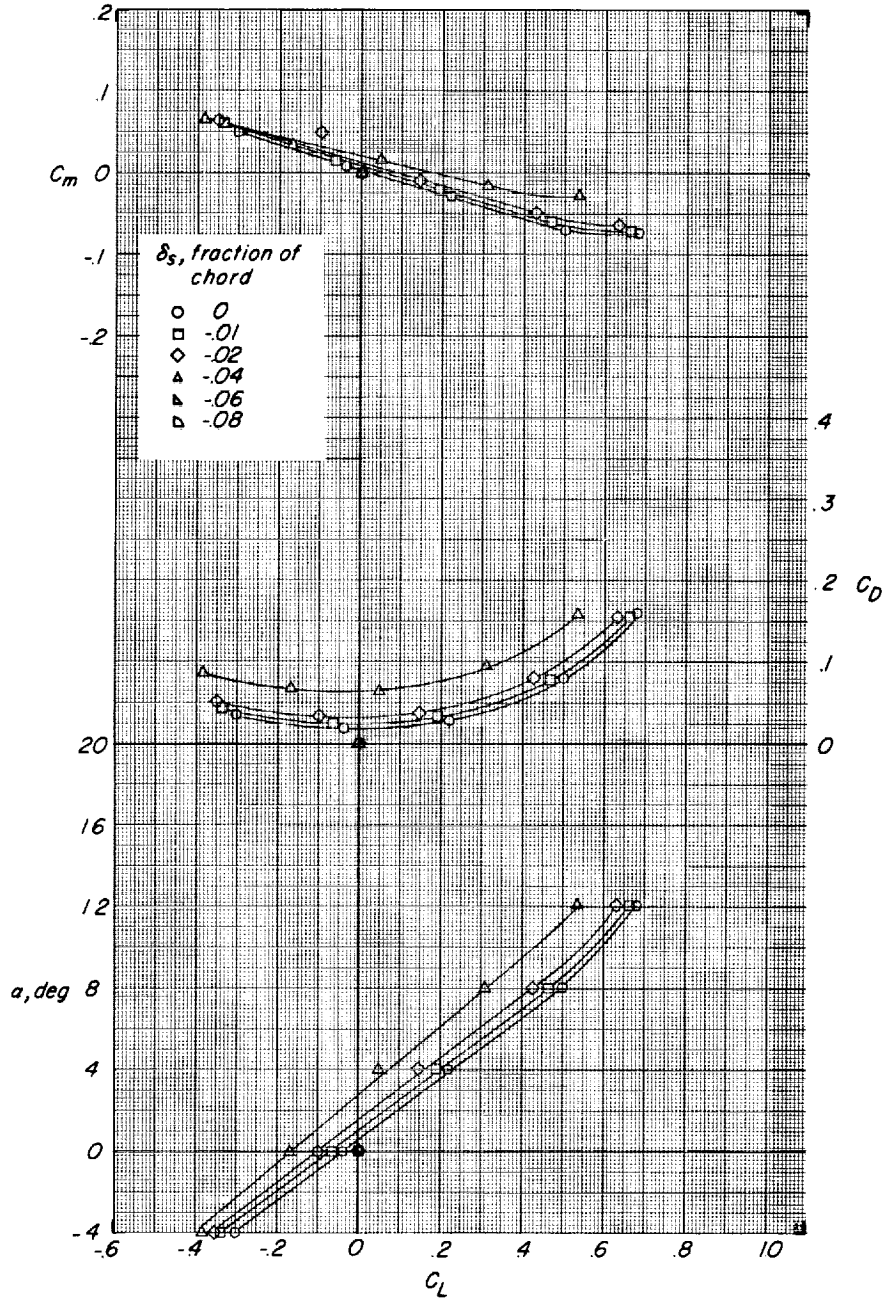

(d) M = 0.91.

Figure 6.- Continued.

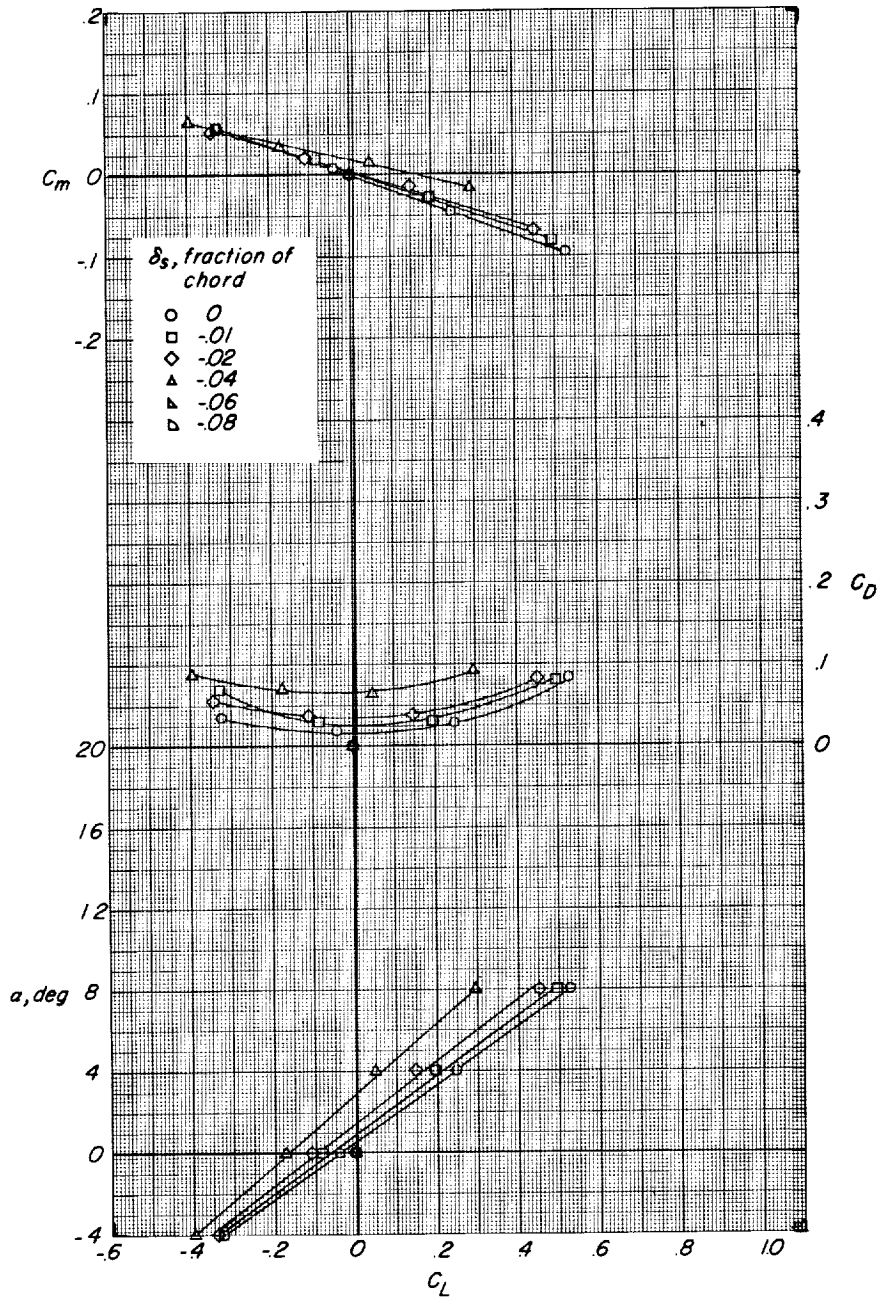

(e) M = 0.95.

Figure 6.- Concluded.

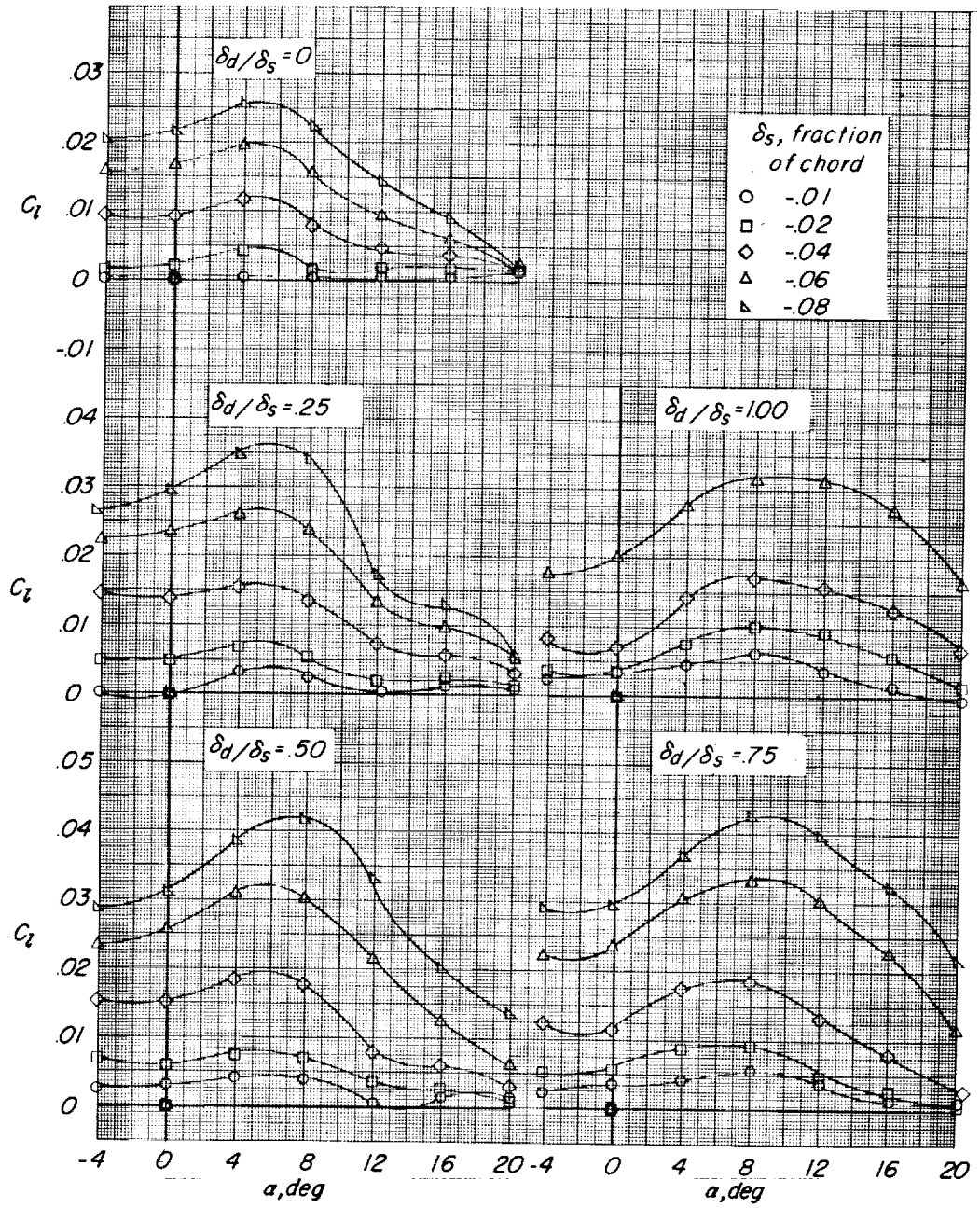

(a) M = 0.60.

Figure 7.- Variation of the rolling-moment coefficients with angle of attack for the 45° sweptback wing equipped with spoiler-slot-deflector configurations having deflector-to-spoiler projection ratios (δ_d/δ_s) of 0 to 1.0.

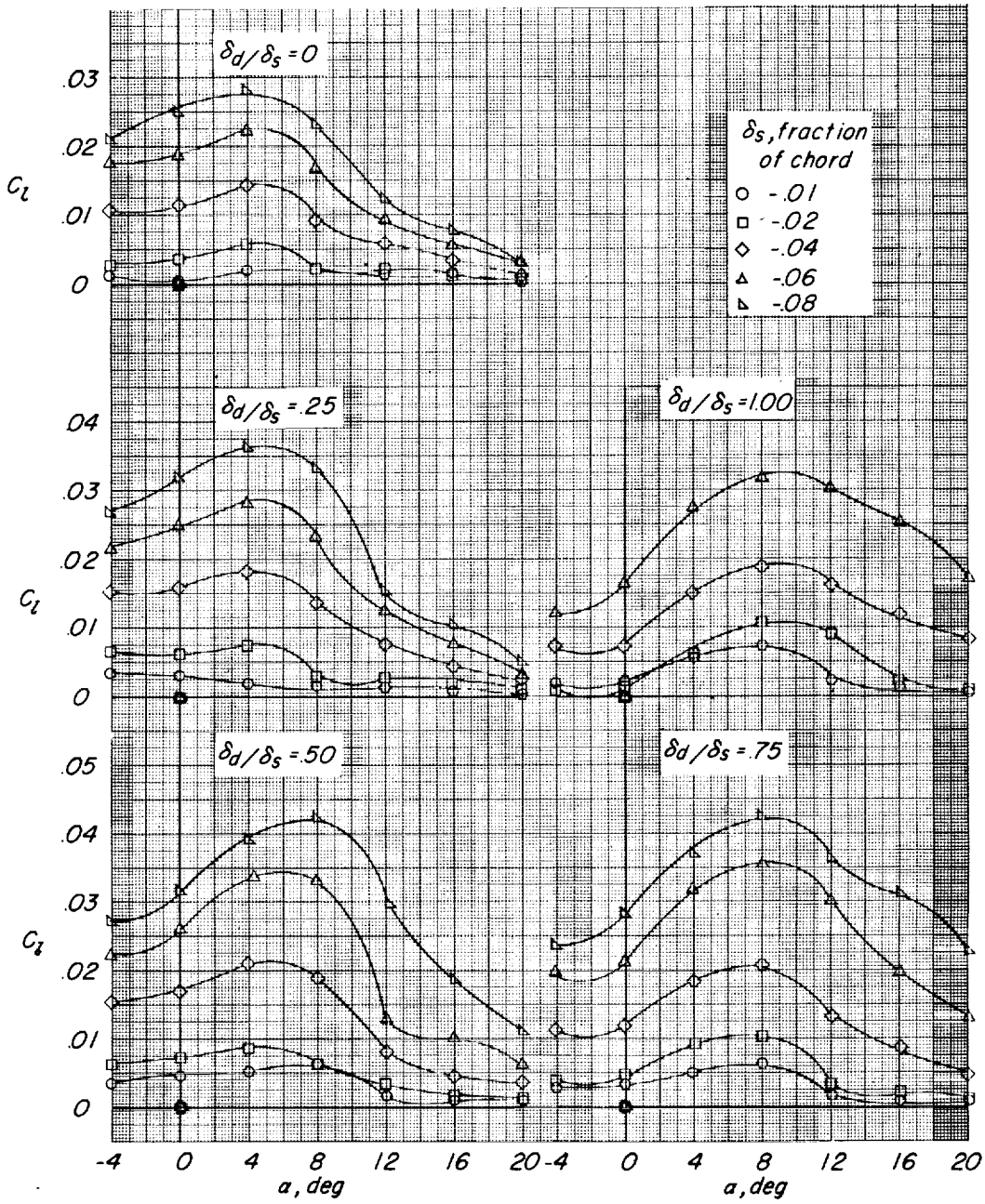

(b) M = 0.80.

Figure 7.- Continued.

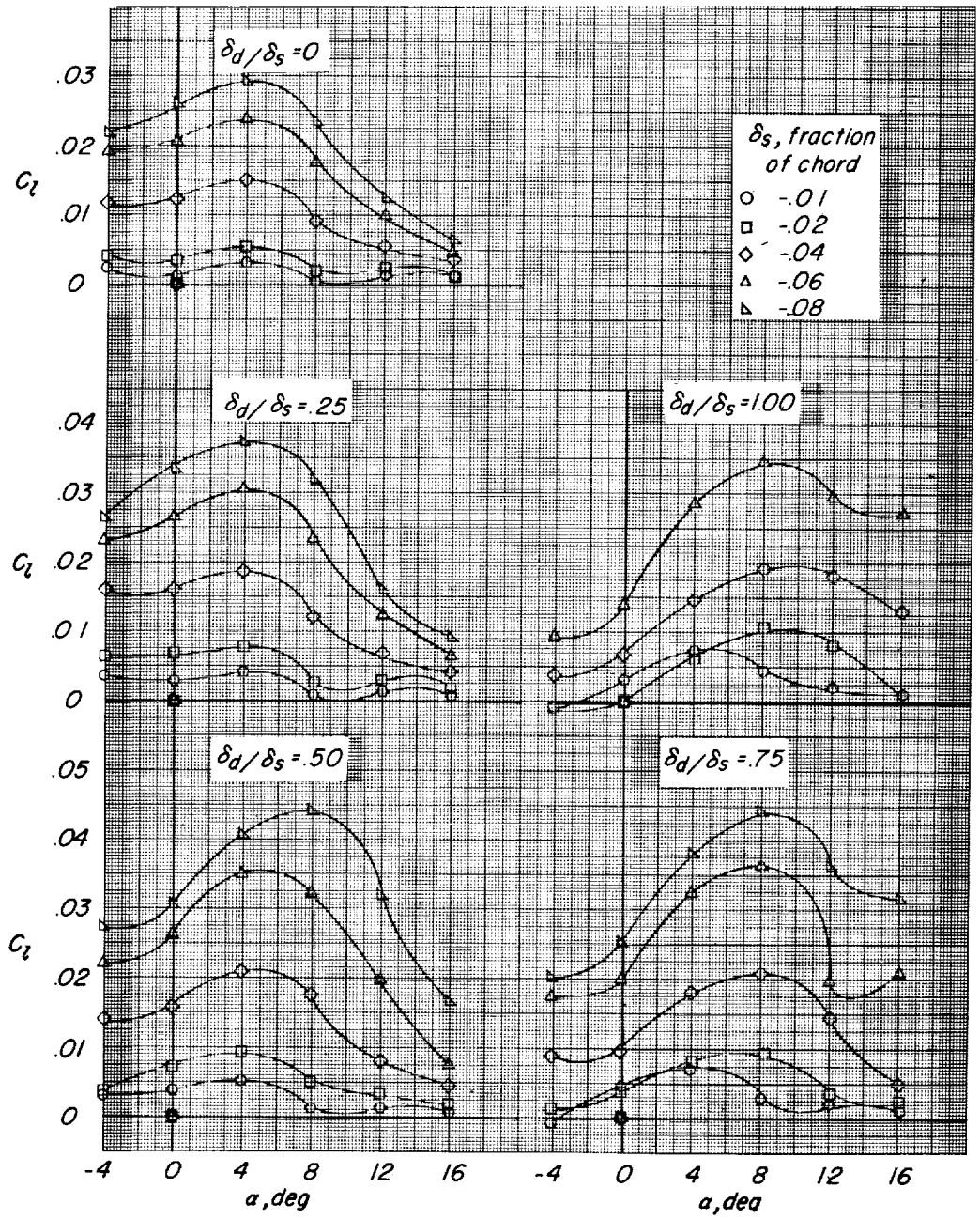

(c) M = 0.85.

Figure 7.- Continued.

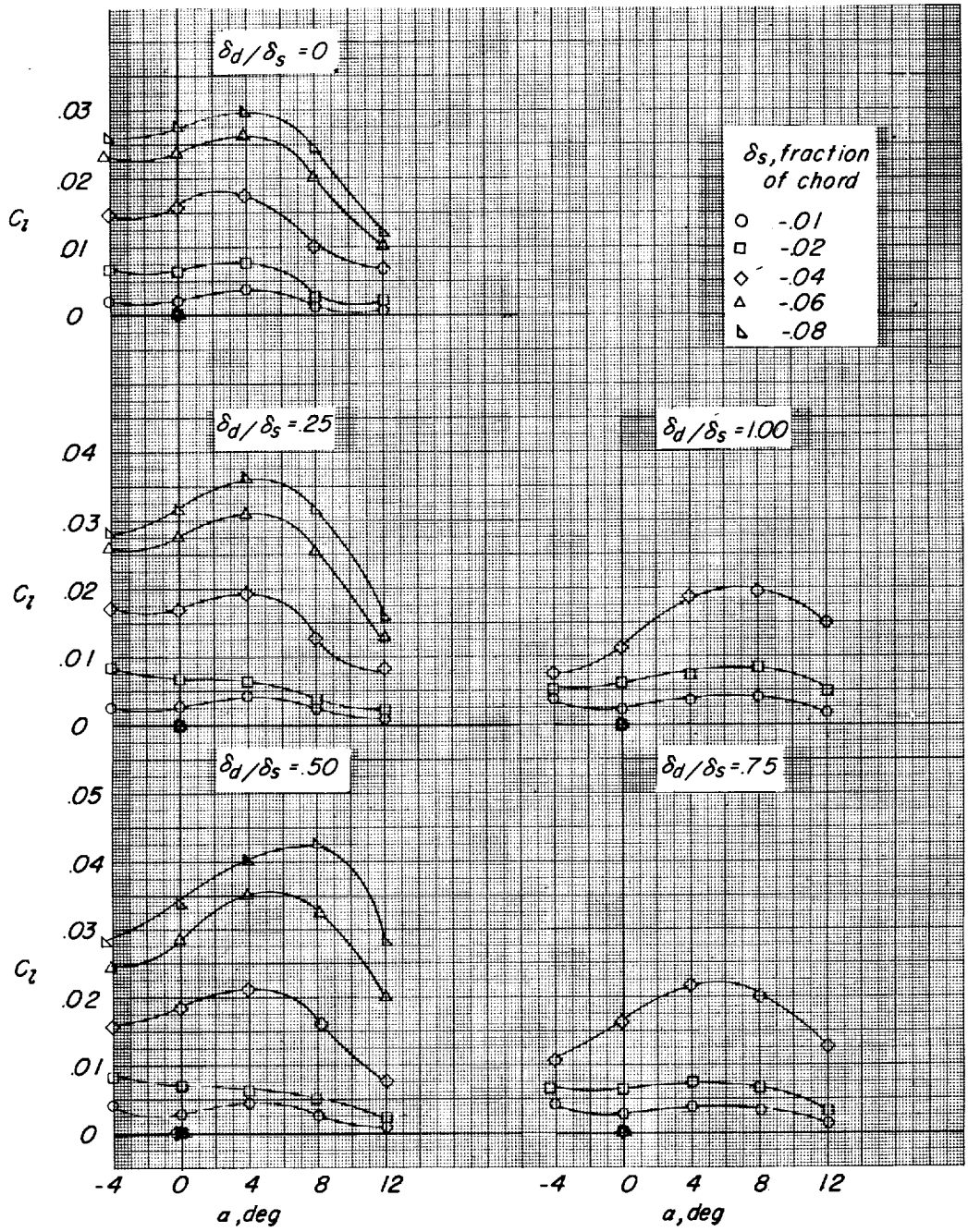

(d) M = 0.91.

Figure 7.- Continued.

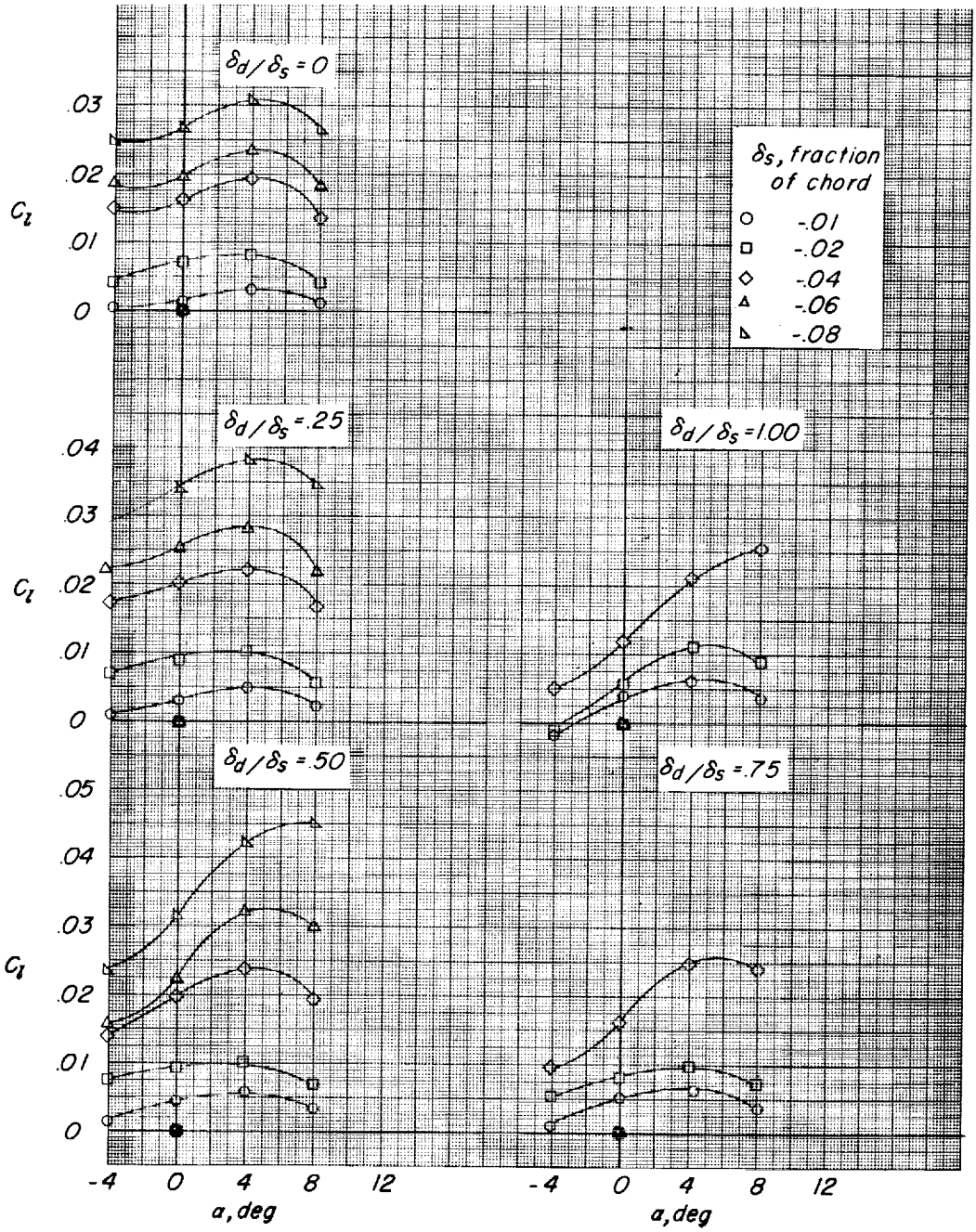

(e) M = 0.95.

Figure 7.- Concluded.

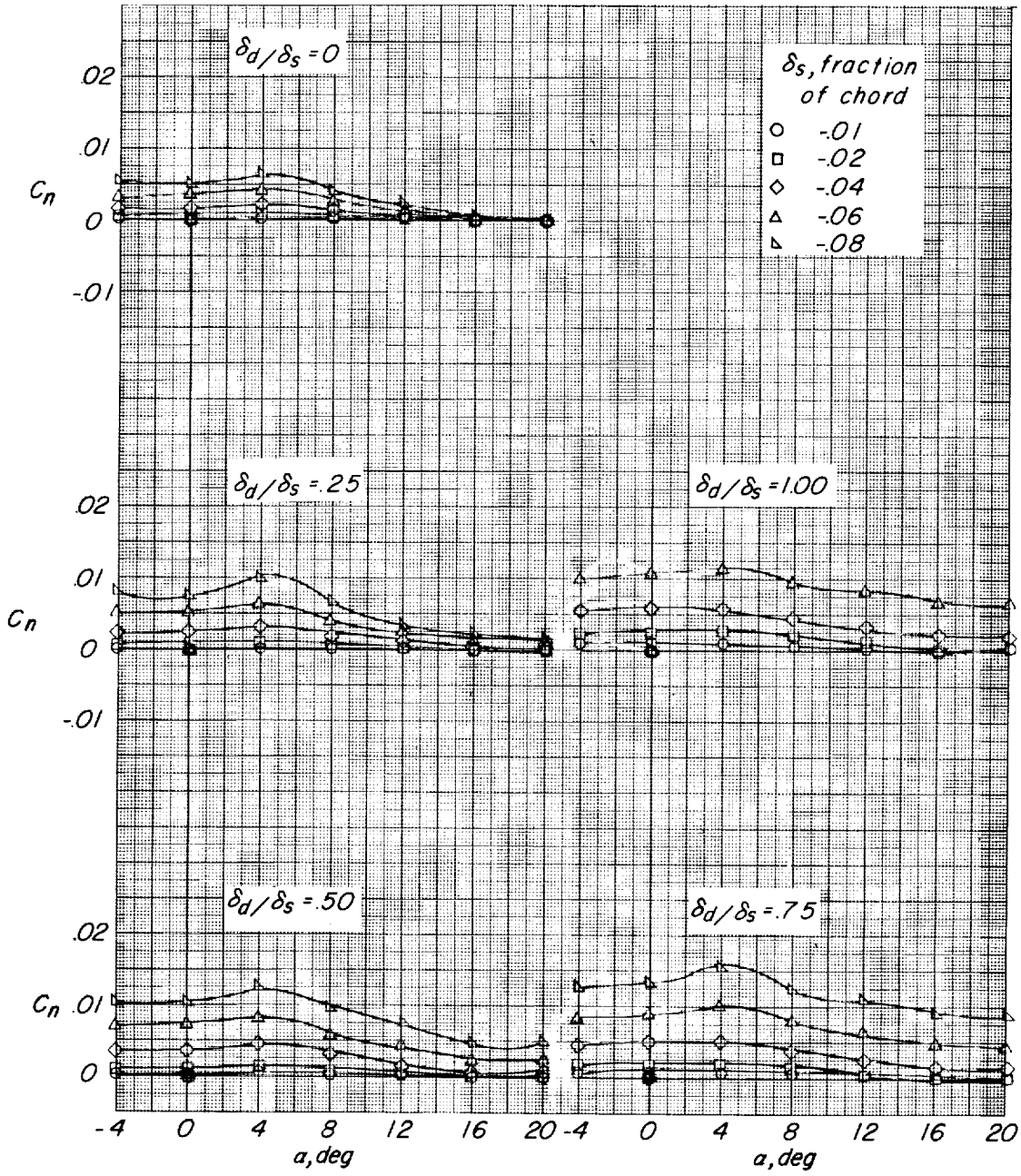

(a) M = 0.60.

Figure 8.- Variation of the yawing-moment coefficients with angle of attack for the 45° sweptback wing equipped with spoiler-slot-deflector configurations having deflector-to-spoiler projection ratios (δ_d/δ_s) of 0 to 1.0.

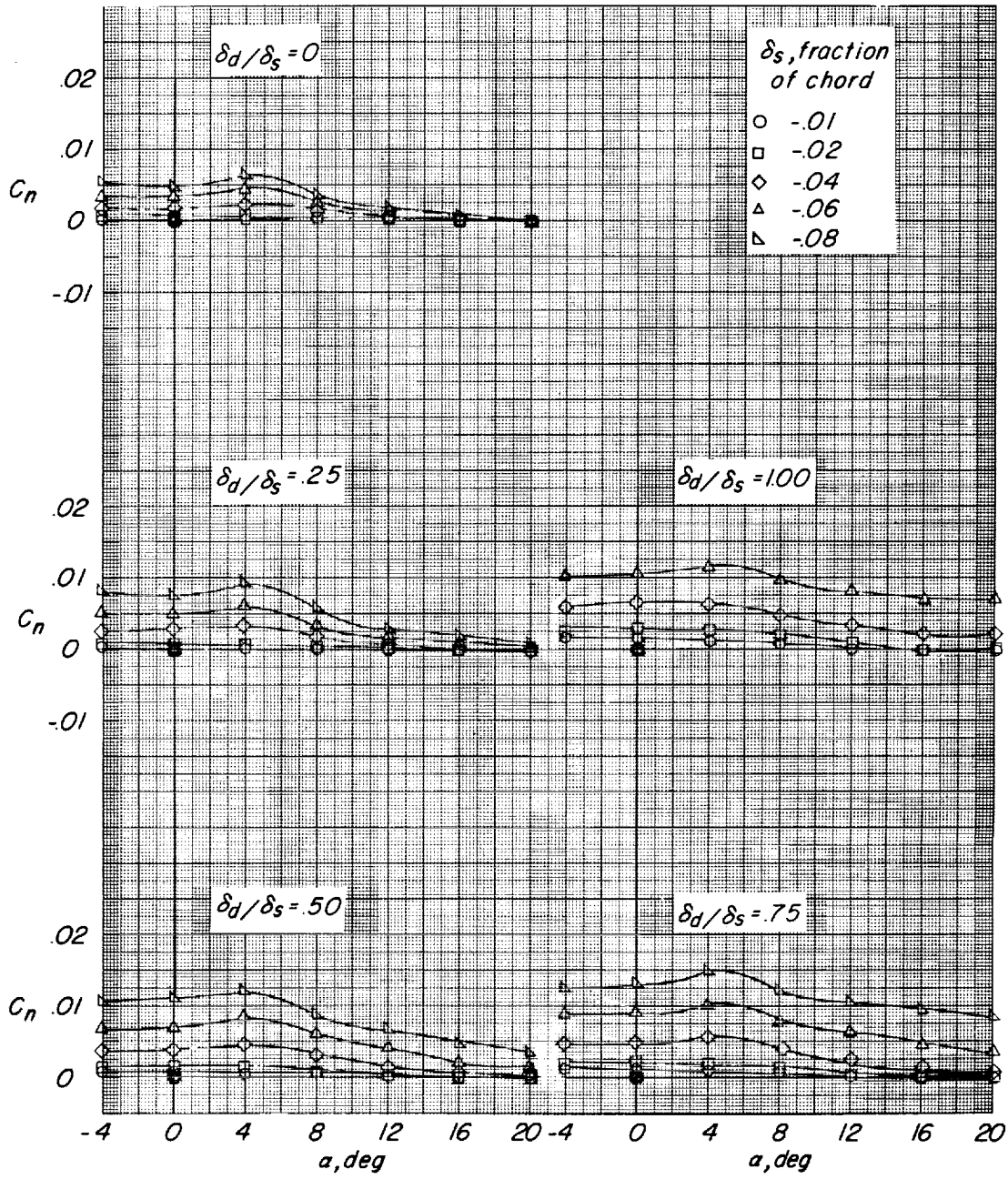

(b) M = 0.80.

Figure 8.- Continued.

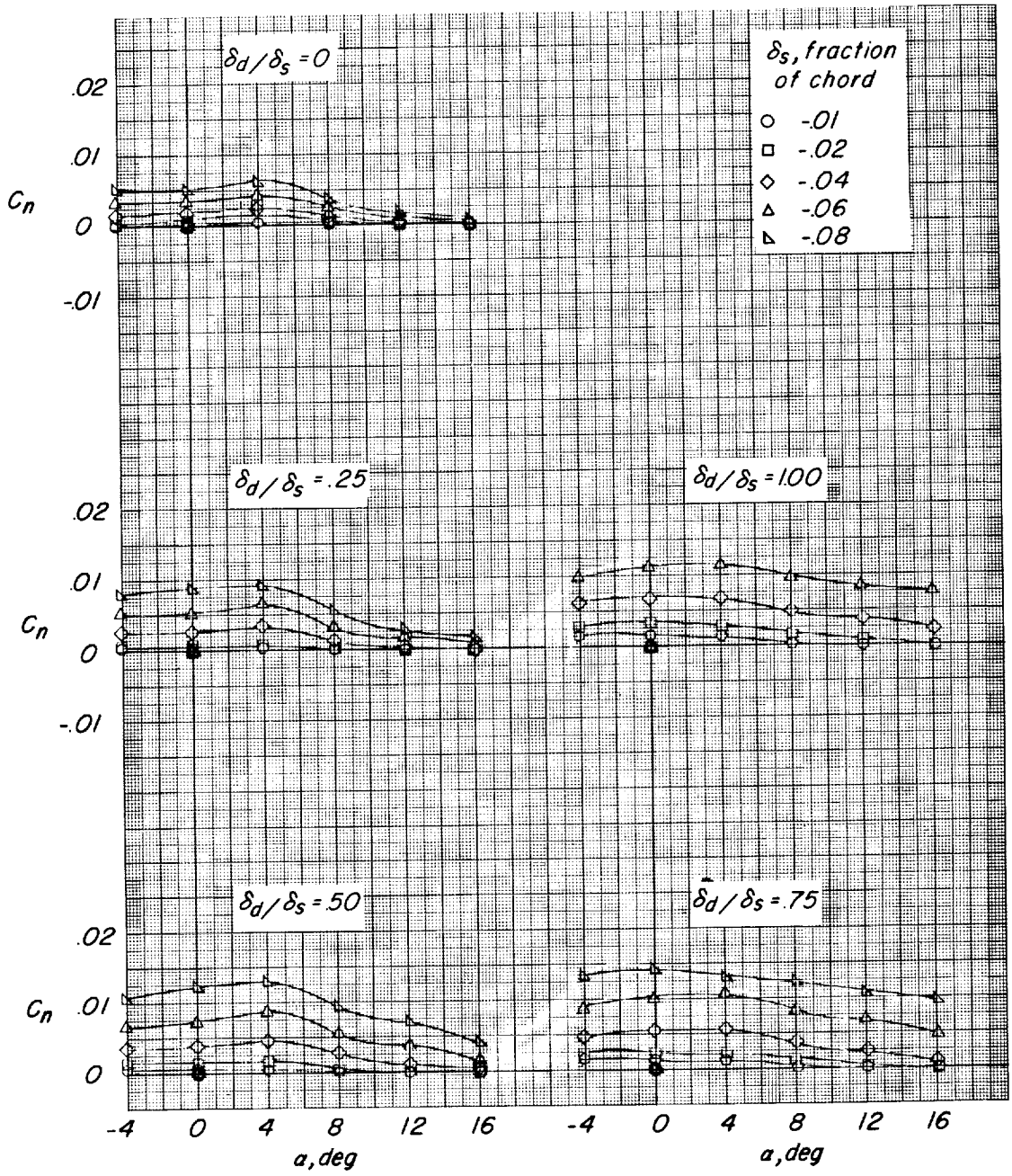

(c) M = 0.85.

Figure 8.- Continued.

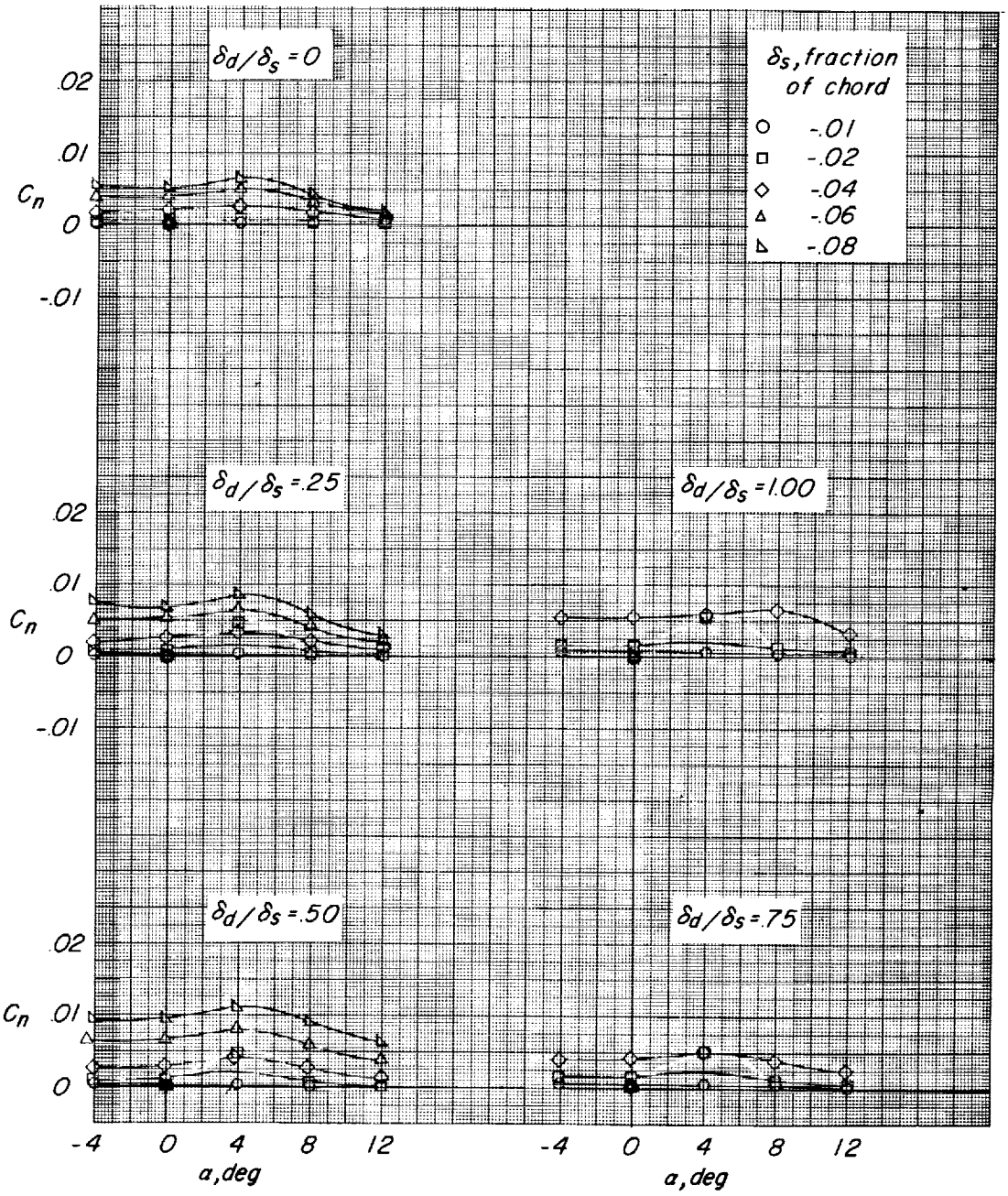

(d) M = 0.91.

Figure 8.- Continued.

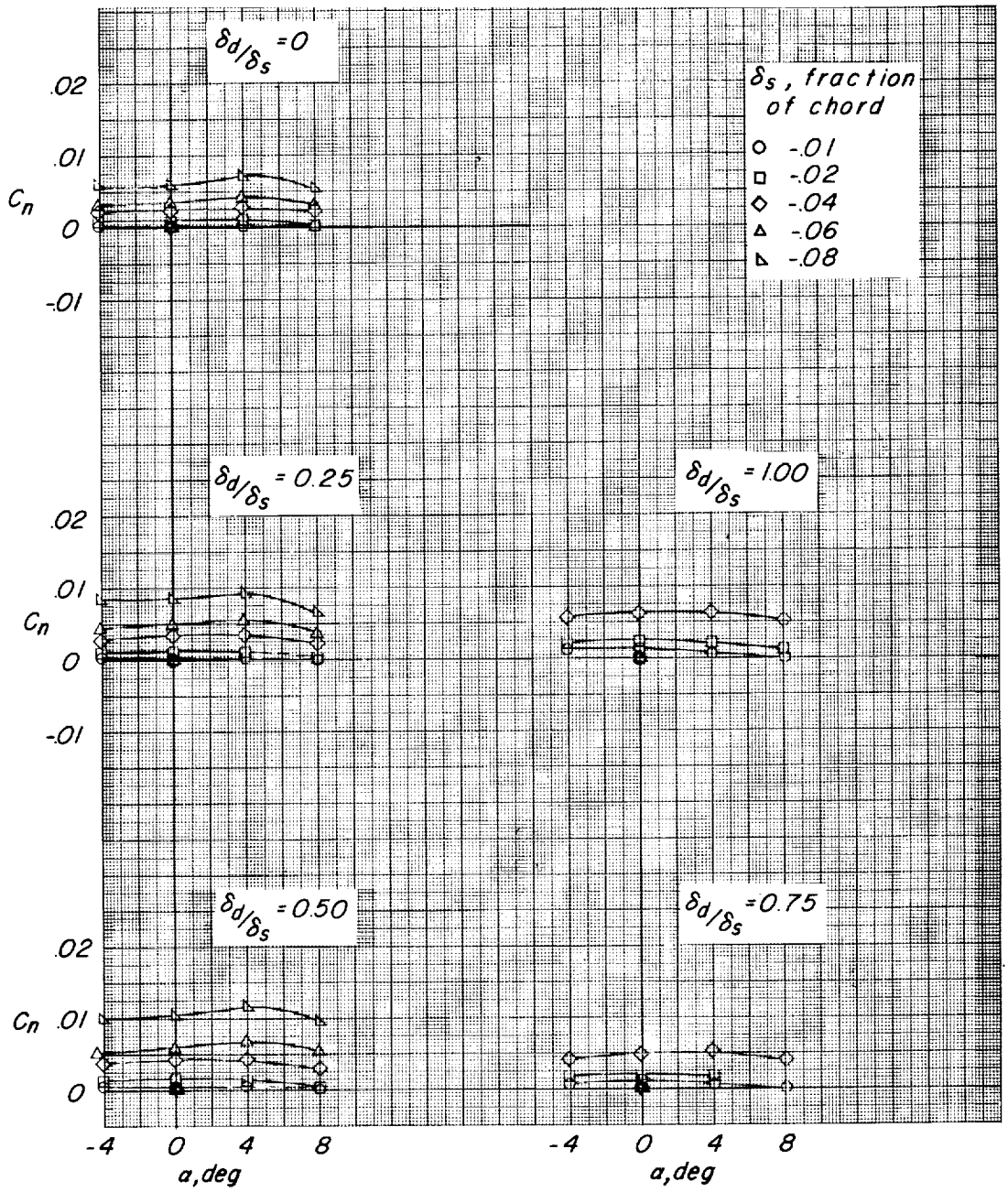

(e) M = 0.95.

Figure 8.- Concluded.

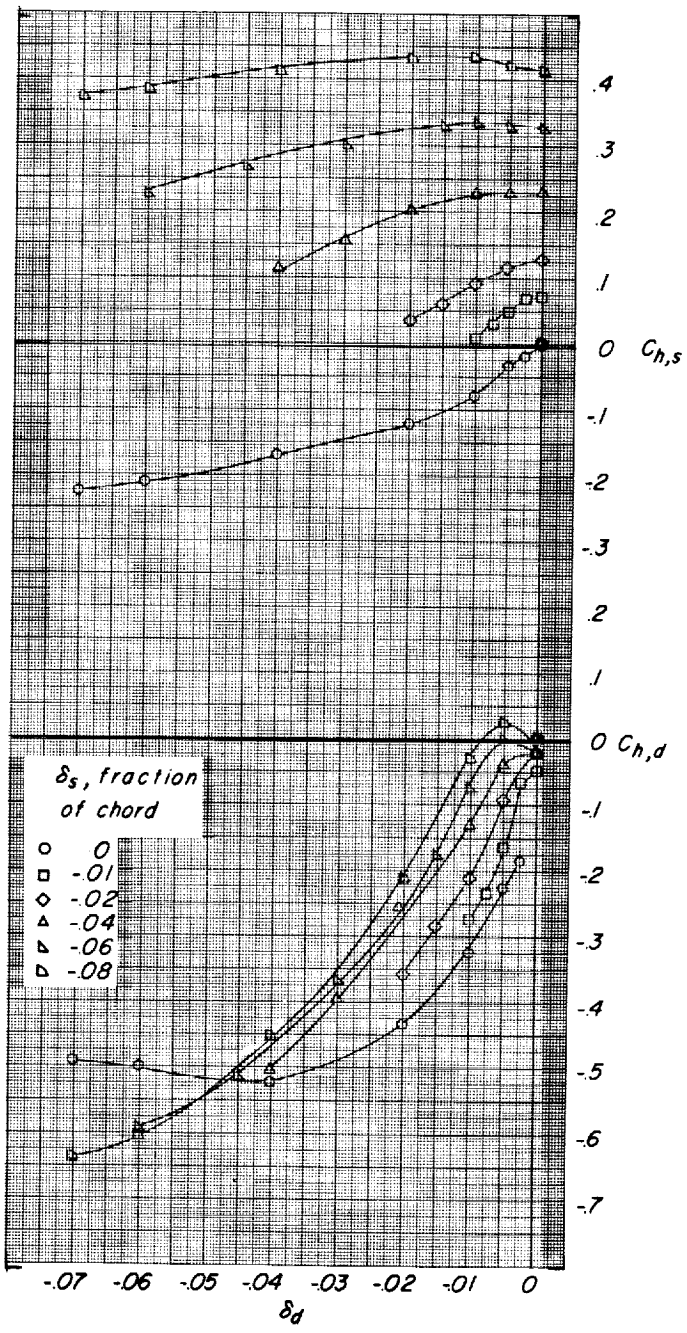

(a) $\alpha = -4^{\circ}$.

Figure 9.- Variation of the spoiler and deflector hinge-moment coefficients with deflector projection for various spoiler projections at M = 0.60.

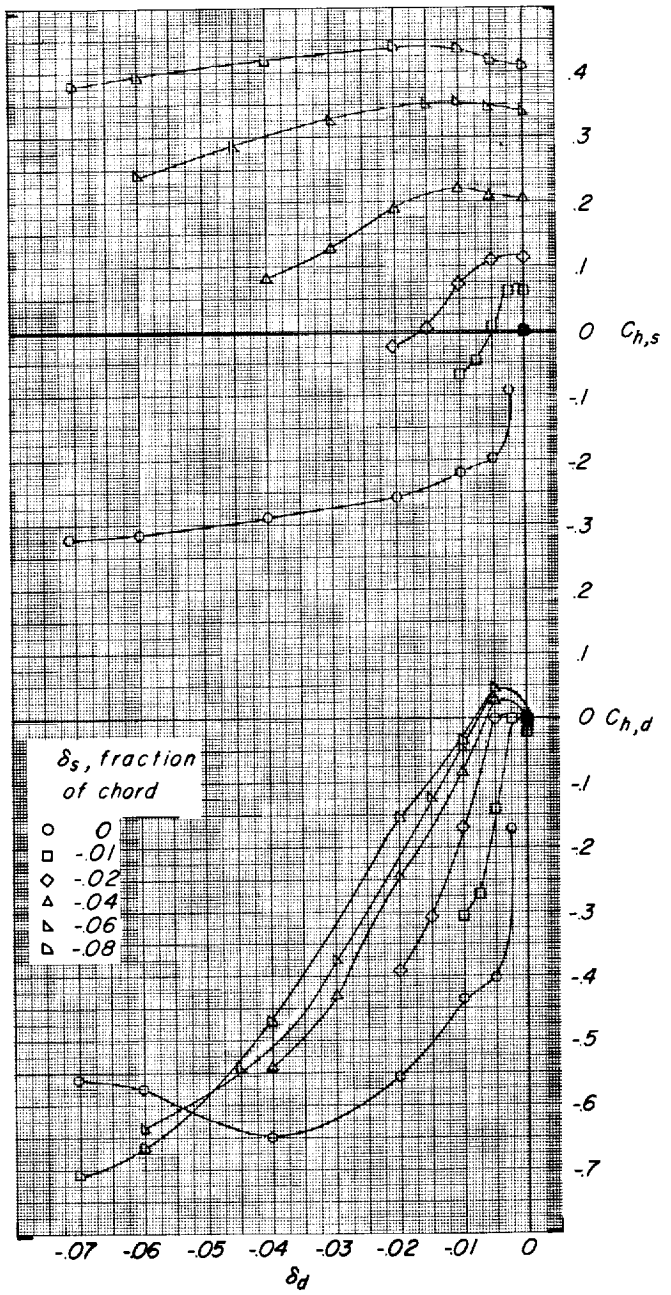

(b) $\alpha = 0^{\circ}$.

Figure 9.- Continued.

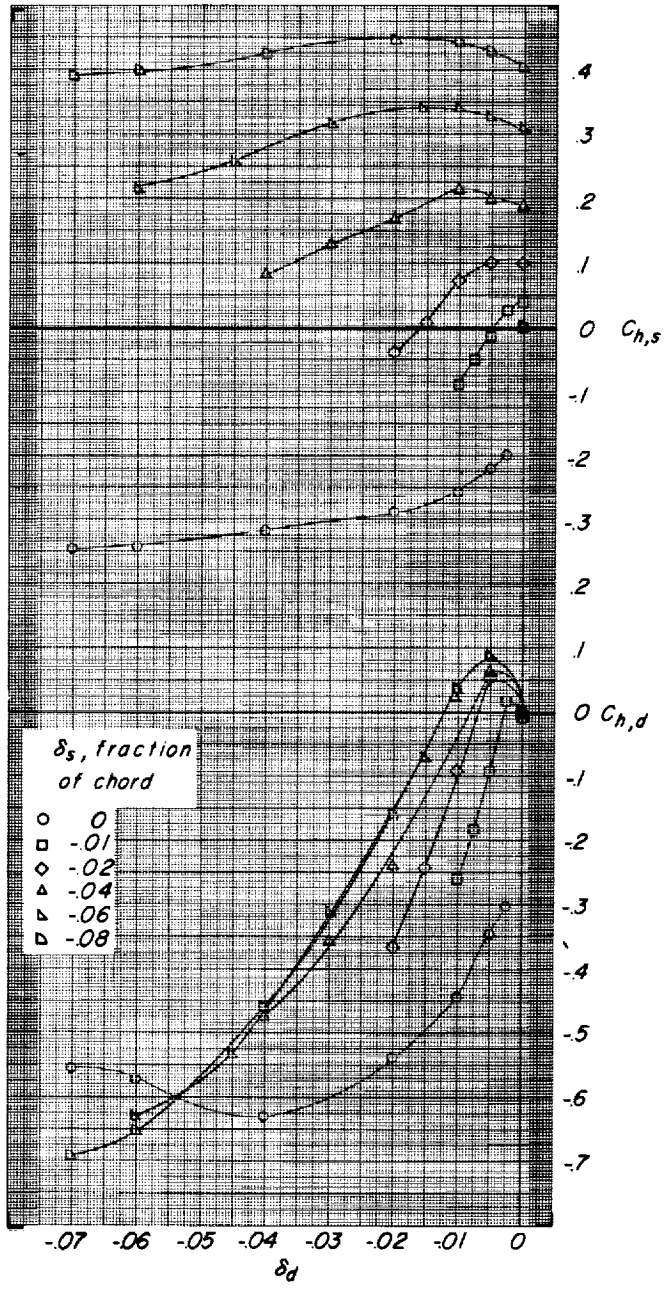

(c) $\alpha = 4^{\circ}$.

Figure 9.- Continued.

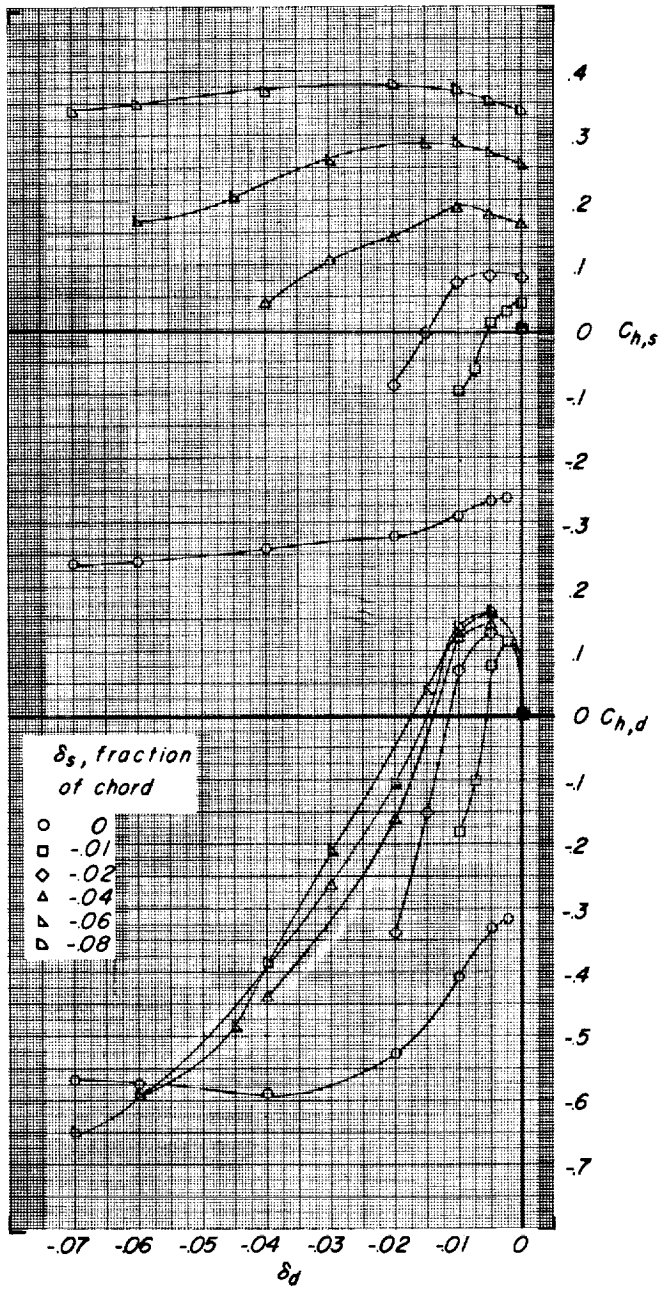

(d) $\alpha = 8^{\circ}$.

Figure 9.- Continued.

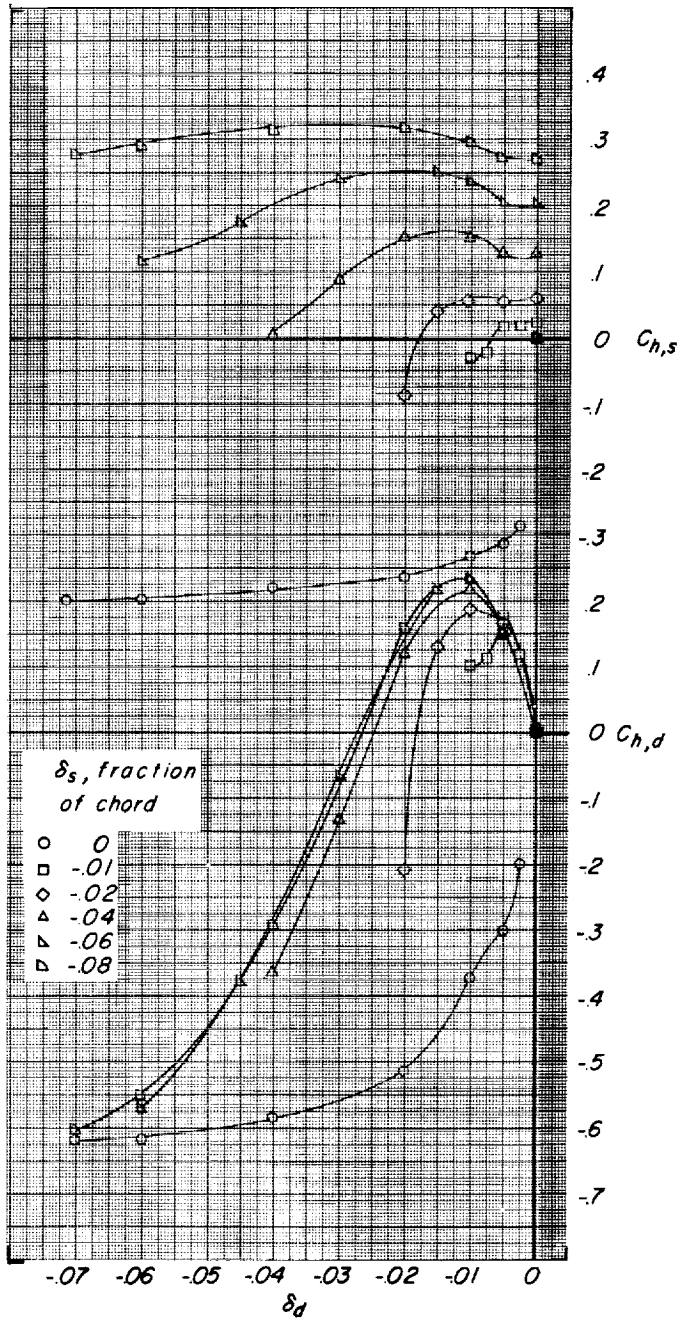

(e) $\alpha = 12^{\circ}$.

Figure 9.- Continued.

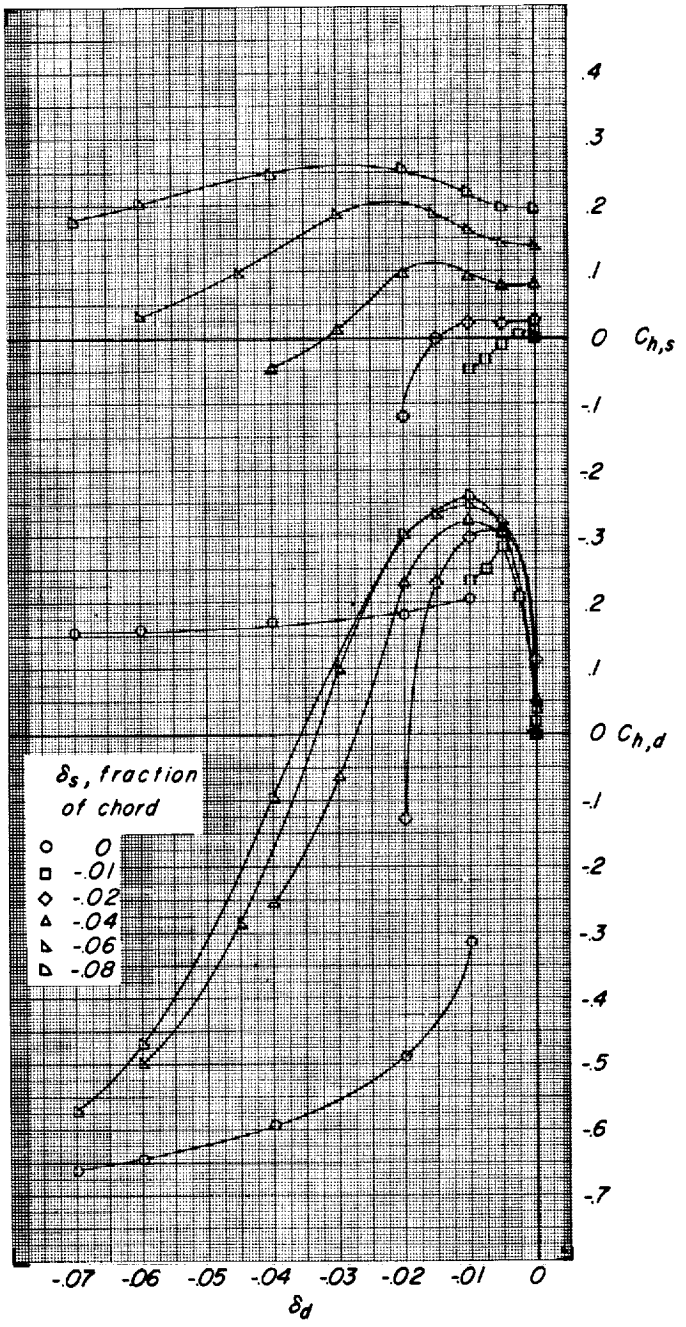

(f) $\alpha = 16^{\circ}$.

Figure 9.- Continued.

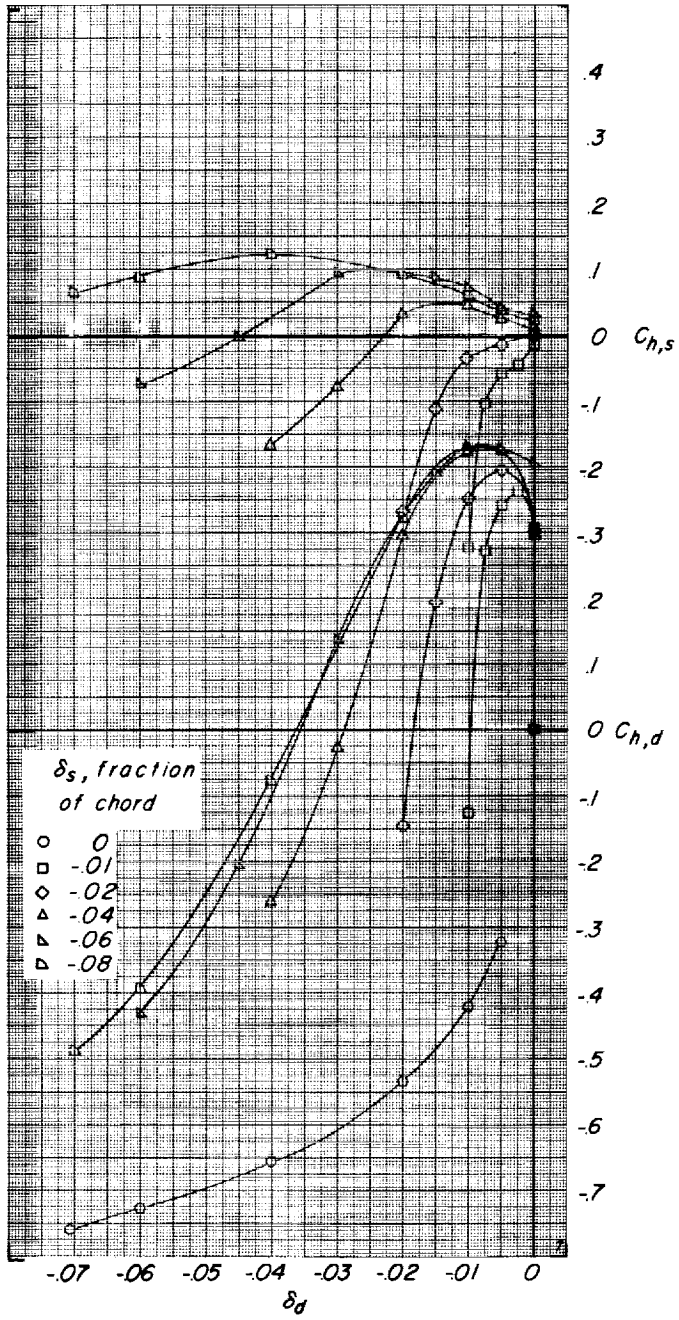

(g) $\alpha = 20^{\circ}$.

Figure 9.- Concluded.

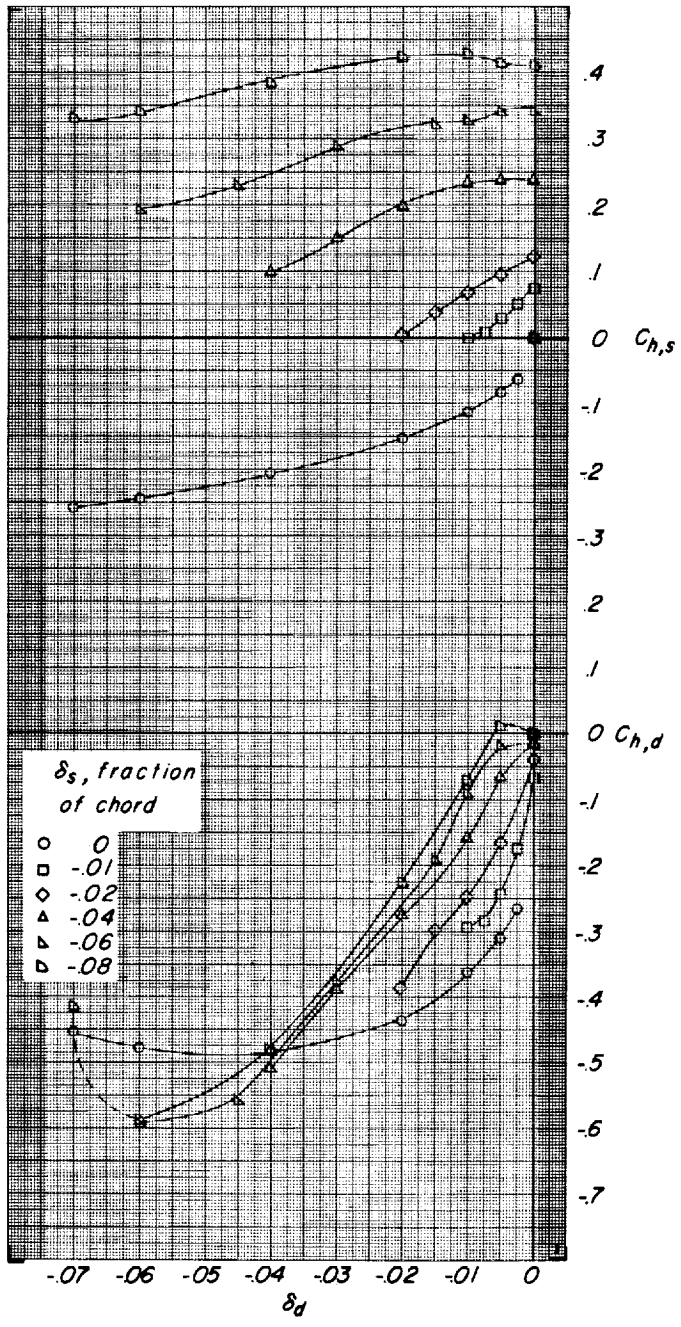

(a) $\alpha = -4^{\circ}$.

Figure 10.- Variation of the spoiler and deflector hinge-moment coefficients with deflector projection for various spoiler projections at M = 0.80.

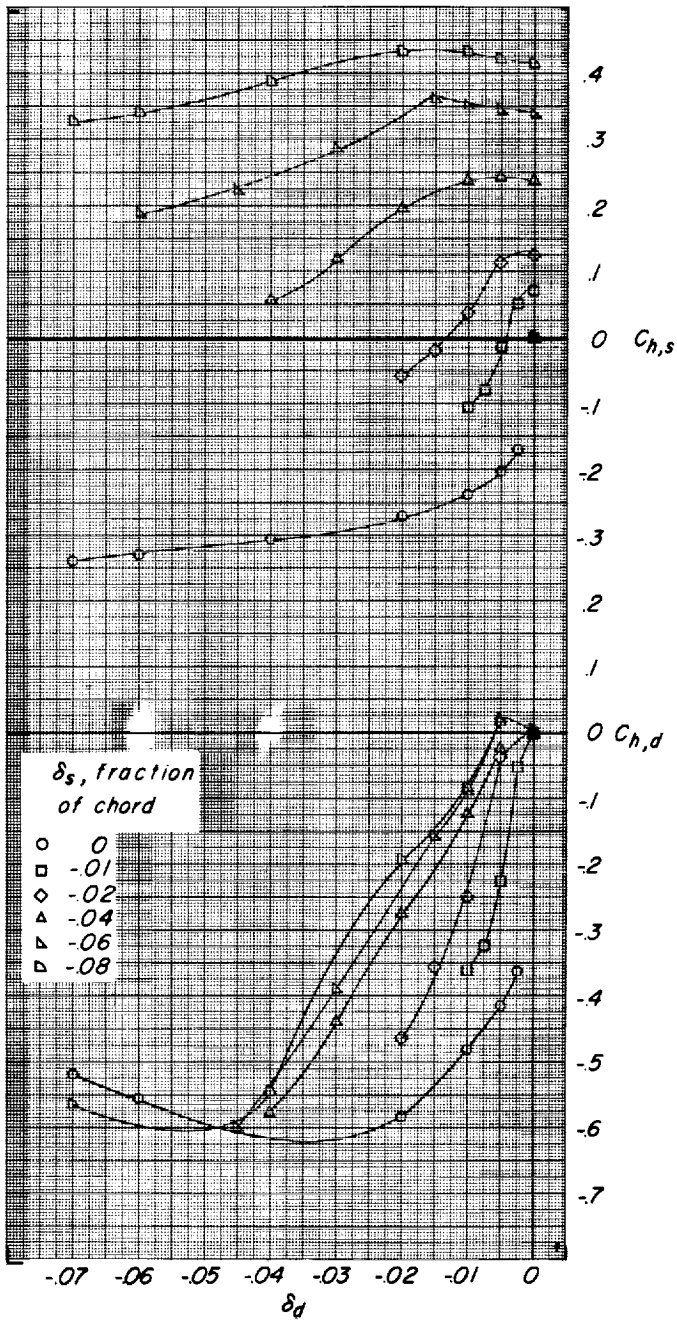

(b) $\alpha = 0^{\circ}$.

Figure 10.- Continued.

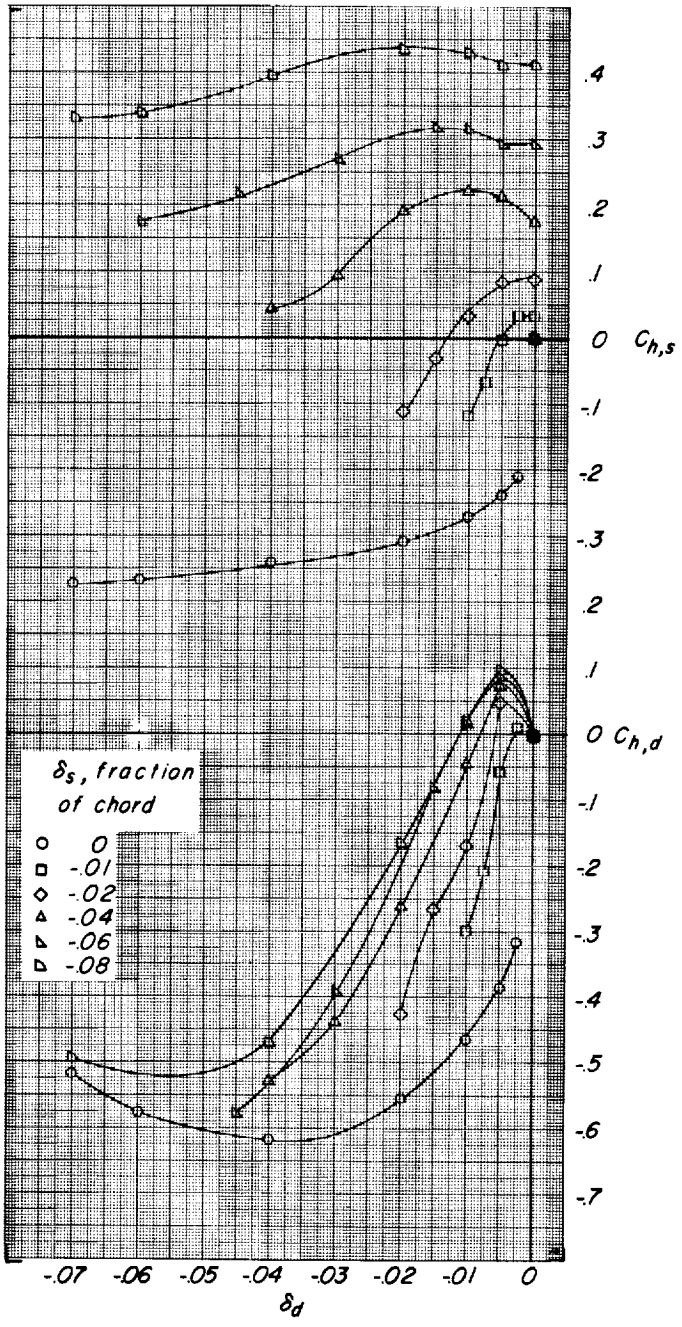

(c) $\alpha = 4^{\circ}$.

Figure 10.- Continued.

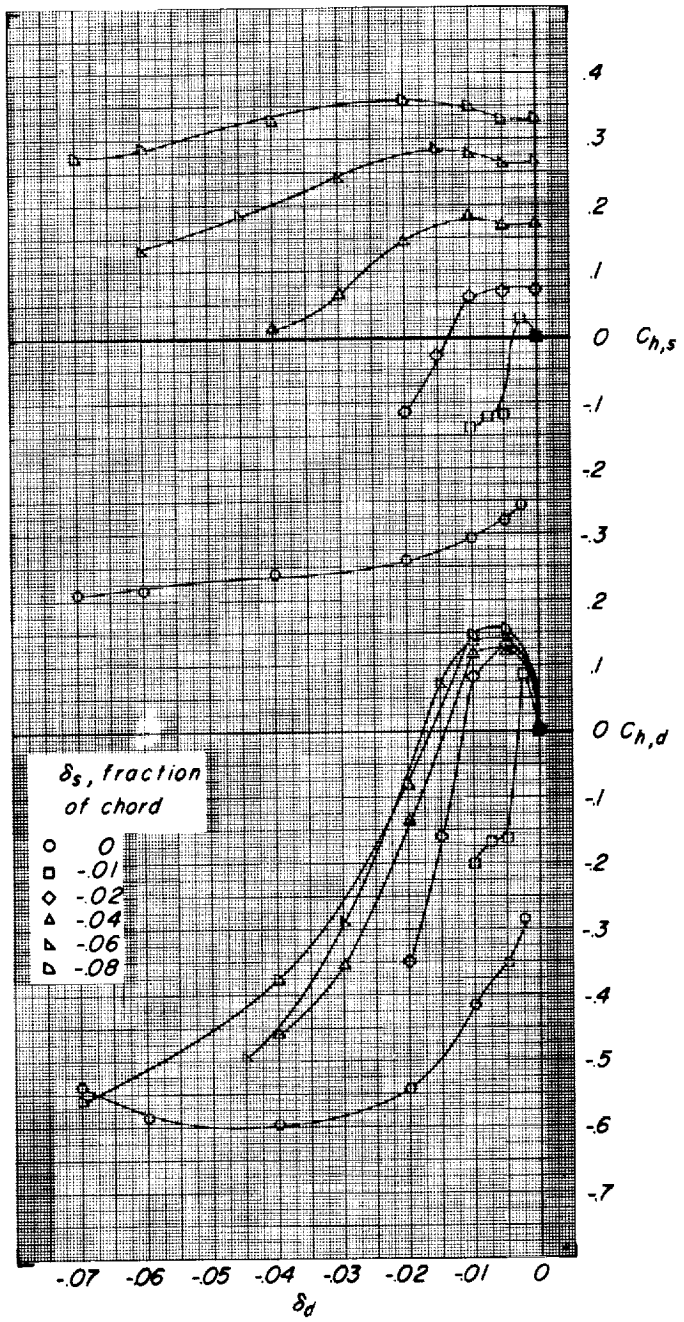

(d) $\alpha = 8^{\circ}$.

Figure 10.- Continued.

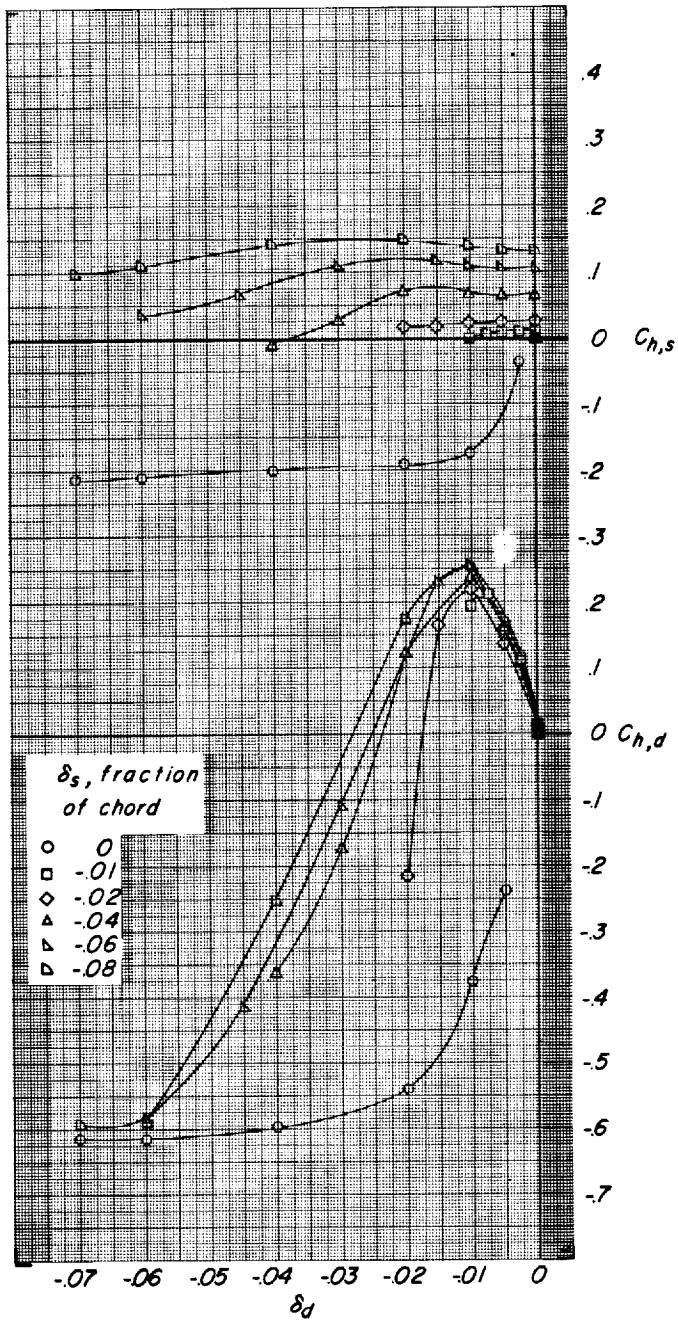

(e) $\alpha = 12^{\circ}$.

Figure 10.- Continued.

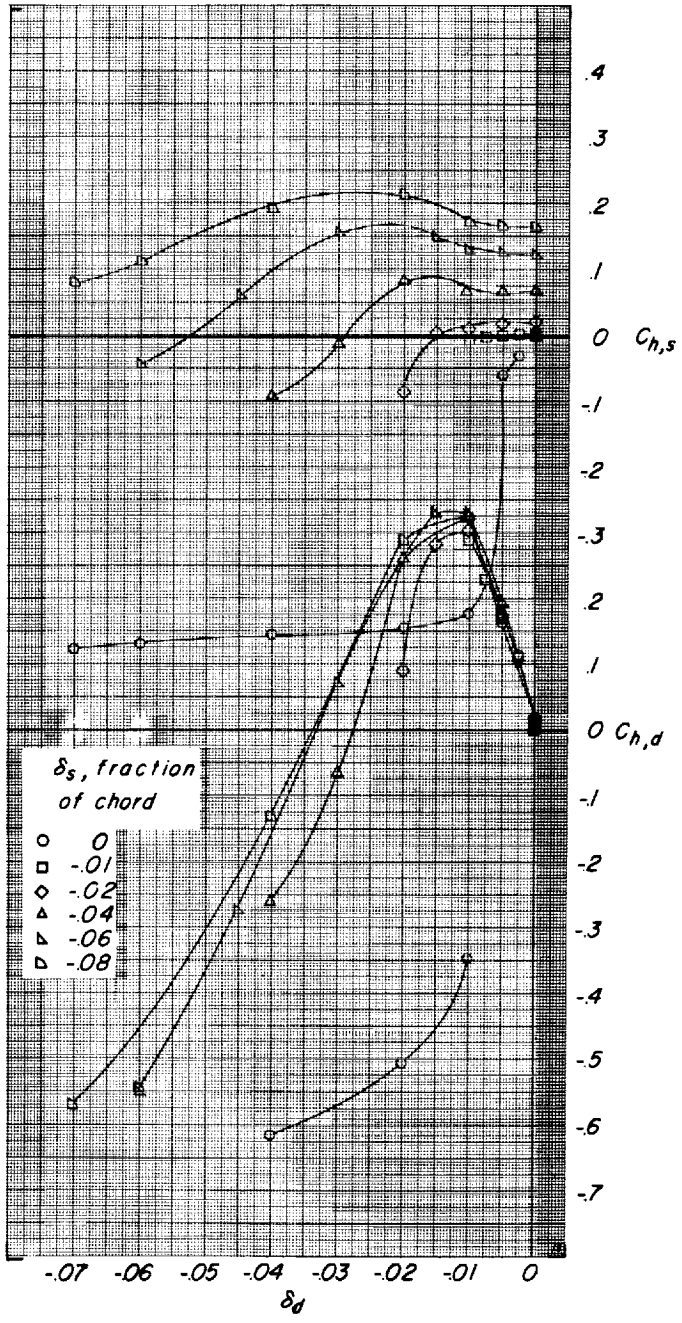

(f) $\alpha = 16^{\circ}$.

Figure 10.- Continued.

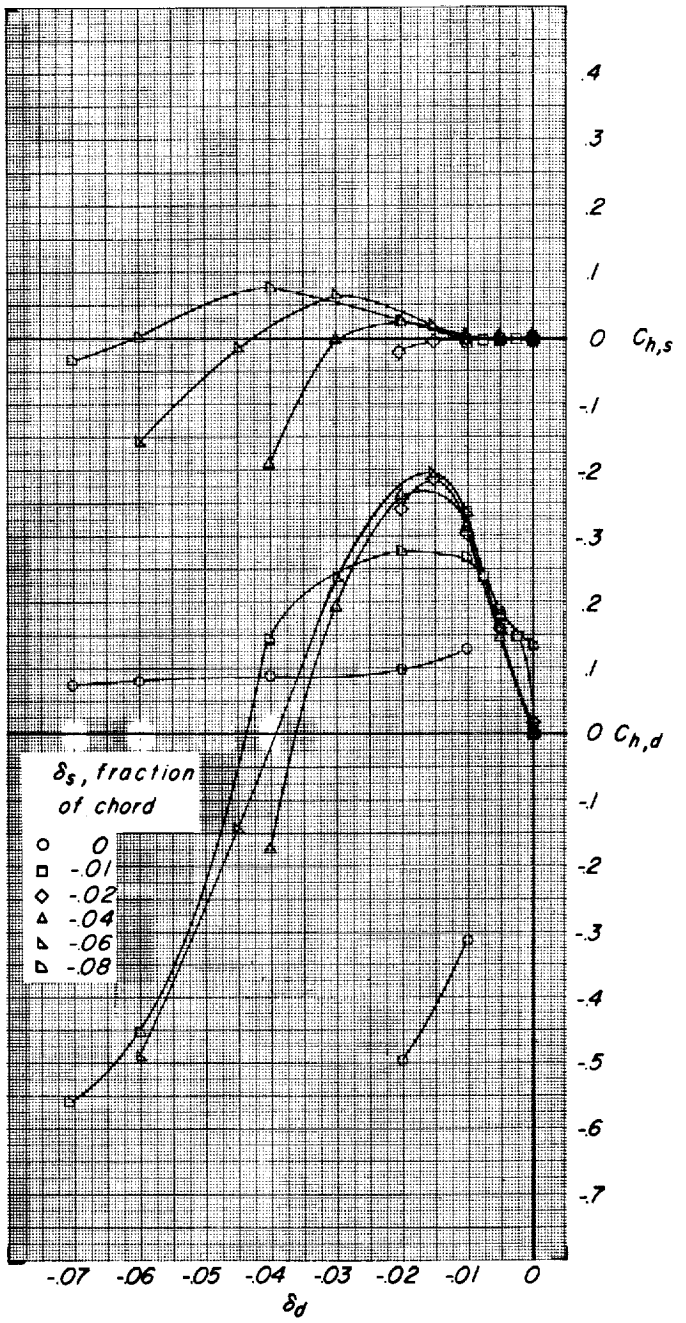

(g) $\alpha = 20^{\circ}$.

Figure 10.- Concluded.

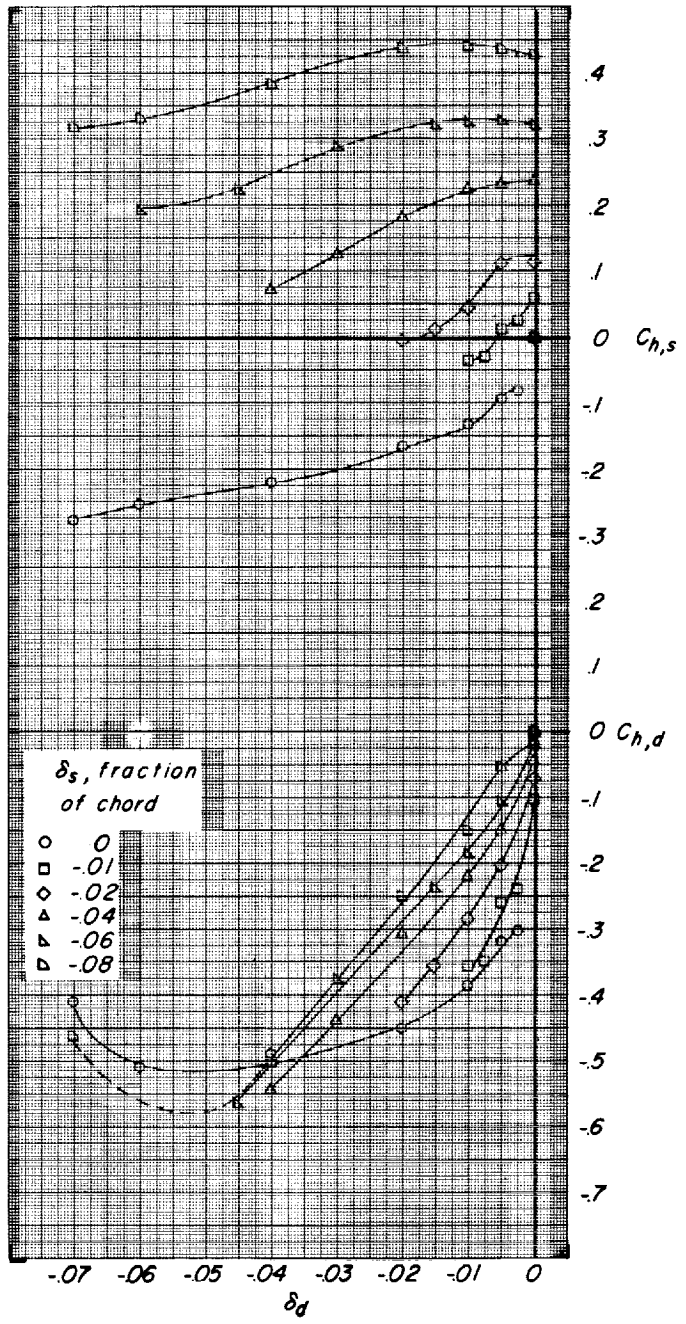

(a) $\alpha = -4^{\circ}$.

Figure 11.- Variation of the spoiler and deflector hinge-moment coefficients with deflector projection for various spoiler projections at M = 0.85.

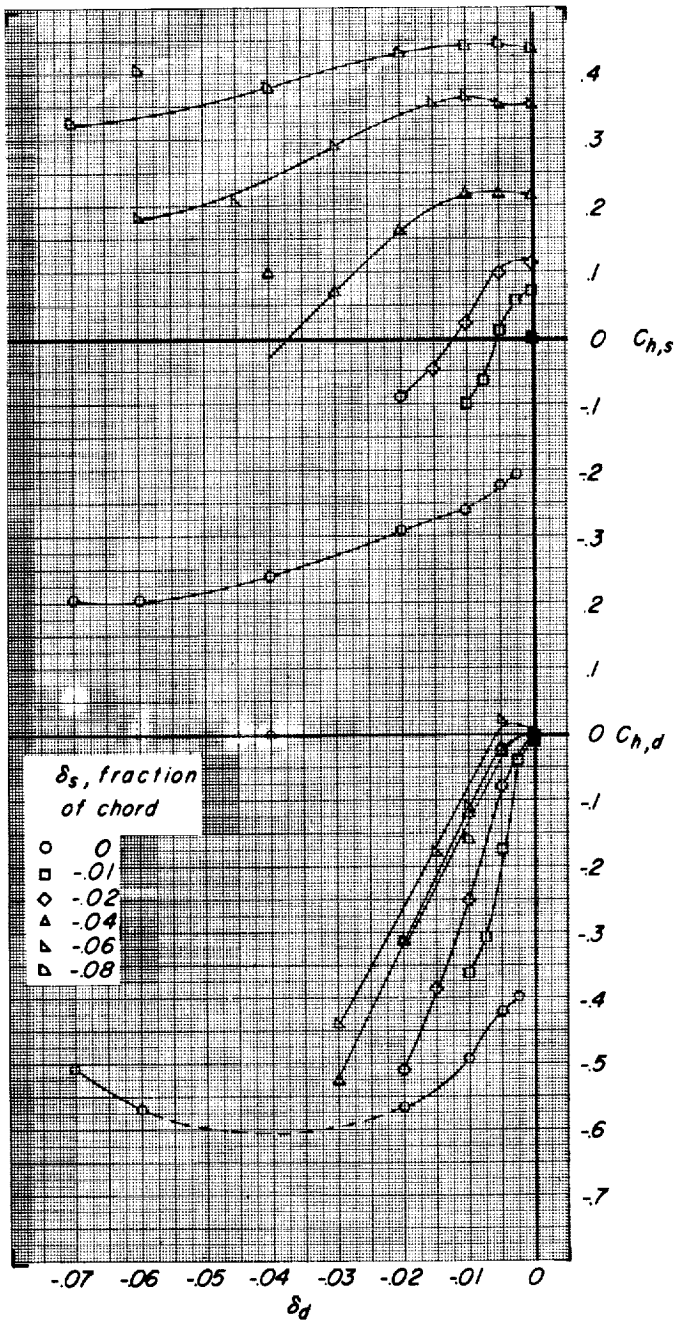

(b) $\alpha = 0^{\circ}$.

Figure 11.- Continued.

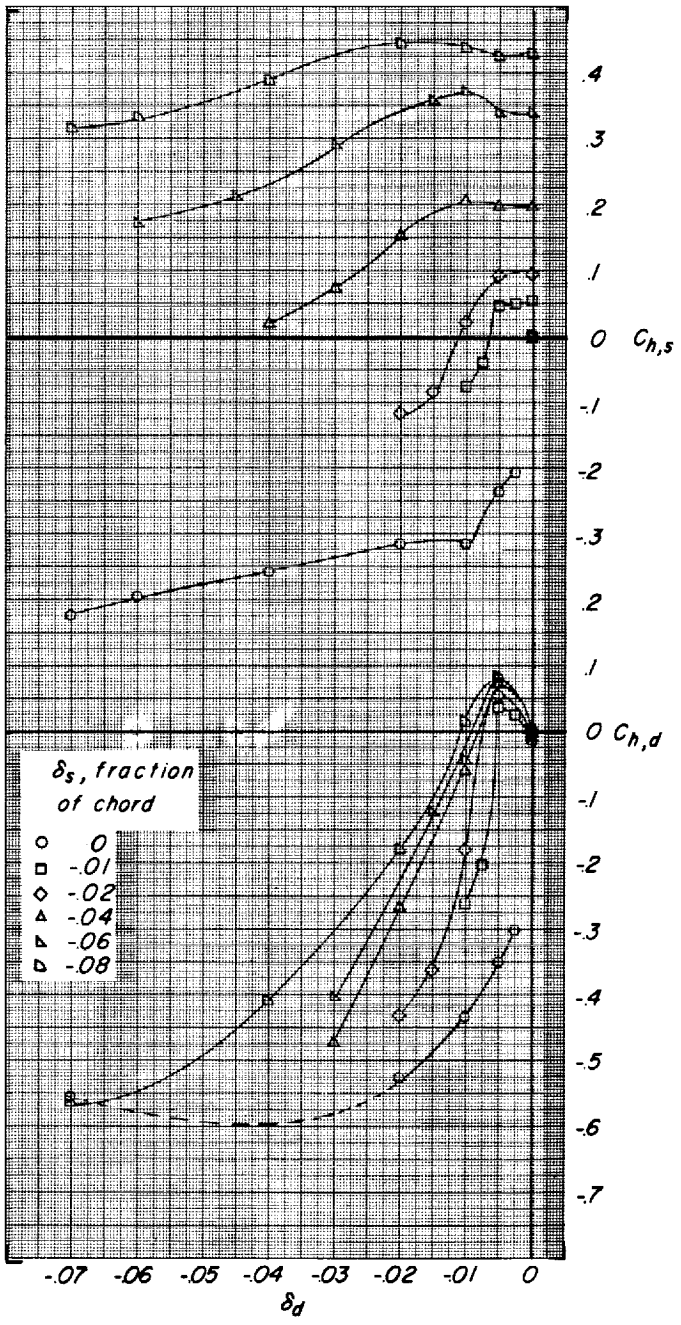

(c) $\alpha = 4^{\circ}$.

Figure 11.- Continued.

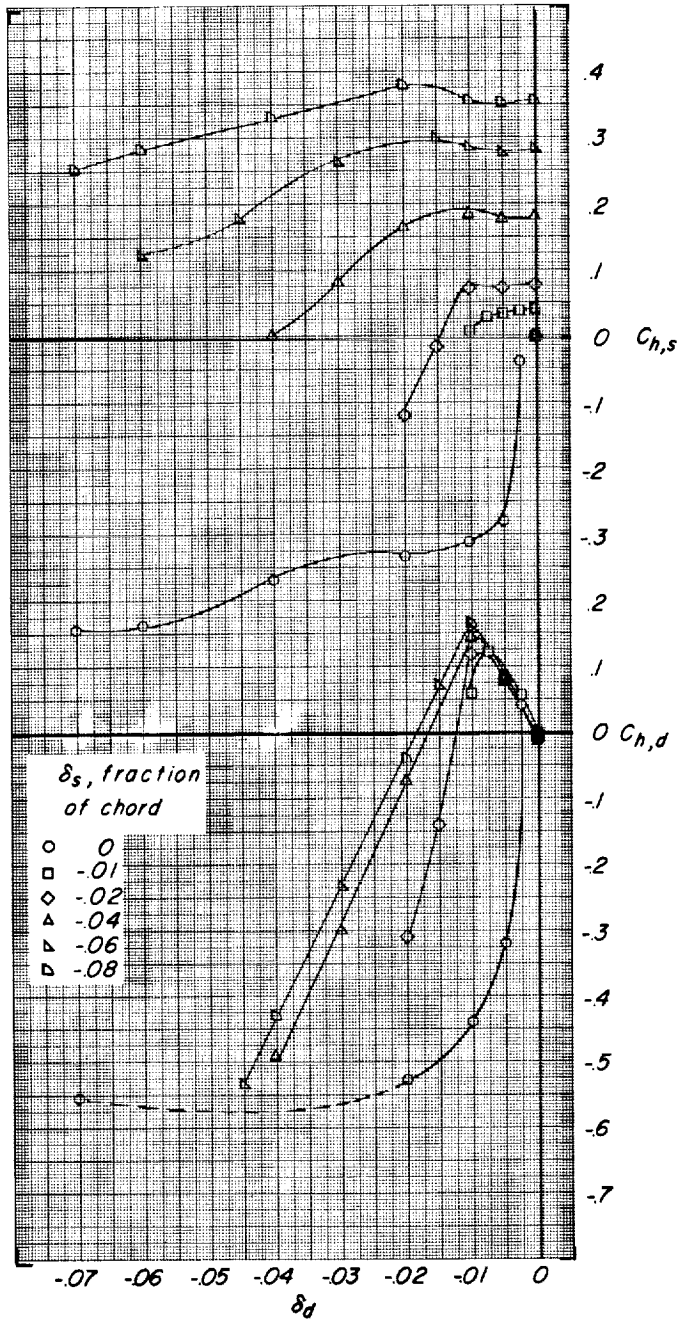

(d) $\alpha = 8^{\circ}$.

Figure 11.- Continued.

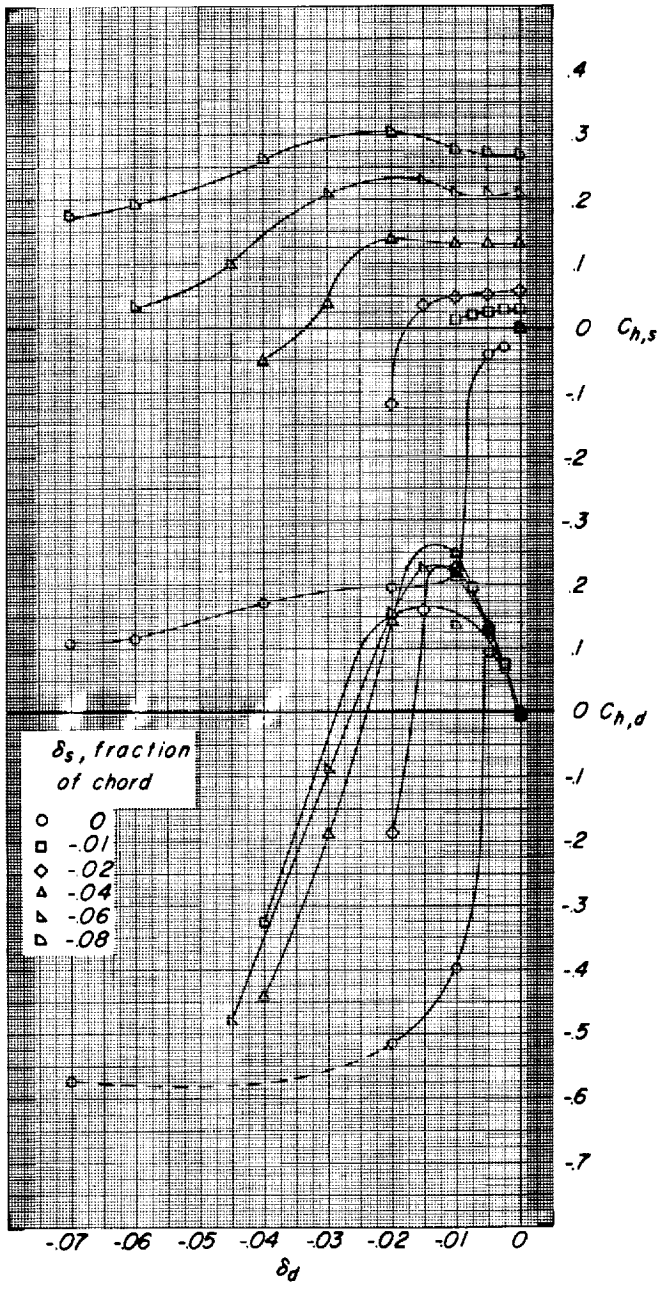

(e) $\alpha = 12^{\circ}$.

Figure 11.- Continued.

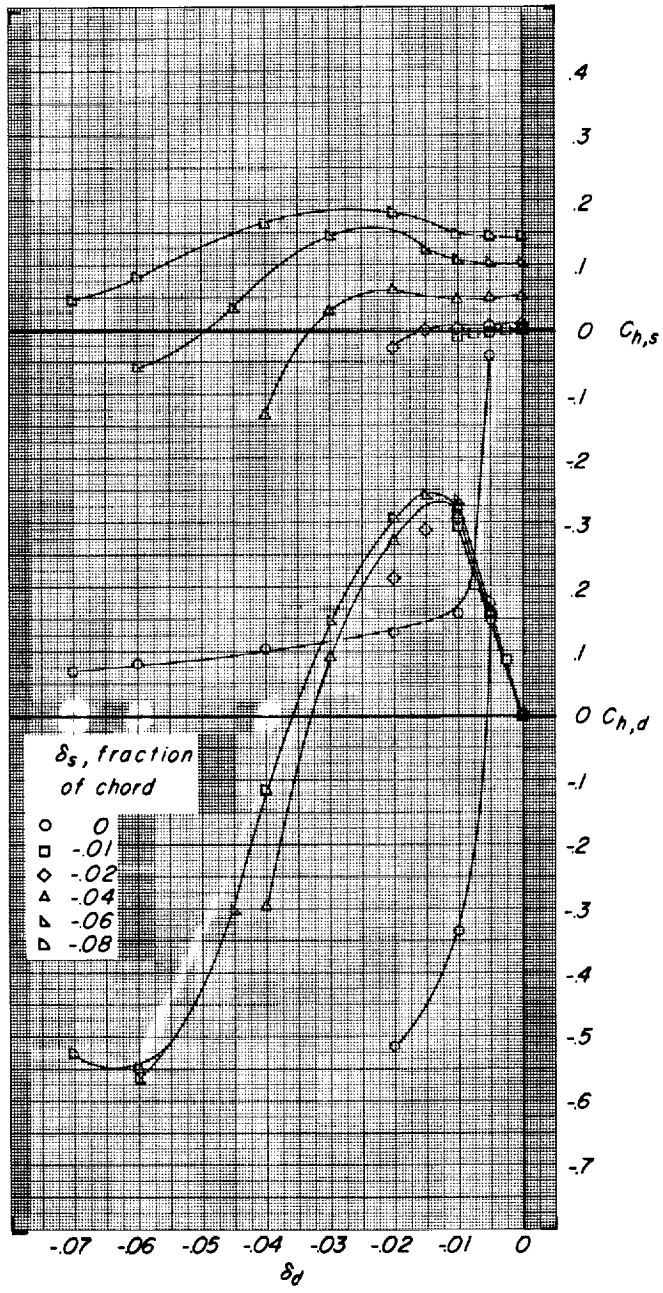

(f) $\alpha = 16^{\circ}$.

Figure 11.- Concluded.

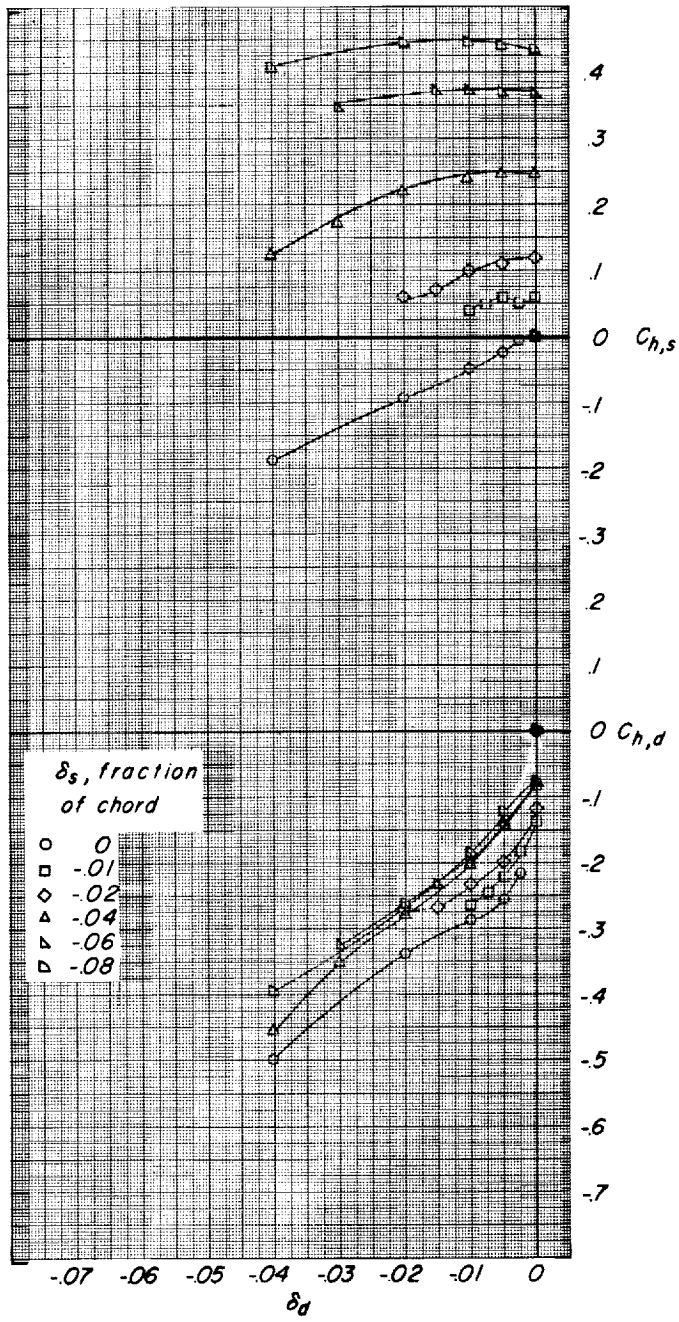

(a) $\alpha = -4^{\circ}$.

Figure 12.- Variation of the spoiler and deflector hinge-moment coefficients with deflector projection for various spoiler projections at M = 0.91.

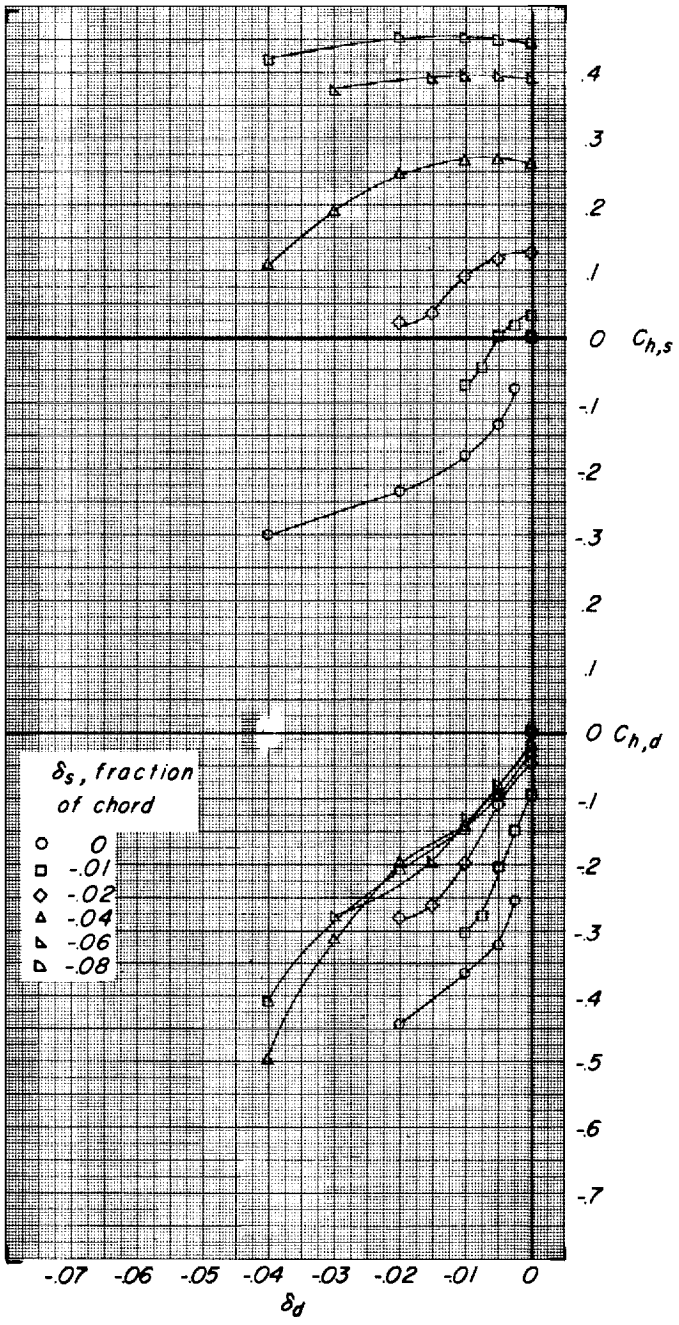

(b) $\alpha = 0^{\circ}$.

Figure 12.- Continued.

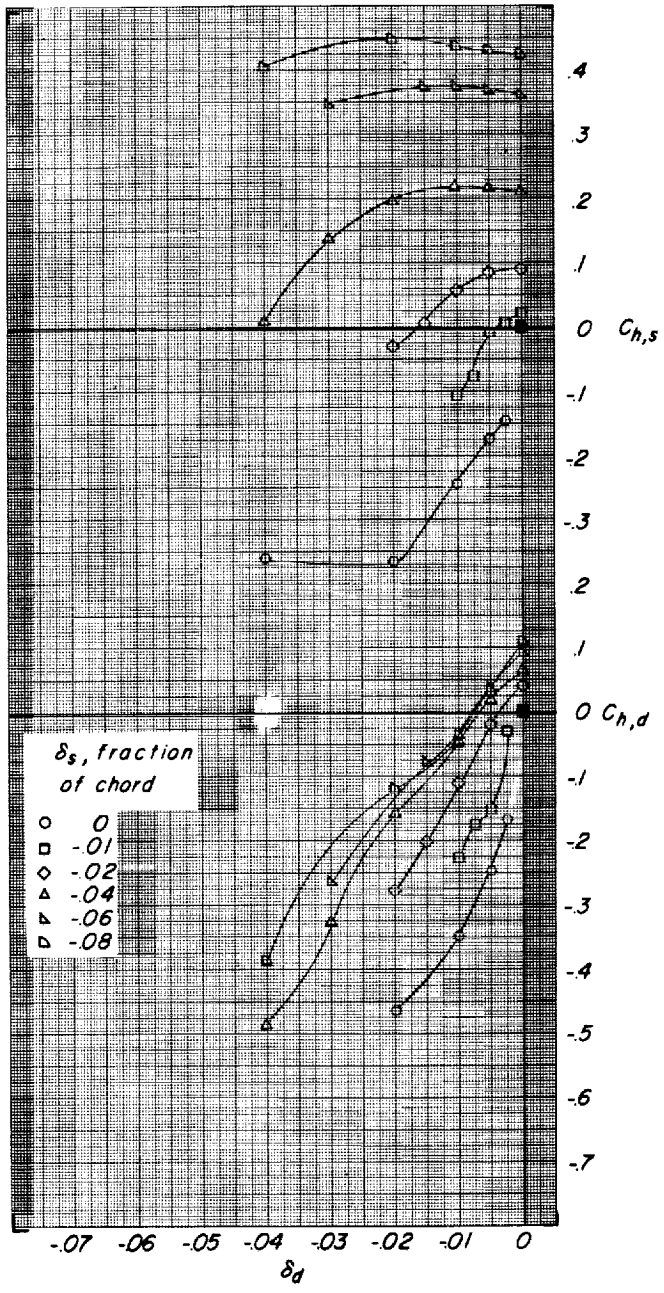

(c) $\alpha = 4^{\circ}$.

Figure 12.- Continued.

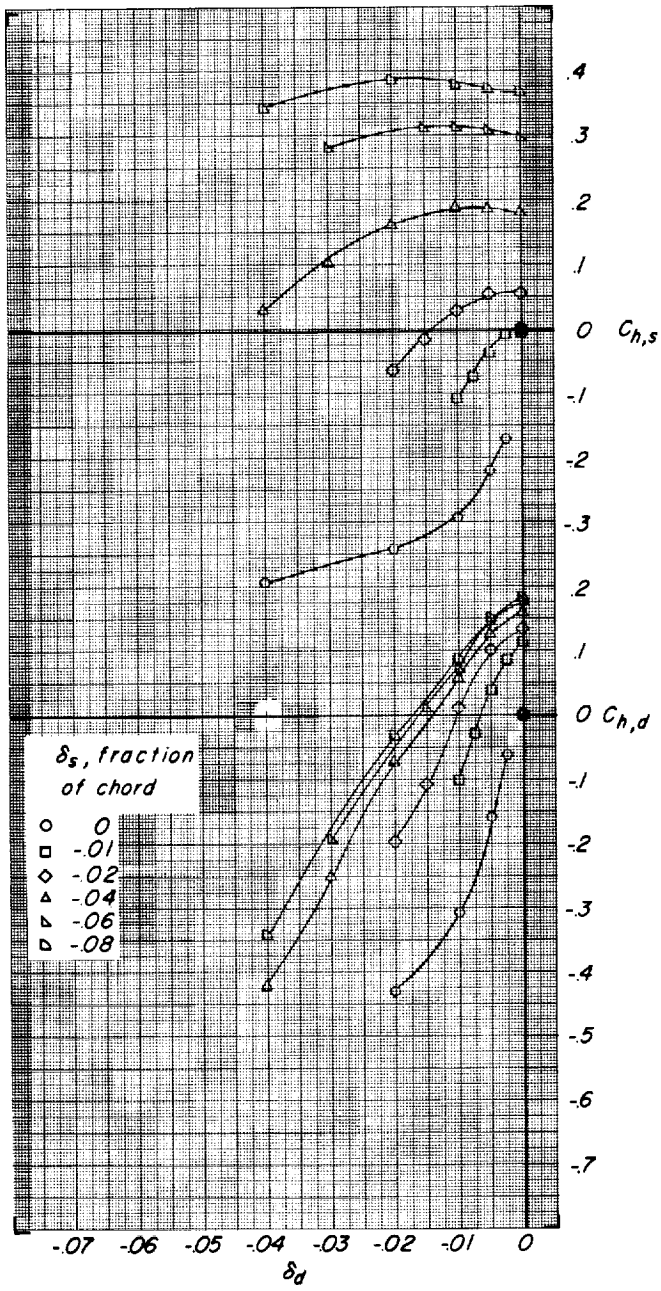

(d) $\alpha = 8^{\circ}$.

Figure 12.- Continued.

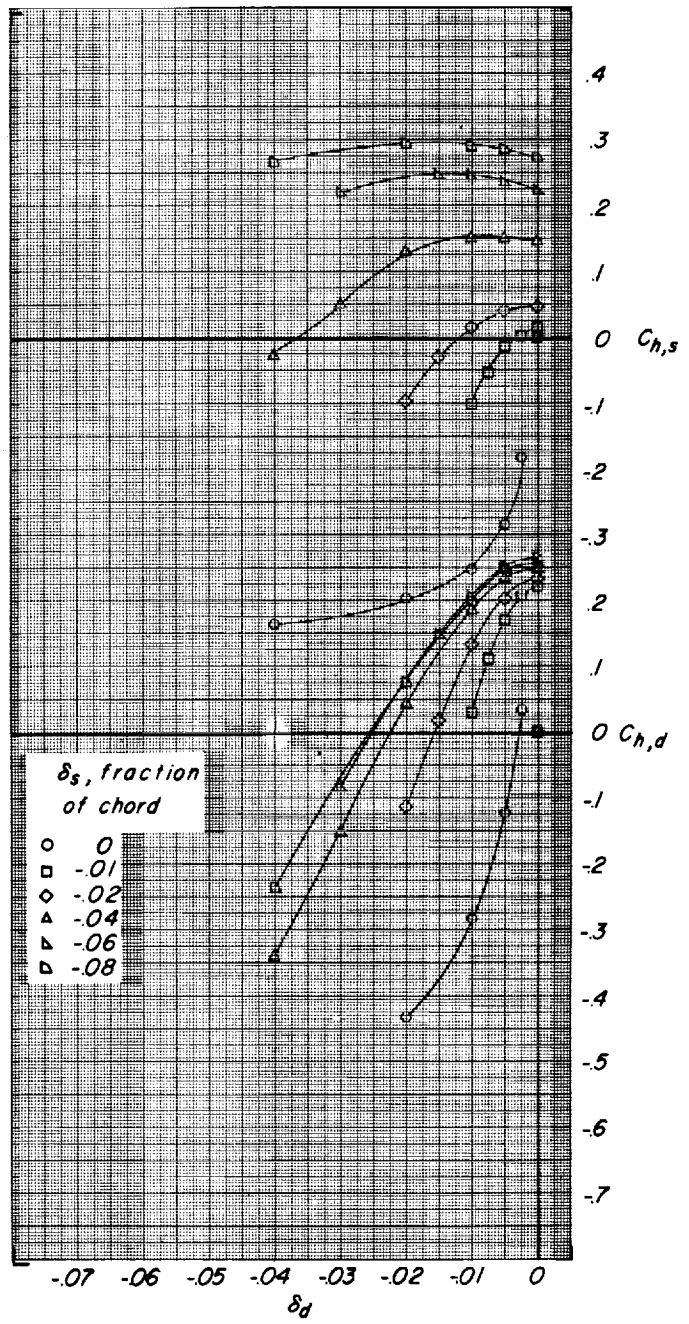

(e) $\alpha = 12^{\circ}$.

Figure 12.- Concluded.

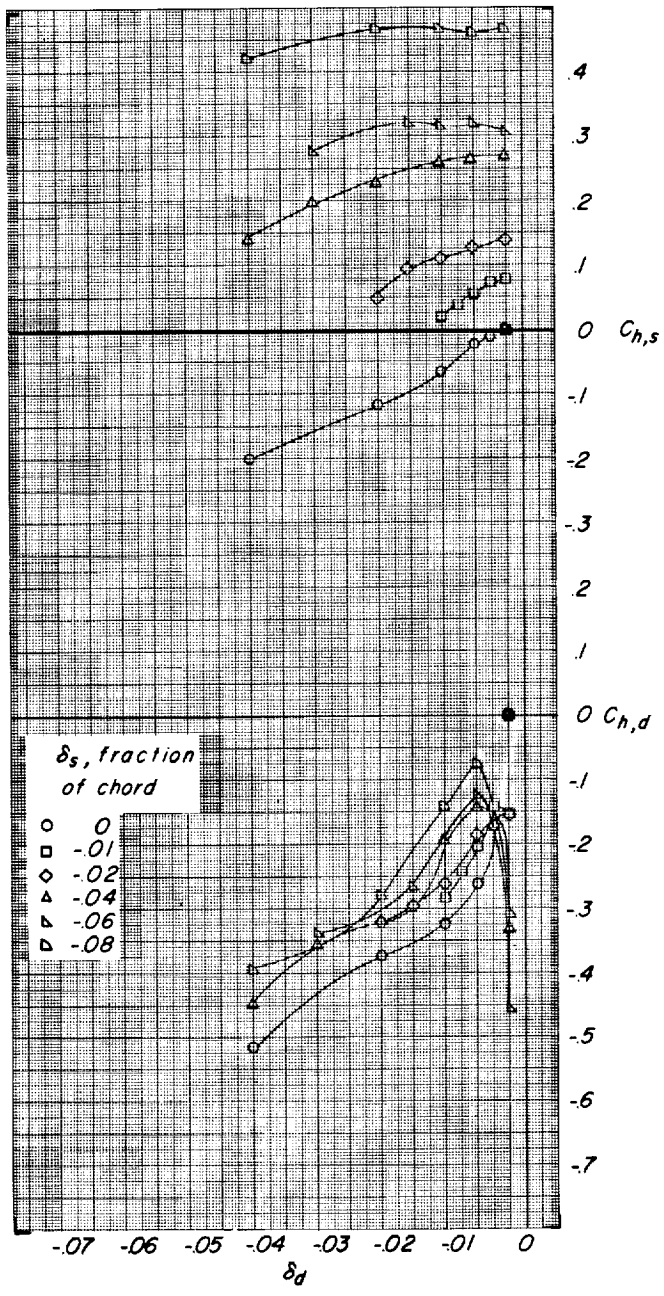

(a) $\alpha = -4^{\circ}$.

Figure 13.- Variation of the spoiler and deflector hinge-moment coefficients with deflector projection for various spoiler projections at M = 0.95.

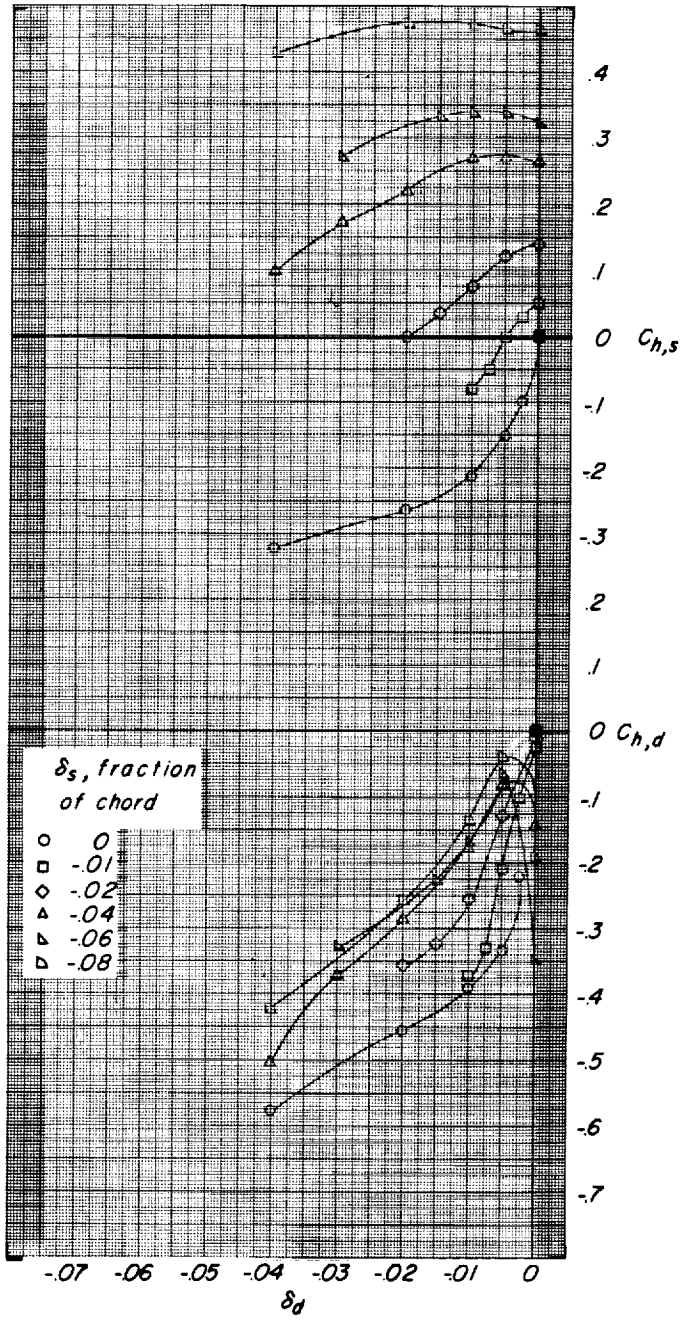

(b) $\alpha = 0^{\circ}$.

Figure 13.- Continued.

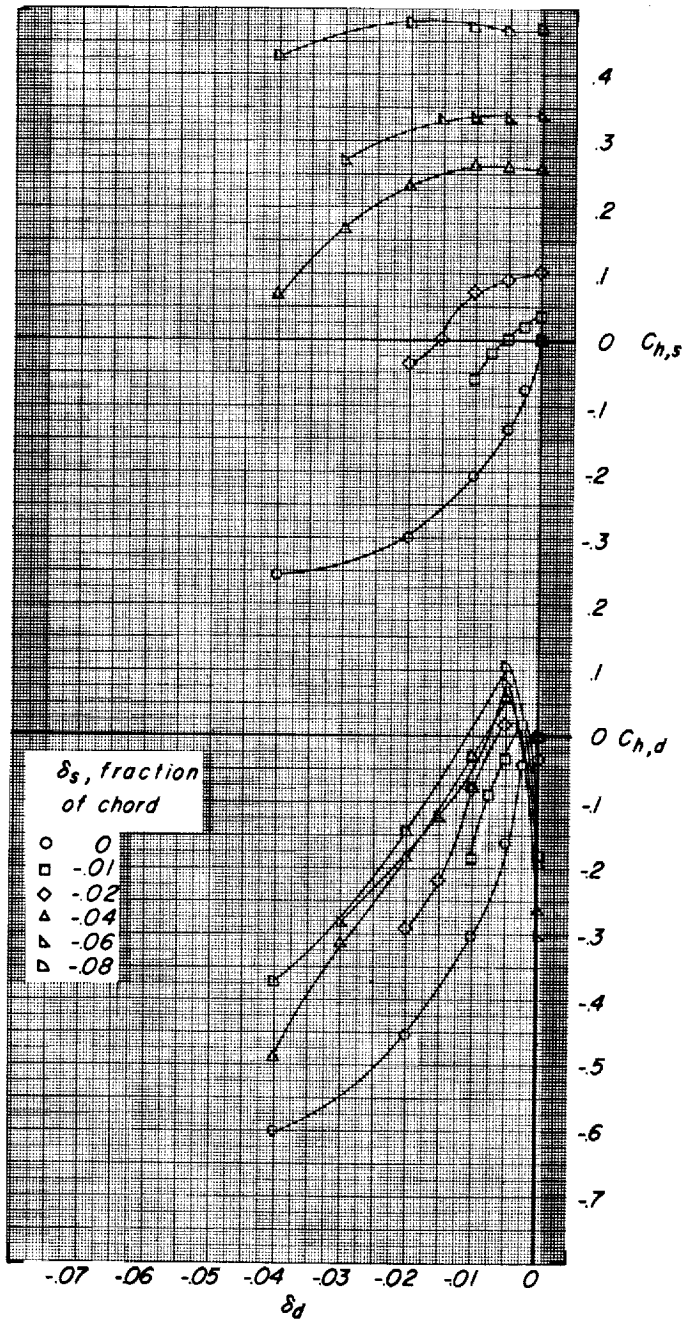

(c) $\alpha = 4^{\circ}$.

Figure 13.- Continued.

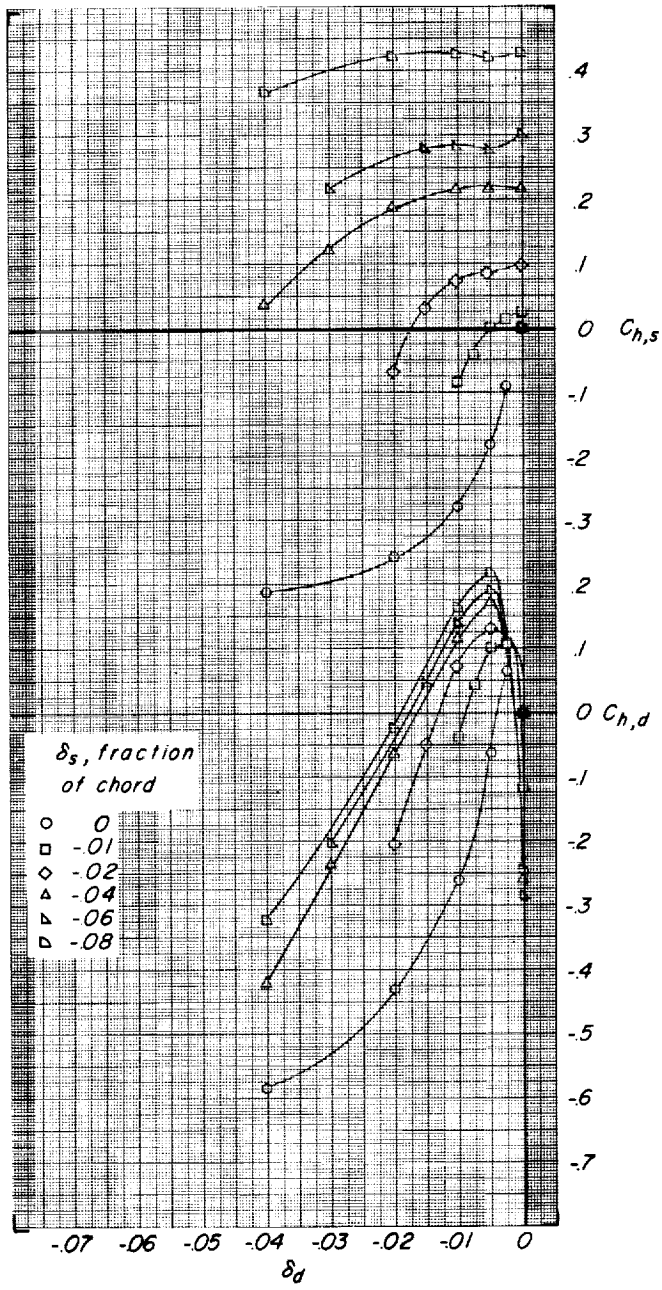

(d) $\alpha = 8^{\circ}$.

Figure 13.- Concluded.